

Nanyang Technological University

School of Mechanical & Aerospace Engineering

**Synthesis of robust and multifunctional microcapsules for protective
coatings used in marine and offshore environments**

By

Sun Dawei

Supervisor: Prof. Fan Zheng

A dissertation submitted to Nanyang Technological University

In partial fulfillment of the requirement for the degree of

DOCTOR OF PHILOSOPHY

2017

Acknowledgement

Firstly, I want to appreciate my previous supervisor, Prof. Yang Jinglei. I cannot achieve current results without his unselfish sharing of knowledge and promising direction. His diligent and scrupulous working attitudes set me a good sample. In addition, I want to show my appreciation to my current supervisor, Prof. Fan Zheng, for his kind support to finish my PhD work and thesis.

My appreciation is also given to Nanyang Technological University for the financial support and the research scholarship of this project.

I also wish to thanks my colleagues and friends who taught me a lot new and unstudied knowledge during my experiments process.

I also want to acknowledge Ms. Koh JooLuang for all the support she has provided unselfishly when I was working in the chemical lab, and all the technical staffs at the School of MAE for their aid in my research work.

Last but not least, I would like to express my heartfelt gratefulness to my family for their continuous support and understanding, and to my girlfriend for her encouragement that really means a lot to me.

Abstract

During service, anticorrosion coatings in seawater are susceptible to wear and scratched damages resulting in the re-exposure of steel substrates. Smart coatings are prepared by formulating microcapsules in polymeric coatings, where healing agents can be released to seal scratches or as lubricant to mitigate wear damages after the microcapsules are broken. Among these microcapsules, isocyanates-loaded microcapsules attracted increasing attentions due to easy operation. However, short service life in moist environments, poor stability in organic solvents and weak mechanical strength of microcapsules restrict their further applications. Therefore, further development of robust microcapsules is of great importance.

4,4'-methylenebis (cyclohexyl isocyanate) (HMDI) was encapsulated successfully in water resistant microcapsules by combining interfacial polymerization and modified in situ polymerization in an oil-in-water emulsion system. The water resistant microcapsules were characterized through various analytical methods, and the influence of agitation rate on diameters, shell thickness and core fraction of microcapsules were investigated systematically. The relative residue of core fraction was higher than 80% after 20 days in moist environments including ambient water, open air, warm water, acidic and alkaline aqueous solutions. However, water resistant microcapsules resist poorly to organic solvents.

In addition, HMDI was also encapsulated successfully in double resistant microcapsules possessing superior stability in both aqueous solutions and organic solvents. Besides outstanding stability in aqueous solutions, double resistant microcapsules also possess outstanding stability in organic solvents. The relative residue of core fractions was beyond 90% after 30 days in ambient hexane, xylene and ethyl acetate, respectively. The influences of parameters including

microcapsule size, concentration and immersion duration on the stability of double resistant microcapsules in organic solvents were investigated systematically. However, double resistant microcapsules possess poor stability in acetone and weak mechanical strength.

In order to improve shell strength and acetone resistance of resultant microcapsules, another layer of metal shell was covered on double resistant microcapsules as trifunctional microcapsules. The trifunctional microcapsules were characterized systematically, presenting superior stability in acetone, and higher mechanical strength than that of double resistant microcapsules.

In order to investigate the influence of metal shell on microcapsules, systematic comparison was conducted between double resistant microcapsules and trifunctional microcapsules. The trifunctional microcapsules possess shell strength several times higher than that of double resistant microcapsules. Even in polymeric matrix, the multifunctional composite coatings containing trifunctional microcapsules also possess higher compressive strength and compressive modulus than those containing double resistant microcapsules. Self-healing samples and self-lubricating samples were fabricated successfully by dispersing two types of microcapsules in epoxy resin. Both double resistant microcapsules and trifunctional microcapsules showed superior self-healing anticorrosion performance towards steel panels. However, trifunctional microcapsules possess marginal self-lubricating performances in epoxy resin due to the existence of metals shell, comparing with outstanding self-lubricating performance of double resistant microcapsules.

Robust microcapsules were fabricated successfully through various encapsulation techniques. However, further investigations are still needed to improve the shortages of current microcapsules.

Contents

Acknowledgement.....	I
Abstract	II
Contents	IV
List of figures.....	IX
List of abbreviations	XVI
Chapter 1 Introduction.....	1
1.1 Background	1
1.2 Objective	3
1.3 Scope.....	4
1.4 Novelty and originality	5
1.5 Report outline.....	6
Chapter 2 Literature Review	8
2.1 Protective materials used in marine and offshore structures	8
2.1.1 Protective surface coatings	10
2.1.2 Polymeric coatings used in offshore risers	14
2.2 Microcapsules based smart protective coatings.....	19
2.2.1 Anticorrosion mechanisms.....	20
2.2.2 Microencapsulation methods	26

2.3	Current issues	32
Chapter 3	Experiments.....	35
3.1	Materials	35
3.2	Synthesis of microcapsules	35
3.2.1	Synthesis of water resistant microcapsules.....	35
3.2.2	Synthesis of double-resistant microcapsules	40
3.2.3	Synthesis of trifunctional microcapsules	43
3.3	Characterization of microcapsules	45
3.4	Stability tests of microcapsules in water and organic solvents.....	47
3.5	Mechanical property tests	47
3.5.1	Mechanical property of microcapsules	47
3.5.2	Compression test of epoxy composites containing microcapsules	48
3.6	Preparation and test of multifunctional composite coatings	49
3.6.1	Preparation of anticorrosion coatings	49
3.6.2	Evaluation of anticorrosion performance.....	49
3.6.3	Preparation of self-lubricating samples	50
3.6.4	Evaluation of self-lubricating performance	50
Chapter 4	Study of water resistant microcapsules.....	51
4.1	Motivation.....	51
4.2	Overview of preparing water resistant microcapsules	53

4.2.1 Synthesis of water resistant microcapsules.....	53
4.2.2 The influence of agitation rate on water resistant microcapsules	55
4.3 Characterization of water resistant microcapsules.....	58
4.3.1 Morphology of water resistant microcapsules	58
4.3.2 Chemical composition of water resistant microcapsules	59
4.3.3 Thermal property and core fraction of water resistant microcapsules	60
4.4 Stability of water resistant microcapsules in water.....	62
4.4.1 Stability in aqueous solutions with various pH values	62
4.4.2 Pot life.....	64
4.4.3 Stability in organic solvents.....	64
4.5 Resistance mechanism of microcapsules to organic solvents.....	66
4.6 Summary	67
Chapter 5 Study of double resistant microcapsules.....	69
5.1 Motivation.....	69
5.2 Overview of preparing double resistant microcapsules	70
5.3 Characterizations of double resistant microcapsules	71
5.3.1 Morphology of double resistant microcapsules	71
5.3.2 Chemical composition of core materials.....	73
5.3.3 Core fraction and thermal stability of double resistant microcapsules	73
5.4 Stability of double resistant microcapsules in organic solvents and water.....	75

5.4.1 Shell functions of double resistant microcapsules	75
5.4.2 Stability of double resistant microcapsules in water.....	78
5.4.3 Stability of double resistant microcapsules in organic solvents	79
Chapter 6 Study of tri-functional microcapsules	86
6.1 Motivation.....	86
6.2 Overview of preparing trifunctional microcapsules	87
6.3 Characterization of trifunctional microcapsules	88
6.3.1 Morphology of trifunctional microcapsules.....	88
6.3.2 Chemical determination of core materials	90
6.3.3 Core fraction and thermal stability of trifunctional microcapsules	90
6.4 Stability of trifunctional microcapsules in organic solvents and water	92
6.4.1 Stability of trifunctional microcapsules in organic solvents.....	92
6.4.2 Stability of trifunctional microcapsules in water	93
6.5 Summary	96
Chapter 7 Mechanical, anticorrosion and tribological performances of multifunctional composite coatings	97
7.1 Motivation.....	97
7.2 Mechanical properties of resultant microcapsules.....	97
7.2.1 Mechanical properties of shell materials	98
7.2.2 Influence of microcapsules on mechanical properties of epoxy composites.....	99

7.3 Influence of resultant microcapsules on anticorrosion performance of multifunctional composite coatings.....	102
7.3.1 Anticorrosion performance of self-healing coatings towards steel panels	103
7.3.2 Self-healing anticorrosion process monitored by EIS	104
7.4 Tribology performance	105
7.4.1 The influence of normal loads on tribology of epoxy composites.....	106
7.4.2 The influence of sliding velocities on tribology of epoxy composites	115
7.5 Summary	122
Chapter 8 Conclusions and future work.....	124
8.1 Conclusions.....	124
8.2 Future work.....	126
References	128
List of Publications	148

List of figures

Chapter 2

Figure 2.1 Serious corrosion occurs to (a) marine and (b) offshore structure.	8
Figure 2.2 Corrosion profile of steel piling at different locations in seawater [13].	9
Figure 2.3 Typical metallic coating on metal substrates.	10
Figure 2.4 Offshore field development components include subsea system, FL/PL/Riser, Processing and Fixed/Floating Structures [78].	15
Figure 2.5 Function of drilling riser is to transport crude oil to topside system [80].	16
Figure 2.6 Components of a riser with liner as the innermost layer [81], polymeric liner as the innermost layer was coated on the surface of carcass for anticorrosion.	17
Figure 2.7 Different wear mechanisms corresponding to different conditions [82].	17
Figure 2.8 Anticorrosion mechanism of microcapsules-based self-healing coatings.	20
Figure 2.9 The anticorrosion process of cations corrosion inhibitors towards polymeric coatings [38].	25

Chapter 3

Figure 3.1 The first step of preparing water resistant microcapsules applied the reaction between amine and isocyanates. The rapid reaction between amino functional groups and NCO functional groups can produce dense polyurea shells [145].	36
Figure 3.2 The second step of preparing water resistant microcapsules applied the rapid formation of PUF resins in acidic environments [146].	38
Figure 3.3 The first step to prepare double resistant microcapsules is the same with the first step of preparing water resistant microcapsules.	39

Figure 3.4 The second step of preparing double resistant microcapsules is to coat highly crosslinked PUF resin on microcapsules with inner-layered polyurea shells in acidic environments [147].	41
Figure 3.5 The preparation process of microcapsules with catalyst on the surface. The newly formed Pd particles was prepared by reducing Pd^{2+} with Sn^{2+} .	43

Chapter 4

Figure 4.1 Reaction mechanism between isocyanate and water.	52
Figure 4.2 Schematic formation process of water resistant microcapsule.	54
Figure 4.3 Diameter and shell thickness of microcapsules prepared at different agitation rates..	56
Figure 4.4 Core fraction of water resistant microcapsules prepared at different agitation rate....	56
Figure 4.5 Core fractions of microcapsules prepared under different fractions of Suprasec 2644, and the inset pictures are the corresponding interior morphology of related microcapsules.....	58
Figure 4.6 (a) Overview of water resistant microcapsules; (b) Morphology of single microcapsule; (c) Inner structure of microcapsules, and (d) Shell profile.....	58
Figure 4.7 Comparison of FTIR spectrums of water resistant microcapsule's shell, processed shell materials, core materials, Suprasec 2644 and HMDI.....	60
Figure 4.8 Thermal performances of water resistant microcapsules and constituent materials. ..	61
Figure 4.9 The relative core fractions (Residual/original core fraction) of water resistant microcapsules varied with durations after immersed in aqueous solutions with different pH values.	63
Figure 4.10 Relative core fractions of water resistant microcapsules varied with immersion durations after exposed in open air and water under different temperature.	63
Figure 4.11 Stability of water resistant microcapsules in organic solvents.....	65

Figure 4.12 Schematic diagrams showing different release mechanisms of liquid core through shell after microcapsules immersion in weakly or nonpolar organic solvents (a), polar aprotic organic solvents (b), and ambient water (c).....	67
-------------------------------------------------------------------------------------------------------------------------------------------------------------------------------------------------------------------------------------------	----

Chapter 5

Figure 5.1 (a) Overview of double resistant microcapsules; (b) Morphology of single double resistant microcapsule; (c) Inner structure of double resistant microcapsule, and (d) Shell profile of double resistant microcapsules.	72
Figure 5.2 Comparison of ^1H -NMR spectras of pure HMDI (a) and core materials (b).	73
Figure 5.3 Thermal stability of double resistant microcapsules, shell, broken double resistant microcapsules and HMDI.	74
Figure 5.4 The morphologies of microcapsules with inner-layered polyurea shells (a, b) and double resistant microcapsules (c, d) after immersion in water (a, c) for 20 days and hexane (b, d) for 5 days.....	76
Figure 5.5 The residual core fraction of double resistant microcapsules as a function of immersion time in ambient water.	79
Figure 5.6 Morphology (a) and inner structure (b) of double resistant microcapsules after being immersed in ambient water for 20 days.....	79
Figure 5.7 Stability of typical microcapsules in hexane, xylene and ethyl acetate.	81
Figure 5.8 Morphology of microcapsules after 30 days in hexane (a), xylene (b) and ethyl acetate (c). (d) is the morphology of microcapsules after 2 days in acetone	82
Figure 5.9 Core fractions of double resistant microcapsules with different size before and after immersion in ethyl acetate for 5 days.	82

Figure 5.10 The thickness of outer-layered shell of microcapsules with diameters of 158.1 ± 42.3 μm (a), 79.7 ± 21.5 μm (b), 59.1 ± 16.9 μm (c).	84
-----------------------------------------------------------------------------------------------------------------------------------------------------------------------------------------------------	----

Figure 5.11 The influence of microcapsules concentration on the release performance of typical microcapsules in ethyl acetate.	84
-------------------------------------------------------------------------------------------------------------------------------------	----

Chapter 6

Figure 6.1 (a) Overview of trifunctional microcapsules; (b) Morphology of single trifunctional microcapsule; (c) Trifunctional microcapsules showed hollow inner structure; (d) The three-layered shell structure of trifunctional microcapsules.	89
--------------------------------------------------------------------------------------------------------------------------------------------------------------------------------------------------------------------------------------------------------	----

Figure 6.2 (a) The test area of metal shell; (b) Elements composition of metal shell, and (c) EDX spectrum of metal shell.	89
---------------------------------------------------------------------------------------------------------------------------------	----

Figure 6.3 Comparison of FTIR curves of core materials and pure HMDI.....	91
---------------------------------------------------------------------------	----

Figure 6.4 TGA weight loss curves of trifunctional shell materials, trifunctional microcapsules and pure HMDI as a function of temperature.	91
--------------------------------------------------------------------------------------------------------------------------------------------------	----

Figure 6.5 The residual core fraction of trifunctional microcapsules as a function of immersion durations after being immersed in hexane, xylene, ethyl acetate and acetone, respectively.	94
-------------------------------------------------------------------------------------------------------------------------------------------------------------------------------------------------	----

Figure 6.6 The outer morphology and inner structure of trifunctional microcapsules after being immersed in hexane (a ₁ , a ₂), xylene (b ₁ , b ₂), ethyl acetate (c ₁ , c ₂) and acetone (d ₁ , d ₂), respectively.	94
----------------------------------------------------------------------------------------------------------------------------------------------------------------------------------------------------------------------------------------------------------------------------------------------------------------------	----

Figure 6.7 The residual core fraction of trifunctional microcapsules as a function of durations after being immersed in ambient water.....	95
--------------------------------------------------------------------------------------------------------------------------------------------	----

Figure 6.8 The outer morphology (a) and inner structure (b) of trifunctional microcapsules after being immersed in water for 20 days.....	96
-------------------------------------------------------------------------------------------------------------------------------------------	----

Chapter 7

Figure 7.1 Typical load-displacement curves of double resistant microcapsules and trifunctional microcapsules.....	98
Figure 7.2 Normalized shell strength of double resistant microcapsules and trifunctional microcapsules.....	99
Figure 7.3 Compressive strength of composites containing double resistant microcapsules and trifunctional microcapsules as a function of microcapsules concentration.	101
Figure 7.4 Compressive modulus of composites containing double resistant microcapsules and trifunctional microcapsules as a function of microcapsules concentration.	102
Figure 7.5 The corrosion performances and detailed information in scratches of coatings including neat epoxy coating (a ₁ , a ₂), self-healing coatings containing double resistant microcapsules (b ₁ , b ₂), and self-healing coatings containing trifunctional microcapsules (c ₁ , c ₂).	103
Figure 7.6 (a) The schematic picture of EIS experiment model; (b) The equivalent circuit applied to obtain the resistance due to healing (R_{healing}) by curve fitting.	104
Figure 7.7 The healing resistance (R_{healing}) of scratched self-healing coating containing double resistance microcapsules (a) and trifunctional microcapsules (b) as a function of immersion durations.....	105
Figure 7.8 Friction coefficient of samples as a function of durations under different normal loads (3N, 5N, and 10N) at sliding velocity of 50 REV. (a) Pure epoxy samples; (b) Composites Tri-10wt%; (c) Composites Tri-30wt%, and (d) composites DR-10wt%.....	107
Figure 7.9 The detailed morphology of the wear track of pure epoxy samples (a), composites Tri-10wt% (b), composites Tri-30wt% (c) and composites DR-10wt% (d) under normal loads of 3N (a ₁ , b ₁ , c ₁ and d ₁), 5N (a ₂ , b ₂ , c ₂ and d ₂) and 10N (a ₃ , b ₃ , c ₃ and d ₃).	108

Figure 7.10 The friction coefficient of pure epoxy samples, composites Tri-10wt%, composites Tri-30wt% and composites DR-10wt% as a function of normal loads (3N, 5N and 10N).	111
Figure 7.11 (a) The topography of wear track of pure epoxy samples (5N, 50 REV); (b) Profile of related wear track.....	112
Figure 7.12 The wear width of pure epoxy samples, composites Tri-10wt%, composites Tri-30wt% and composites DR-10wt% as a function of normal loads (3N, 5N and 10N).....	114
Figure 7.13 The wear depth of pure epoxy samples, composites Tri-10wt%, composites Tri-30wt% and composites DR-10wt% as a function of normal loads (3N, 5N and 10N).....	114
Figure 7.14 Friction coefficient of pure epoxy samples (a), composites Tri-10wt% (b), composites Tri-30wt% (c) and composites DR-10wt% (d) as a function of durations under normal load of 5N at sliding rates of 25 REV, 50 REV and 100 REV.....	116
Figure 7.15 The detailed morphology of the wear track of pure epoxy samples (a), composites Tri-10wt% (b), composites Tri-30wt% (c) and composites DR-10wt% (d) at sliding rate of 25 REV (a ₁ , b ₁ , c ₁ and d ₁), 50 REV (a ₂ , b ₂ , c ₂ and d ₂) and 100 REV (a ₃ , b ₃ , c ₃ and d ₃).....	117
Figure 7.16 The friction coefficient of pure epoxy samples, composites Tri-10wt%, composites Tri-30wt% and composites DR-10wt% as a function of sliding velocities (25 REV, 50 REV and 100 REV).	119
Figure 7.17 The wear width of pure epoxy samples, composites Tri-10wt%, composites Tri-30wt% and composites DR-10wt% as a function of sliding velocities (25 REV, 50 REV and 100 REV).	121
Figure 7.18 The wear depth of pure epoxy samples, composites Tri-10wt%, composites Tri-30wt% and composites DR-10wt% as a function of sliding velocities (25 REV, 50 REV and 100 REV).	122

List of tables

Table 2.1 Mechanism based on different anticorrosion agents.....	21
Table 2.2 Encapsulation methods	25

List of abbreviations

CNT	Carbon nanotube
DCPD	Dicyclopentadiene
DI water	Deionized water
DPO	Benzyl peroxide
EDX	Energy dispersive X-ray spectroscopy
EIS	Electrochemical impedance spectroscopy
EMA	Ethylene maleic anhydride
FTIR	Fourier transform infrared spectroscopy
HCl	Hydrochloride acid solution
HDI	Hexamethylene diisocyanate
HMDI	4,4'-Methylenebis(cyclohexyl isocyanate)
H-NMR	¹ H-Nuclear Magnetic Resonance Spectroscopy
IPDI	Isophorone diisocyanate
KBr	Potassium bromide
LPO	Lauroyl peroxide
MDI	Methylenediphenyl diisocyanate

NaOH	Sodium hydroxide
NaCl	Sodium Chloride
PUF	Poly(urea-formaldehyde)
TEPA	Tetraethylenepentamine
TGA	Thermogravimetric analysis

Chapter 1 Introduction

1.1 Background

Marine and offshore structures are susceptible to corrosion from seawater resulting in serious economic consumption and safety hazards. In order to retard corrosion process, protective coatings including metallic coatings, inorganic coatings and polymeric coatings were widely applied on steel surface to isolate the substrates from corrosive seawater. However, high fabrication cost and weak adjustability restricted the wide applications of metallic and inorganic coatings. Polymeric coatings attract numerous attentions due to outstanding anticorrosion performance towards steel substrates and easy operations. During the exploration process of offshore petroleum, steel pipelines were extensively served as carcass for the transportation of crude oil. With the development of material science and engineering techniques, polymeric coatings were coated on the internal surface of carcass as protective layer to improve anticorrosion property of steel pipelines. However, protective coatings usually possess short service life under repeated attacks from marbles or asperities within surrounding environments. Therefore, it is highly necessary to design and fabricate a new multifunctional self-healing and self-lubricating coating which can repair cracks and retard wear automatically at the site of damages.

Recent years, self-healing anticorrosion coatings have drawn numerous attentions due to their automatic healing ability to damages. When damages occur to polymeric matrix, the propagation of cracks breaks microcapsules easily resulting in the release of healing agents, which can isolate steel substrates from corrosive environments after cure. Typical healing agents include isocyanates, linseed oil, and corrosion inhibitors. Among these alternatives, isocyanate based

one-component self-healing coatings drew numerous attentions because of their outstanding anticorrosion performance toward metal substrates. The released isocyanates can react rapidly with surrounding moisture with the formation of polyurea film to seal the cracks. Yang *et al.* [1] firstly encapsulated successfully isocyanate (IPDI) within polyurethane shell via interfacial polymerization. Subsequently, Huang and Yang [2] presented efficient anticorrosion performance of scratched one-component self-healing coating towards steel panels by embedding encapsulated hexamethylene diisocyanate (HDI) within epoxy coating. Besides, Keller *et al.* [3] evaluated the self-healing performance of microcapsule-based intelligent coating under erosion conditions.

Besides self-healing functions, polymeric coatings containing microcapsules were also imparted self-lubricating capability to resist wear damages from solid asperities. Khun *et al.* [4, 5] incorporated encapsulated HDI and encapsulated liquid wax within epoxy resin to inhibit wear damages from steel balls. The released liquid wax as liquid lubricant can decrease significantly friction coefficient, while the released HDI can also realize self-healing of wear track under abrasion conditions besides decreasing friction coefficient. Therefore, incorporating encapsulated isocyanates in polymeric coatings can achieve simultaneously self-healing and self-lubricating functions [4, 6].

However, some existing shortages of encapsulated isocyanates restrict resultant self-healing and self-lubricating performances. When encapsulated isocyanates were applied to protective coatings, weak shell strength of microcapsules degrade mechanical behavior of polymeric matrix, and poor stability in organic solvents and water shortened the service life of these smart materials. Increasing investigations were focused on the improvement of shell properties of microcapsules containing isocyanates. Sun *et al.* [7] used double-layered polyurea shell to

improve successfully the stability of encapsulated HDI in organic solvents with weak and medium polarities. Wu *et al.* [8] synthesized silica/polyurea hybrid shells encapsulating HDI presenting outstanding resistance to xylene. Yi *et al.* [9] improved microcapsules stability in ambient water by introducing inorganic fillers within polyurea shells. However, all improvements to shell properties still fail to fabricate microcapsules with high mechanical strength and, outstanding stability in organic solvents and water, simultaneously. Herein, we intend to design and fabricate one new type of microcapsules (named as double resistant microcapsules) with outstanding stability in both organic solvents and water. Subsequently, the metal shell was coated on double resistant microcapsules to boost the mechanical strength as trifunctional microcapsules. Finally, two types of microcapsules were formulated in epoxy resin as protective coatings, and self-healing and self-lubricating performances were compared systematically.

1.2 Objectives

The main objectives of this thesis work are:

- To fabricate water resistant microcapsules, which possess outstanding stability in aqueous environment to address applications in waterborne coatings or paints.
- To enhance the stability of water resistant microcapsules in organic solvents to address applications in solvent-borne materials.
- To increase the mechanical strength of double resistant microcapsules for engineering applications.

- To investigate the compressive behaviors of the resultant microcapsules and develop anticorrosion and self-lubricating polymer composites modified by the resultant microcapsules.

1.3 Scope

To realize the proposed objectives, the following work scopes are initiated.

- The water resistant microcapsules will be prepared by combining interfacial polymerization and in situ polymerization. Inner-layered polyurea shells were firstly fabricated to encase HMDI based on its dense matrix structure from higher crosslink density. The higher crosslink density of polyurea than polyurethane was mainly due to the faster reaction rate of amines towards isocyanates [10]. Subsequently, outer-layered PUF shells with linear structure were covered on microcapsules with inner-layered polyurea shells, and the water resistant microcapsules were fabricated successfully. The resultant microcapsules are characterized via Scanning Electron Microscope (SEM), Fourier Transform Infrared Spectroscopy (FTIR) and Thermogravimetric analysis (TGA). The effect of agitation rate on diameters, shell thickness and core fraction of microcapsules is to be investigated systematically. Subsequently, the stability of the resultant microcapsules in water and organic solvents will be tested.
- The double resistant microcapsules will be prepared by combining interfacial polymerization and new in situ polymerization process. Inner-layered polyurea shells were firstly applied to encapsulate HMDI. Subsequently, outer-layered PUF shells with highly cross-linked structure were coated on the surface of microcapsules with inner-layered polyurea shells. Finally, the double resistant microcapsules were fabricated successfully.

The resultant microcapsules are characterized via SEM, FTIR and TGA. The stability of microcapsules in both ambient water and organic solvents will be evaluated by immersing microcapsules in various solvents.

- The trifunctional microcapsules will be fabricated by covering a layer of Nickel-P alloy on double resistant microcapsules through chemical plating techniques. This resultant microcapsule was named as tri-functional microcapsule. The resultant microcapsules were characterized via SEM, FTIR and TGA, and EDX. The stability of resultant microcapsules in both water and organic solvents resistance will be tested.
- The final part is to investigate the influence of metal shell on the mechanical properties of microcapsules, including shell strength and composites strength. In addition, the anticorrosion performance and tribological performance of multifunctional composite coatings containing double resistant microcapsules and trifunctional microcapsules will be investigated systematically.

1.4 Novelty and originality

The novelty and originality of this research is listed below.

- 1) One of the open issues of isocyanate-capsule-based self-healing coatings is its vulnerability in water environment, which is to be solved by forming cross-linked polyurea shell to achieve long-term aqueous resistance potentially for waterborne coatings or paints.
- 2) Another issue is the poor survivability of current microcapsules in solvent-borne resins. Therefore, solvent resistant function is introduced to the water-resistant microcapsules to form double resistant microcapsules, which will be also investigated in epoxy composite coatings in terms of self-healing and self-lubricating performances for the first time.

3) Lastly, mechanical integrity of composites modified by microcapsules is also very important for certain engineering applications. Therefore, metal shell is additionally formed on the double resistant capsules to obtain mechanically strong structure. The mechanical strengths of individual metal shell microcapsules and their polymer composites are proved. The self-healing and self-lubricating performances of composites containing metal shell microcapsules are also investigated.

Although the metal shell microcapsules behave multifunctional performances, each of these three types of microcapsules can fit for a niche application independently at a cost-effective manner.

1.5 Report outline

The first chapter introduces the background about the protective coatings and highlights the objectives and scope of my project.

Chapter 2 reviews protective coatings, risers, tribology, smart polymeric coatings and recent advances in microencapsulation techniques. Especially, the development of microcapsules shell materials is presented. Finally, conclusion and motivation are given.

Chapter 3 introduces the preparation strategies of various microcapsules and lists related sample preparation processes and test methods.

Chapter 4 introduces the preparation strategy of water resistant microcapsules loading HMDI as core, and stability of final microcapsules in water are measured and presented.

Chapter 5 is to improve the stability of water resistant microcapsules in organic solvents, and the final microcapsules (named as double-resistant microcapsules) present outstanding stability in both water and organic solvents.

Chapter 6 improves the mechanical properties of double-resistant microcapsules by plating a layer of metal shell, and the final microcapsules were named as tri-functional microcapsules, the stability of resultant microcapsules in water and organic solvents are presented.

Chapter 7 compares mechanical properties of double resistant microcapsules with that of tri-functional microcapsules. Both types of microcapsules were formulated in epoxy resin as multifunctional composite coating, whose compressive strength, compressive modulus, self-healing performance and tribology performance of final composites were presented systematically.

Chapter 8 provides the conclusion of current work and gives some designs about future work.

Chapter 2 Literature Review

2.1 Protective materials used in marine and offshore structures

With the development of science and engineering techniques, the exploration of ocean resources attracts increasing attentions. However, there are abundant of electrolytes, dissolved oxygen, microorganism and decomposing organic matters in seawater. All the existing constituents corrode easily the immersed metal constructions including marine (Figure 2.1a) and offshore structures (Figure 2.1b) resulting in numerous economic cost and potential safety hazard. As far as known, corrosion brings greatest consumption of metal materials, and annual economic loss as high as billions of dollars in developed nations [11]. Comparing with direct economic loss, indirect loss was higher while more difficult to evaluate. The estimation of annual indirect economic loss was around 300 billion dollars in United States of America. More seriously, corrosion occurring to structural parts probably causes safety failure possessing dramatic consequences for human and environments [12, 13]. Numerous reports about the failure of aircrafts, pipelines, and ships are reported annually.

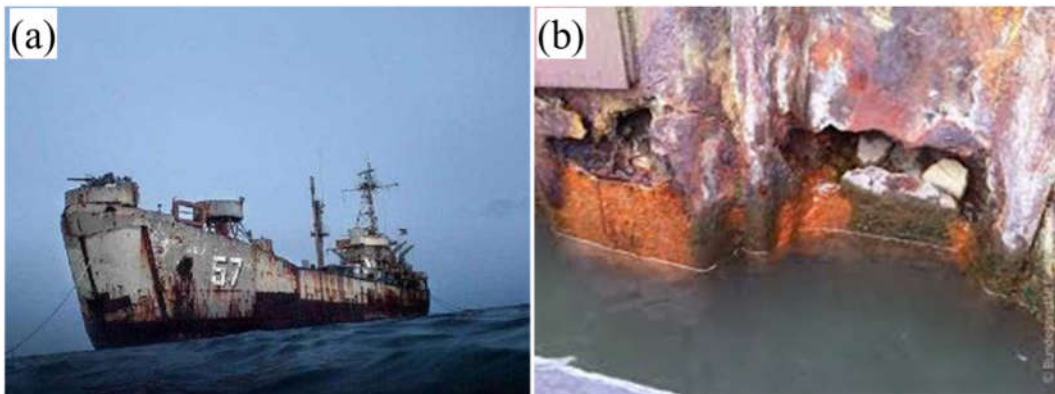


Figure 2.1 Serious corrosion occurs to (a) marine and (b) offshore structure.

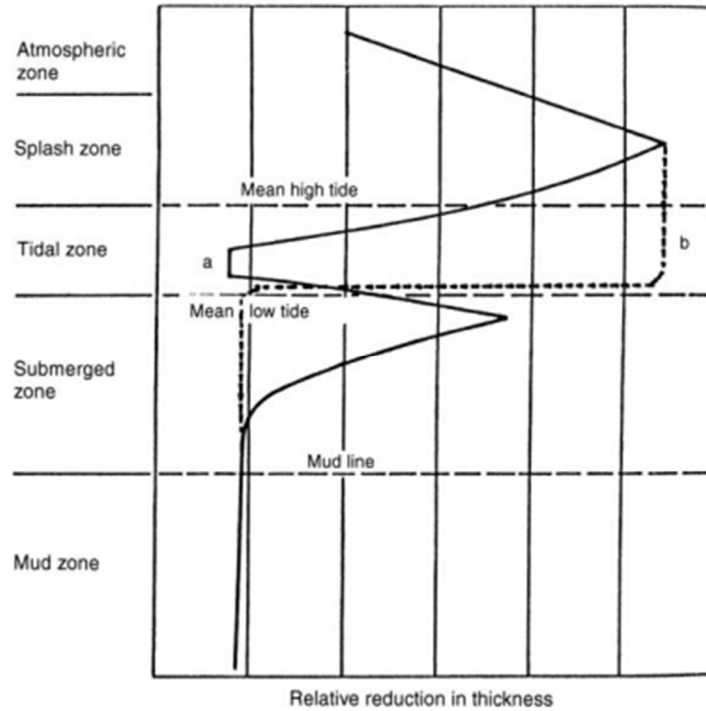


Figure 2.2 Corrosion profile of steel piling at different locations in seawater [14].

When metal materials were immersed in seawater at different sea levels, different corrosion rates were observed, as shown in Figure 2.2. The positions of metal materials in seawater can be roughly divided into atmospheric zone, splash zone, submerged zone and mud zone. The most serious corrosion occurs in splash zone, because this area is oxygen-rich atmosphere with continuous supply of electrolytes from seawater [15]. However, the corrosion of steel in tidal zone is relative mild due to the galvanic protection by the splashed area [14]. Normally, the corrosion rate of steel materials in seawater was mainly influenced by the supply rate of dissolved oxygen, which is controlled by temperature and electrolyte concentration. In seawater, the electrolyte concentration varied slightly at different locations resulting in minor influence on corrosion rate. Therefore, temperature is the main factor controlling corrosion rate. Temperature changed significantly with the latitude from $-2\text{ }^{\circ}\text{C}$ in the Arctic area to $35\text{ }^{\circ}\text{C}$ in the tropical area. Under higher temperature, the diffusion velocity of oxygen was faster resulting in more serious

corrosion of metal materials. In order to retard corrosion process, protective surface coatings were widely applied to steel materials to isolate the metal substrates from surrounding environments.

2.1.1 Protective surface coatings

Various coatings were widely applied in anticorrosion fields of steel materials in seawater. Three types of coatings need to be mentioned including metallic coatings, inorganic coatings and polymeric coatings.

Metallic coatings

Metallic coatings are conventionally applied to metallic and ceramic substrates as protective coatings, and they can be fabricated through various methods including thermal spraying [16], chemical vapor deposition [17], physical spraying, dip coating [18], sputtering [19] and immersion, and so on. Normally, metallic coatings are covered metal substrates with a thin thickness, and typical metallic coatings on substrates were shown in Figure 2.3.



Figure 2.3 Typical metallic coating on metal substrates.

Two basic rules including barrier effect and cathodic protection [20] need to be obeyed during fabrication of metallic coatings. Barrier effect means that metallic coatings need good impermeability to isolate metal substrates from corrosive environments by retarding the transportation of electrolytes [21].

Barrier effect can be achieved through surface passivation. For example, the surface of aluminum substrates can be oxidized into dense and nonporous oxidation film as protective layer in acid environments. Normally, the barrier effect of coating is influenced insignificantly by the density and thickness of coatings [22], and thicker and denser coating corresponds to better anticorrosion performance. Cathodic protection is achieved by coating a layer of metal layer with lower potential (zinc or aluminum) on steel substrates [23]. The cell can be formed in corrosive environments, and the steel substrates are then protected as cathode. However, the low potential of protective layer usually tends to result in hydrogen embrittlement of metal substrates [24, 25].

Metallic coatings experience rapid development under the concern of environment and economy. Due to outstanding anticorrosion performance, cadmium [26] and chromium-containing [27] metallic coatings were widely applied in anticorrosion of steel materials. However, cadmium and chromium was prohibited gradually due to potential hazard towards natural environments [28]. Some novel metallic coatings were developed for environmental concern including zinc-nickel [26] and aluminum alloy [29]. Besides environmental concern, economic concern is another force to drive the development of anticorrosion coatings. Some indium-containing coatings with lower price were developed to improve the anticorrosion performance of steel in thermal environments [30]. However, shortages still exist and restrict the development of metallic coatings. Aluminum and zinc containing coatings can hardly to survive in acidic environments, and hydrogen can be produced gradually with corrosion process resulting in

hydrogen embrittlement of metal substrates [31]. In addition, the weak adhesion with metal substrates and high costs of metallic coatings push the development of inorganic coatings and polymeric coatings.

Inorganic coatings

As representative inorganic coatings, ceramic materials are used in highly critical environments due to expensive cost. Inorganic coatings can be manufactured by embedding natural inorganic compounds including quartz, minerals, and inorganic mineral colorants as pigments in polymeric matrix. The most popular inorganic compound was zinc silicates [32]. Higher concentration of inorganic components in host matrix brought better barrier effects to anticorrosion coatings. However, polymeric matrix containing high contents of solid are susceptible to mud cracking [33]. Therefore, applying zinc silicates to polymeric matrix for anticorrosion aim needs further debates [34, 35]. In addition, sol-gel process can also be used to fabricate inorganic coating for anticorrosion, including ZnO, SiO₂, and SiO₂-TiO₂ [36-38]. Inorganic materials possess high density to provide outstanding anticorrosion performance towards steel substrates. However, sol-gel process can hardly to fabricate large-scale coatings due to its high process temperature [39]. In addition, the inorganic coatings made from sol-gel process are susceptible to cracks or pores resulting in more severe corrosion of metal substrates.

Polymeric coatings

Polymeric coatings are widely applied in anticorrosion field of steel panels due to low cost, easy operation and adjustable properties [40]. However, the polymeric coatings are susceptible to external damages resulting in the re-exposure of metal substrates in corrosive environments. Therefore, smart coatings are developed gradually for economic and environmental concerns [41]. Herein, we present several smart coatings.

Zinc-rich coatings

Zinc-rich coatings have been applied as anticorrosion coatings for a long time [42]. When galvanic corrosion occurs, the steel can be protected electrochemically by more active metal Zn, which serves as a cathode in cells [43]. As a kind of fillers, zinc was frequently dispersed in epoxy resin [44, 45] and alkyd resin [46, 47], and showed outstanding anticorrosion performance. The size [48, 49] and shape [50, 51] of zinc pigments were investigated systematically, and a combination of spherical and lamellar shape has the best anticorrosion performance [44].

Micro- and nano-container based anticorrosion coatings

In order to eliminate the health [52] and environmental incompatibilities, corrosion inhibitors are usually encapsulated within microcapsules to avoid the direct exposure. Various encapsulation methods can be applied to encapsulate corrosion inhibitors including porous or hollow ceramic microcapsules [53, 54], stimuli-responsive microcapsules [55] and polymer containers [56, 57], which can be introduced in polymeric coatings. The release of corrosion inhibitors was influenced by many factors including shell thickness, chemical structures of shell materials, and the matrix where microcapsules were dispersed [58]. The good dispersibility of containers in matrix influences insignificantly the barrier properties of coatings. Lower concentration of microcapsules responds to less release of corrosion inhibitors while better barrier properties of coatings. Although microcapsules with higher concentrations in coatings can release more corrosion inhibitors, the barrier properties of coatings can be damaged seriously [59].

Conductive polymers based anticorrosion coatings

Conductive polymers attract numerous attentions due to their capability to retard corrosion of steel substrates. The conductive polymers can maintain metal surface in a passive states by

forming a layer of oxide film covering the metal substrates [60]. The conductive polymers can be synthesized through chemical or electrochemical oxidation methods [61, 62], and showed outstanding anticorrosion performances [63]. Polyaniline [64, 65], polypyrrole [66, 67], and polythiophene [68, 69] are mostly used as conductive polymers to retard corrosion of coatings. Besides changing surface status of metal substrates, impermeable conductive polymers can also restrict the delivery of oxygen from environments to the interfaces [70]. In order improve the impermeability of coatings, copolymerization [71, 72], use of multilayers of conductive polymers [73, 74], and nanostructured conductive polymers composites [75, 76] were developed gradually.

One component self-healing anticorrosion coatings

One component self-healing anticorrosion coatings applied encapsulated healing agents to achieve anticorrosion performances. The healing agents can be released automatically from microcapsules when damages occurs [77], and the healing agent can polymerize with surrounding light, oxygen [78] or moisture [2] into films to seal the scratches. The detailed introduction of one-component self-healing anticorrosion coatings is presented in subsequent part.

2.1.2 Polymeric coatings used in offshore risers

The exploration of deep water petroleum has achieved considerable developments due to the limited onshore oil resources. Polymeric coatings can be applied as the liners of risers to retard the corrosion of steel pipelines during exploration process.

Introduction of liners of risers

A typical structure of offshore drilling system consists of four parts, subsea system, flowline/pipeline/riser system, fixed/floated structures and topside processing system [79], as shown in Figure 2.4.

The riser is the pipeline that extends from the drilling platform down to the seafloor. Crude oil including mud and cuttings from the borehole are transported to the platform through the riser. The top of the riser is attached to the drillship, while its bottom is secured at the seafloor. The main functions of a riser system are production/injection, export/import or circulate fluids, drilling and completion workover [80]. The drilling riser function as a conduit to transport unprocessed liquid including gas or crude oil from the subsea oil well to topside system, as shown in Figure 2.5. The conveyed fluid is a multi-phase mixture consisting of paraffin, sea water and other solids like sand and marbles.

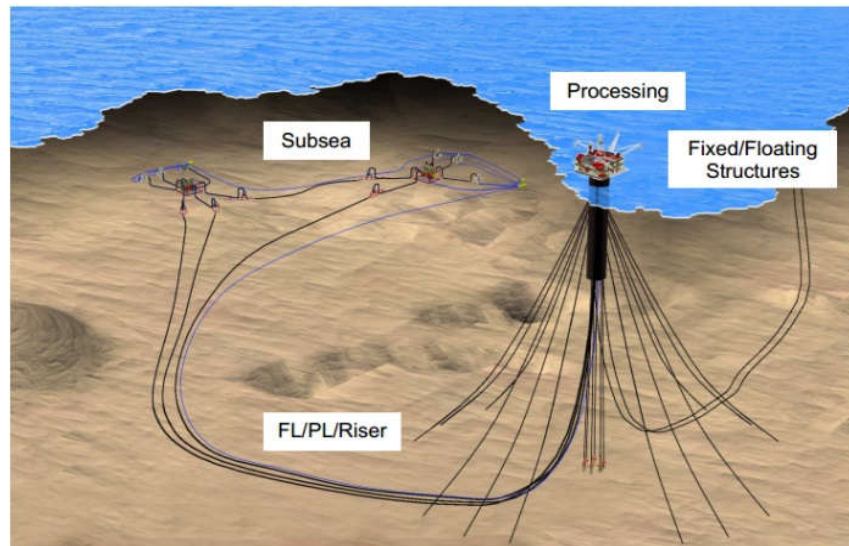


Figure 2.4 Offshore field development components include subsea system, FL/PL/Riser, Processing and Fixed/Floating Structures [79].

A traditional riser includes carcass, barrier, pressure armor, anti-wear layer, tensile armor and outer sheath, as shown in Figure 2.6. The main function of the outer sheath is as a barrier against sea water while the tensile armor is mainly used to resist the tensile load on the riser. Pressure armor can resist the hoop stress in the pipe wall that is caused by the inner bore fluid pressure. On the other hand, barrier provides a protection of bore fluid integrity. The steel carcass provides protection to pipe due to hydrostatic pressure or build-up of gases in the annulus. However, steel carcasses are susceptible to corruptions by existing electrolytes within crude oil. Therefore, protective coatings as liners are mainly applied to prevent carcass from the corrosion.

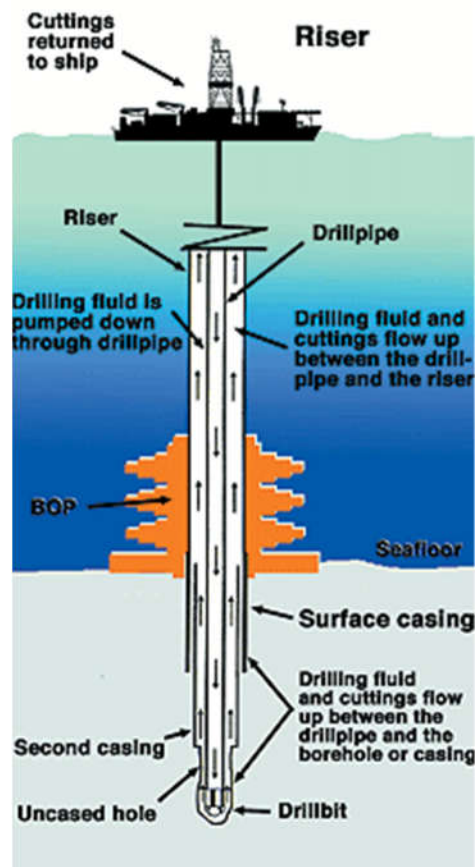


Figure 2.5 Function of drilling riser is to transport crude oil to topside system [81].

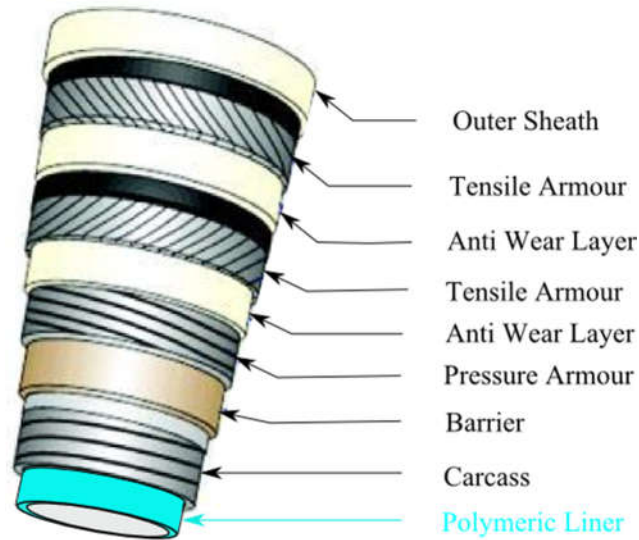


Figure 2.6 Components of a riser with liner as the innermost layer [82], polymeric liner as the innermost layer was coated on the surface of carcass for anticorrosion.

Although polymeric composite coatings are widely applied in anticorrosion field of steel materials, they are susceptible to damages in the form of erosion by asperities including sands and cutting marbles. The interaction between asperities and polymeric composite coatings can be considered as a kind of tribological interactions.

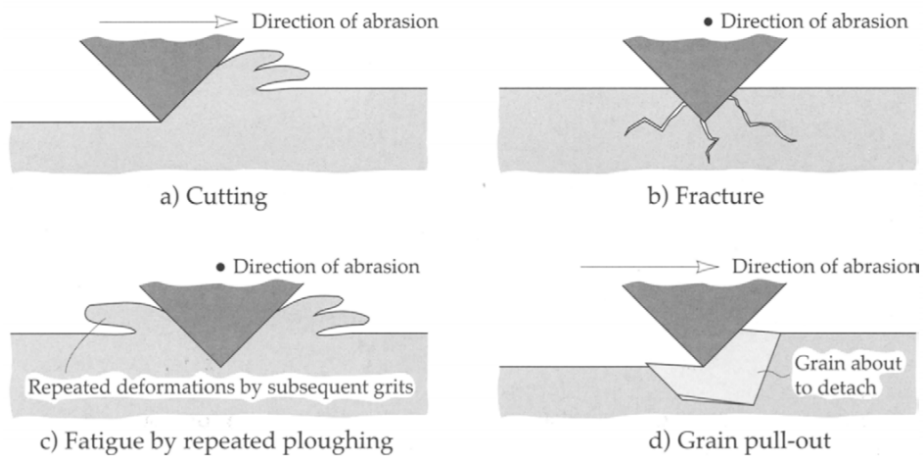


Figure 2.7 Different wear mechanisms correspond to different conditions [83].

Introduction of tribology

The tribological interactions with solid wear out polymeric liners from the surface. Major types of wear include friction (adhesion and cohesion), erosion, corrosion and abrasion. Friction phenomenon contains adhesion and cohesion which mean the dissimilar or similar surface tend to cling to each other. Erosion results in wear of surface by exogenic forces including solid or liquid particles to remove the material from the surface. Corrosion means that the metal materials are destructed gradually by reacting chemically with surrounding environments. Abrasion is produced when a rough, hard surface slides across a surface that is relatively softer.

Four types of mechanisms causing abrasive wear include cutting, fracture, fatigues by repeated ploughing and grain pull-out, as shown in Figure 2.7. Cutting is the most popular model where a sharp grit or hard asperity cuts the softer surface. Fracture happens when grits move continuously across the surface of materials, subsequently the produced cracks accumulate gradually and cause the release of large quantity of materials. Fatigue was formed because grits can deform repeatedly the surface of a material resulting in metal fatigue. Grain pull-out phenomenon is commonly happens in ceramic materials.

During the service life, coatings as the protective layer of steel substrates were susceptible to repeated attacks from sands and marbles within sea water and crude oil. In order to retard the damages, both solid and liquid lubricants were embedded successfully into polymeric matrix to reduce friction coefficient. Solid lubricants can form a layer of transfer film with low shear strength at the contact interface to reduce the friction coefficient [84], which can also reduce the friction heat resulting in less thermal softening of polymer matrix. Common solid lubricant fillers in polymeric matrix include PTFE, MoS₂, and graphite. Normally, PTFE was the most effective

in decreasing wear rate and it can decrease wear rate of most polymers [85]. In addition, graphite was more effective than MoS₂ in reducing polymer wear rate [86].

Besides solid lubricants, liquid lubricants can also be used to retard the wear of polymeric materials. The lubricating performance depends greatly on the compatibility between liquid lubricants and polymeric matrix [87]. However, liquid lubricants was not applicable to oil-sensitive and oil-contamination-free materials, while encapsulating liquid lubricant within solid shells can settle efficiently this problem. Microcapsules containing liquid lubricants were dispersed successfully within polymeric matrix as self-lubricating materials, which release liquid lubricant from broken microcapsules during friction process. Guo *et al.* [88] incorporates microcapsules containing lubricant oil into epoxy composites achieving ultra-low friction coefficient. Khun *et al.* [4, 5] prepared successfully self-lubricating materials by embedding encapsulated liquid wax in silicone and encapsulated HDI in epoxy resin, obtaining interesting effects. Final tribological performance of microcapsules-based self-lubricating materials was improved obviously under higher core fraction and larger microcapsules sizes.

However, penetrating damages of coatings still exist and result in the re-exposure of steel panels in moist environments. Herein, self-healing microcapsules was intended to be incorporated into protective coating for the re-storage of barrier function after being damaged.

2.2 Microcapsules based smart protective coatings

As the outmost layer of marine and offshore infrastructures, polymeric coatings have to face many attacks from surrounding environments including chemical, water and mechanical damages. Especially, polymer coatings are susceptible to scratched damages by marbles or sands from marine environments due to weak mechanical strength, resulting in the re-exposure of steel

substrates in corrosive environments and great economic loss. Additionally, the corroded marine and offshore structures brought potential safety hazard during service life. However, the damages in marine and offshore infrastructures are hard to detect and manual repair costs a lot. In order to solve this problem, reactive agents based microcapsules are embedded into protective coatings to retard the corrosion of marine and offshore structures when damages occur. This method was an efficient route to extend service life and reduce maintenance cost.

2.2.1 Anticorrosion mechanisms

Self-healing anticorrosion coatings containing microcapsules can perform self-healing function automatically without external intervention. The healing mechanism was schematically shown in Figure 2.8.

When scratched damages are initiated within coatings, the approaching cracks can rupture embedded microcapsules, and healing agents were then released automatically from broken microcapsules in damaged area through capillary forces. After cure of healing agents, the barrier function of coatings was recovered, and the corrosion of metal substrates at damaged area was retarded efficiently [2].

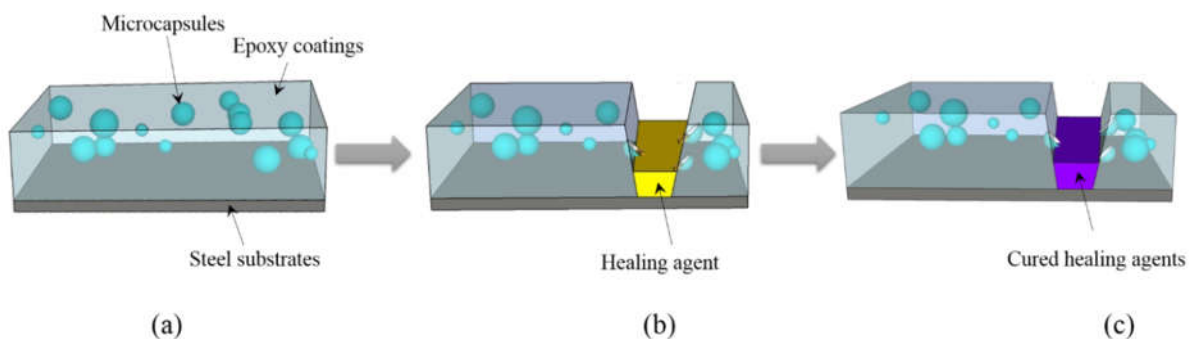


Figure 2.8 Anticorrosion mechanism of microcapsules-based self-healing coatings.

Table 2.1 Mechanism based on different anticorrosion agents

Self-healing system	Mechanisms
Isocyanate	Isocyanates can react with atmospheric moisture with the production of polyurea film [2].
Organic siloxane	Organic siloxane with hydroxyl or vinyl groups can polymerize into hydrophobic film via polycondensation and polyaddition reaction.
Linseed oil	Linseed oil [89] or tung oil [90] can achieve anticorrosion function by react with aerial oxygen with the formation of a layer of polymer film.
Corrosion inhibitors	Corrosion inhibitors like 8-hydroxyquinoline [91] or benzotriazole [54] tend to initiate additional passivation on metal substrates surface with the formation of dense film to retard the transportation of electrolytes.
Rare earth metal salts	The rare earth metal salts can retard corrosion of metal substrates by stifling cathodic oxygen reduction [39].
Anionic clays	Harmful chlorides can be absorbed and inhibiting ions are released to retard corrosion [92, 93].

Different agents perform anticorrosion function based on different mechanisms. Until now, many anticorrosion agents were encapsulated successfully and applied in anticorrosion coatings. The detailed information is discussed as following in Table 2.1.

Isocyanates as healing agent

Isocyanates as a kind of ideal one-component healing agent are encapsulated successfully and applied to self-healing anticorrosion coatings. The self-healing performance of isocyanates is

based on its reaction with atmospheric moisture or tetrathiol [94]. Yang *et al.* [1] successfully encapsulated isophorone diisocyanate (IPDI) within polyurethane shell via interfacial reaction between polyurethane prepolymer and 1, 4-butanediol and optimized process parameters for the first time, while without demonstrating self-healing performance in polymeric coating. Subsequently, Huang *et al.* [2] encapsulated more reactive HDI within polyurethane shell through interfacial polymerization method. After being incorporated into epoxy coating, the encapsulated HDI showed superior self-healing capability towards scratched coatings and anticorrosion performance towards steel panels under accelerated corrosion process in salt aqueous solutions [2] and even under erosion conditions [3]. Subsequently, various isocyanates were encapsulated and showed satisfying anticorrosion performance. IPDI was loaded within multi-layered shell via Pickering emulsions method and achieved outstanding anticorrosion performance. Besides isocyanates monomers, UV-curable polyurethane prepolymer was also encapsulated for anticorrosion applications [95]. Most of the microcapsules containing isocyanates are mainly applied to anticorrosion coatings due to their high reactivity to environmental moisture.

Siloxane as healing agent

Until now, three types of siloxanes were applied to build self-healing system based on different mechanisms. The first mechanism is polycondensation polymerization between an alkoxy end-capped siloxane prepolymer and a hydroxyl end-capped cross-linker under the action of catalyst (dilauryldibutyltin) [77, 96]. However, low healing efficiency was presented in epoxy matrix due to the mismatch of healing agent with host matrix. The second mechanism is the polyaddition reaction between hydrosilylation and vinyl-functionalized siloxane [97], and it displayed excellent healing performance to elastomeric poly(dimethylsiloxane). The third

mechanisms is to apply the reaction between hydrolysable organic silane and water [98], and it showed superior anticorrosion performance in scratched smart coatings towards steel substrates. In addition, CA-PDMS was also encapsulated as healing agent to achieve repeatable self-healing performance [99], where coating scratches were healed by photo-irradiated polymerization of released healing agent.

Linseed oil as healing agent

Linseed oil can polymerize with aerial oxygen with the formation of dense polymer film to heal scratches in self-healing anticorrosion coatings [89, 100]. Suryanarayana *et al.* [78] encapsulated linseed oil within PUF shells and applied successfully them in self-healing anticorrosion coatings. In order to improve the drying rate of linseed oil, tung oil containing more unsaturated glycerides of long chain fatty acids was encapsulated, and showed outstanding anticorrosion performance in in short term [90, 101]. However, short shelf life of linseed oil in open air is still a long term challenge.

Corrosion inhibitors

Corrosion inhibitors are a kind of N-heterocyclic compounds, which can react with metal surface with the formation of passivation layer to prevent the contact between metal and corrosive environments. The typical corrosion inhibitors including quinolone [91], pyrimidine [102], triazole [103], oxadiazole [104], pyrazole [105], and benzimidazole [106] have been applied successfully to polymeric coatings for anticorrosion of steel substrates. However, the direct addition of corrosion inhibitors in coatings influence in a negative way on coatings barrier property and anticorrosion efficiency of inhibitors. Encapsulating corrosion inhibitors in micro- or nano- containers can solve efficiently this problem. Various encapsulation techniques were used to load corrosion inhibitors. Benzotriazole [106-108] and NaVO_3 [109] have been

successfully loaded in hollow nanoparticles. However, low core fraction is an unavoidable issue, and restricts practical anticorrosion performance. In order to increase core fractions, new encapsulation techniques were developed. Koh *et al* [110] encapsulated successful isosorbide derivatives through interfacial polymerization between dimer ester diisocyanate and 1, 4-butanediol. The typical core fractions of resultant microcapsules was around 40-45 wt%. By modifying reaction conditions, the core fractions of encapsulated corrosion inhibitors can be improved to 67 wt% [110]. The influence of experiments conditions on morphologies, structures, and thermal properties of microcapsules was also investigated systematically [111]. Besides, in situ polymerization techniques were also applied to load hydrophobic corrosion inhibitors, and presented superior anticorrosion performance in PU coatings [112]. However, the existence of N-heterocyclic structure within corrosion inhibitors tends to retard the reaction of in situ polymerization resulting in poor qualities of resultant microcapsules.

Rare earth metal salts

The alkaline earth cations (Ca^{2+} , Mg^{2+} , Sr^{2+} , and Ba^{2+}) can inhibit the corrosion of steel surface by stifling cathodic oxygen reduction. When coatings containing alkaline cations were immersed in NaCl solutions, the alkaline earth cations can diffuse in underfilm by exchanging with Na^+ in surrounding environments, as shown in Figure 2.9B. In alkaline environments, the alkaline earth cations can hydrolyze partially with the formation of precipitation film covering metal substrates. The mentioned film can retard corrosion process by decreasing the electrical conductivity and ion mobility on metal surface, as shown in Figure 2.9C. The alkaline earth cations can dissolve in aqueous solutions resulting in difficult encapsulation in oil-in-water systems, and can only be encapsulated in ion-exchange clays.

Anionic ions

Special anions including $V_2O_7^{2-}$ [93] and MoO_4^{2-} [92] have been reported to possess anticorrosion functions, which were achieved through two ways. The anions in coatings can absorb harmful chloride in corrosive environments through ion exchange method, and release inhibiting ions on steel surfaces [93]. The anions are usually encapsulated in layered double hydroxide nanocontainers (LDH) through direct synthesis corrosion inhibitors or anion exchange in LDH precursor [113]. The resultant microcapsules presented obvious anticorrosion performance in water-based epoxy resin towards to aluminum alloy.

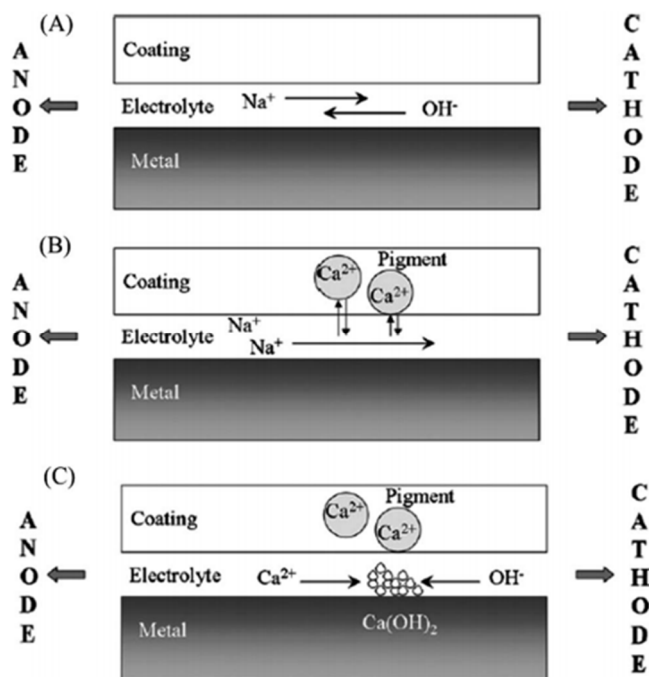


Figure 2.9 The anticorrosion process of cations corrosion inhibitors towards polymeric coatings [39].

Table 2.2 Encapsulation methods

Encapsulation method	Mechanisms

In situ polymerization	The particles produced from the reaction between urea and formaldehyde aggregate and deposit on droplets surface to form a layer of Urea-Formaldehyde shell [85].
Interfacial polymerization	Two reactants react at the oil/water interface to form a layer of polymer shell covering liquid core in an emulsion system [1].
Polyelectrolyte multilayers microcapsules	Polyelectrolytes can be covered on nanoparticles through layer-by-layer techniques [114].
Inorganic nanocapsules	The clays with hollow inner structure were applied to load inhibitors. Inhibitive ions can be loaded in ion-exchange clays through ion change method. Inhibitors can be loaded in hollow mesoporous silica nanoparticles, and then pH-responsive polymers were covered on particles as valves [115, 116] .

2.2.2 Microencapsulation methods

Anticorrosion agents can be encapsulated through various methods, as shown in Table 2.2.

In situ polymerization

In situ encapsulation method applies poly(urea-formaldehyde) resin or poly(melamine-formaldehyde) as shell to encapsulate healing agents. Hitherto, this method has become one of the most versatile methods in self-healing field. In situ encapsulation method was firstly published by S.R. White [85, 117], who encapsulated DCPD within PUF shell for the first time. During the normal preparation process, the hydrophobic healing agents need to be emulsified into finer liquid droplets in surfactant aqueous solution containing reactants under mechanical agitation first. Subsequently, formaldehyde aqueous solution was added into emulsion system followed by the adjustment of system pH value. Then, the system temperature was raised and

sustained for certain duration to complete the encapsulation process. During the encapsulation process, newly formed PUF particles can deposit gradually on the surface of liquid droplet with the formation of PUF shell. Some new method applied prepolymer of UF resin to encapsulate oil droplets increasing shell thickness from several nanometers [85] to several microns [118].

The diameters of microcapsules are influenced significantly by the agitation rate and surfactant concentration, and faster agitation rate and higher surfactant concentration corresponds to smaller microcapsules. Ultrasonic dispersion techniques can emulsify oil phase into nanometer-sized micro-droplets [119]. The thickness of PUF shells is at the level of several hundred nanometers. This approach has been successfully used to encapsulate DCPD [85], epoxy [120], liquid metal [121], tetrathiol [94], linseed oil [78] and HDI [8]. However, poor robustness and weak mechanical strength of PUF microcapsules restrict their practical applications. The robustness of PUF shells can be improved by hybridization, increasing shell thickness and boosting cross-link density. Fan and Zhou [122] improve barrier property of PUF shells by introducing layered silicates. The acid-modified montmorillonite (H-MMT) was dispersed uniformly in aqueous solution, and then co-deposit with PUF particles on droplets surface with the formation of hybrid shells. Wang *et al.* [123] applied oxygen plasma treated carbon nanotubes to improve microcapsules mechanical behavior. Similar with H-MMT, oxygen plasma treated carbon nanotubes can also be embedded in PUF shell. Caruso *et al.* [124] improved shell thickness of PUF microcapsules by introducing polyurethane prepolymer in oil phase. Urea can react with polyurethane prepolymer resulting in the thickening of resultant shells. In order to prepare highly cross-linked shell structure, Wu *et al.* [8] used urea-formaldehyde prepolymer as reactants to encapsulate various core materials. In addition, Ling *et al.* [125] applied melamine to improve shell crosslink density for the encapsulation of evaporable glycidyl methacrylate.

Besides structure of microcapsules shell, the weak interface interaction between shell surface and host matrix was another issue, which can be improved by processing microcapsules surface with couple agent [126]. Although various methods were successfully applied to improve PUF shells, the resultant shells still cannot fulfill the practical requirements.

Interfacial polymerization

Interfacial polymerization is another popular encapsulation method in self-healing field, and it can produce a layer of membrane which thickens over time at the interface between water and oil droplets. In regular preparation process, the first step is to emulsify the mixture of healing agents and reactants into micro-droplets. Subsequently, the water soluble cross-linkers are introduced into water phase to react with the oil phase at the interface with the formation of resultant shells.

Typical shell material is made of polyurethane (or polyurea), which is produced from the polymerization between isocyanates and diol (or amine) [1]. Besides Gum Arabic, other surfactants [77, 127] are also be utilized as emulsion stabilizers. One advantage of interfacial encapsulation method is that it can yield shells with controllable thickness by adjusting reaction time and reactants concentrations. Besides polyurethane or polyurea, epoxy shells can also be produced from interfacial polymerization [128].

Various healing agents including IPDI [1], IPDI trimer [129], HDI [2], catalyst [77], corrosion inhibitor [130], isosorbide derivatives [110], triazole derivative [131] and linseed oil [132] have been encapsulated successfully through interfacial polymerization. However, traditional polyurethane or polyurea shells cannot satisfy practical requirements. Therefore, various techniques were applied to improve the shell properties. Tugba *et al.* [132] prepared UV-triggered released microcapsules by implanting photolabile functional groups in the shell.

McFarland *et al.* [133] studied the influence of amine functionalities on shells morphology and density. Tatiya *et al.* [134] used dendritic functional monomers to improve microcapsules thermal stability by increasing shell cross-link density. Hedao *et al.* [129] used isocyanates trimmer to fabricate microcapsules with more dense shell structure. Inorganic fillers can also be embedded in organic shells to improve shell robustness. Hickey *et al.* [135] deposited clay on the surface of polyurea microcapsules through layer-by-layer techniques. Wu *et al.* [136] improve the stability of encapsulated HDI in organic solvents by embedding silica nanoparticles in polyurethane shells. Besides, inorganic fillers can also be introduced into shells through Pickering emulsion method [9]. Multi-layered shell structure can also be applied to improve the stability of microcapsules in organic solvents. Sun *et al.* [7] prepared double-layered polyurea shells with great stability in medium- and non-polar organic solvents. Kang *et al.* [137] coated a layer of polydopamine to improve the stability of microcapsules in organic solvents. Sun *et al.* [7] applied polyurea shells to improve the stability of encapsulated isocyanates in ambient water. Interfacial encapsulation method can fabricate shells with tunable thickness to fulfill practical requirements, and possess great potential in practical applications.

Polyelectrolyte multilayers microcapsules

Polyelectrolytes were usually covered on inhibitor particles by layer-by-layer technique to prepare microcapsules, providing controlled release of inhibitor in anticorrosion coatings. The microcapsules properties were influenced significantly by shell thickness, which is controlled by the deposition cycles and the types of polyelectrolytes. By adjusting the pH values, the inhibitors can be released in a controlled way to the damaged area of host coatings [114].

Hollow inorganic particles

Besides encapsulated in polymeric shells, corrosion inhibitors can also be loaded in inorganic shells. The hollow halloysite and hydroxyapatite are able to load corrosion inhibitors. Snihirova *et al* [115] used hydroxyapatite microparticles to load corrosion inhibitors, which can be released on demand. In addition, hollow halloysite can also be applied to store corrosion inhibitors [116]. However, the low loading efficiency (below 10 wt%) still restrict the practical application of resultant microcapsules in anticorrosion field.

Mesoporous nanoparticles can also be used to load corrosion inhibitors due to good biocompatibility and excellent stability. Mercaptobenzothiazole have been successfully encapsulated in silica nanoparticles, and applied to retard corrosion of aluminum alloy [138]. The concentration of silica nanoparticles in coatings influences significantly anticorrosion performance. Higher concentration tends to deteriorate the coating integrity, while lower concentration results in the low contents of corrosion inhibitors. In order to develop stimuli-and-response system, nanovalves were applied to adjust the structure of silica nanoparticles [139, 140].

Ion clays are usually applied to load cations and anions corrosion inhibitors. Zeolites and bentonite clay minerals as containers attract numerous attentions and are studied widely. Williams *et al* [141] loaded corrosion inhibitors in bentonite capsules, and presented outstanding anticorrosion performance in organic coatings. Besides, layered double hydroxide nanocontainers were also investigated numerously. The anion inhibitors ($\text{V}_2\text{O}_7^{2-}$, MoO_4^{2-}) are usually stored in the metal hydroxide layers, and can be delivered automatically to the damage area through ions exchanges. Zn/Al and Mg/Al based layered structure containing vanadate have been fabricated successfully [113]. However, layered metal hydroxide containing corrosion

inhibitors still miss effective anticorrosion performances compared with traditional chromated-based pigments.

Thus far, various types of agents have been successfully encapsulated for self-healing function. Isocyanate is a kind of water-reactive chemical, which can polymerize with moisture into dense polyurea film, and thus were widely applied in one-component self-healing anticorrosion coatings. Yang *et al.* [1] firstly encapsulated successfully IPDI through interfacial polymerization. However, efficient anticorrosion performance towards steel substrates was not presented.

Subsequently, Huang *et al.* [2] encased successfully more reactive HDI within polyurethane shells, and displayed excellent anticorrosion performance towards steel panels in epoxy coatings. However, the resultant microcapsules showed poor stability in organic solvents, water, and weak shell strength, restricting their practical application in anticorrosion coatings [6]. In order to improve the stability of encapsulated isocyanates in organic solvents, Wu *et al.* incorporated silica nano-particles into polyurea shell [136] and applied highly cross-linked urea-formaldehyde resin to encapsulate HDI [8], showing outstanding stability in organic solvents with medium and low polarities. Sun *et al.* [7] applied double-layered polyurea shell to load HDI and significant improvement of microcapsules stability in medium and non-polar organic solvents was observed. Besides the stability in organic solvents, improving stability of encapsulated isocyanate in water also attracts numerous attentions. Yi *et al.* [9] introduce nanoparticles within shells to improve efficiently the stability of encapsulated isocyanates in water. Besides, the inorganic components as an isolated shell layer can be applied to improve the stability of encapsulated isocyanates in water [142]. The core fractions of resultant microcapsules dropped around 9.7 wt% after 4 days in ambient water or two weeks exposure in open air. Nguyen *et al.* [143] used fluorinated

aromatic amine to boost the stability of encapsulated isocyanates in water, where the core fraction of resultant microcapsules remains constant after 1 day in ambient water. In addition, improving shell mechanical strength of encapsulated isocyanates also attracts increasing attentions. Patchan *et al.* [144] coated a layer of metals shell with thickness of 2 μm covering encapsulated isocyanate. However, related properties test of metal shell microcapsules was not demonstrated. Although so many investigations tried to improve the shell properties of encapsulated isocyanate, the resultant microcapsules still cannot satisfy the practical requirements of isocyanates-based one component self-healing anticorrosion coatings.

2.3 Current issues

Microcapsule-based smart materials have been attracted great attention attributed to the versatile approaches to synthesize functional and multifunctional microcapsules. However, during processing and service of microcapsule-based materials in engineering applications, a number of harsh environmental factors have to be considered. In the processing stage, microcapsules are normally needed to mix or pre-mix with polymeric resins, which always contain water and/or organic solvents to assist easy processing. In the curing stage of resin, exothermal reaction commonly occurs with quite high localized temperature. After finishing, the composite products will be applied in the environment where erosion or scratch may exist. The resultant microcapsules have to successfully survive in those conditions for feasible applications. In addition, traditional microcapsules always compromise the final mechanical property of the samples [160] due to their low overall-stiffness resulted by liquid core. Therefore, a number of approaches are needed to modify and improve the microcapsule's resistances to water, solvents and heat, and enhance the mechanical strength for mixing process and integrity of the final products.

Increasing attentions were paid on one-component self-healing anticorrosion coatings containing isocyanates-based microcapsules due to the rapid reaction of isocyanates with environmental water. However, during service of microcapsules in anticorrosion coating applications, the humid environments have to be considered. In the service stage, anticorrosion coatings are needed to be exposed in humid environments, where the massive water exists. The isocyanates-based microcapsules have to successfully survive in the moist environments for feasible anticorrosion applications. However, traditional microcapsules containing isocyanates lose all liquid core within several days resulted by the permeability of shells [6]. Although many approaches are applied to improve the stability of microcapsules containing isocyanates in water [9, 143], the resultant microcapsules can still survive in water less than 5 days. Therefore, new approaches are still needed to improve the long-term stability microcapsules containing isocyanates in water.

Improving stability of isocyanates-based microcapsules in water was paid numerous attentions due to superior survivability in humid environments. However, during processing of microcapsules in anticorrosion coating applications, the stability of microcapsules in organic solvents and thermal environments has to be considered. In the processing stage, microcapsules are usually needed to mix with polymeric resin, which always contains organic solvents for easy operations. Besides, during resin curing process, the exothermal reaction occurs with quite high localized temperature. The isocyanates-based microcapsules are required to successfully remain activity in organic solvents and high temperature. Although some investigations tried to boost the stability of microcapsules [7, 8, 136] in organic solvents, the water resistant microcapsules still cannot survive in organic solvents and thermal environments. Introducing solvents and thermal resistant functions to water resistant microcapsules to prepare double resistant microcapsules need to be investigated.

There is big room for enhancing the mechanical strength of core-shelled microcapsules for certain applications. During the service in anticorrosion applications, coatings are susceptible to physical attacks. However, the traditional microcapsules always compromise the coatings strength due to low overall-stiffness resulted by liquid core. The shell strength of isocyanates-based microcapsules has to be enhanced to resist physical attacks. Although a number of approaches are applied to improve the shell strength of microcapsules [123, 144], the results were still unsatisfactory. Plating a layer of metal shell covering microcapsules was probably an efficient method.

Chapter 3 Experiments

3.1 Materials

4,4'-diphenylmethane diisocyanate (MDI) prepolymer Suprasec 2644 was obtained from Huntsman. 4,4'-methylenebis(cyclohexyl isocyanate) (HMDI), gum Arabic, ethylene maleic anhydride (EMA), ammonium chloride (NH_4Cl), tetraethylenepentamine (TEPA), hexane, xylene, ethyl acetate, acetone, ethanol, hydrochloric acid solution (HCl , 0.1 M), potassium bromide (KBr), sodium hydroxide (NaOH), sodium chloride (NaCl), palladium chloride, stannous chloride, Nickel sulfate, sodium hypophosphite monohydrate, sodium acetate, malic acid, lactic acid, thiourea, Tergitol (NP-9) and triethanolamine were purchased from Sigma-Aldrich. Epolam 5015 and hardener 5014 used as epoxy coating were supplied by Axson. All chemicals in this study were used as received without further purification.

3.2 Synthesis of microcapsules

3.2.1 Synthesis of water resistant microcapsules

The water resistant microcapsules containing HMDI as core materials were synthesized by combining interfacial and in situ polymerization. Interfacial polymerization was first applied to prepare the inner-layered polyurea shell of microcapsules, which are then coated by outer-layered PUF shell with linear structure via in situ polymerization.

The inner-layered polyurea shells were prepared via interfacial polymerization in an oil-in-water emulsion system. Firstly, the water phase, 30 ml of deionized (DI) water containing 2.5 wt% of gum Arabic was heated up to 30 °C in a 250 ml beaker, which was placed in a temperature controlled water bath located on a programmable hotplate.

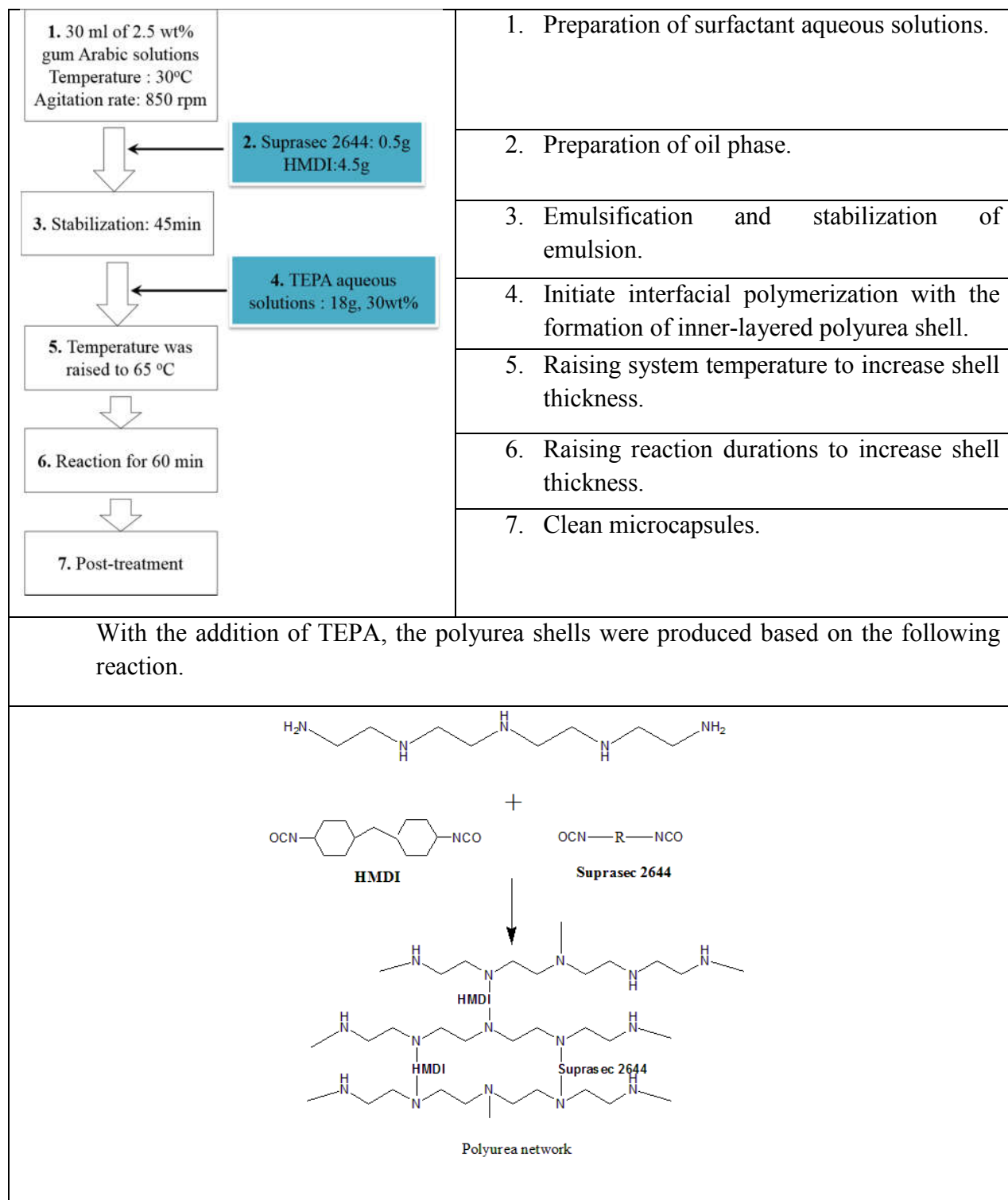


Figure 3.1 The first step of preparing water resistant microcapsules applied the reaction between amine and isocyanates. The rapid reaction between amino functional groups and NCO functional groups can produce dense polyurea shells [10].

Later, the uniform oil phase containing 0.5 g of Suprasec 2644 and 4.5 g of HMDI was emulsified into micro-droplets in the surfactant aqueous solution under certain agitation rate (Caframo, model: BDC6015). After emulsion system was stabilized for 45 min at 30 °C, 18.0 g of TEPA aqueous solution (30 wt%) was added to initiate the interfacial polymerization. Meantime, the system temperature was raised to 65 °C. After reaction for 30 min at the designated temperature, the obtained suspension of microcapsule slurry was rinsed with DI water for 3-4 times as microcapsules with inner-layered polyurea. The specific preparation process was shown in Figure 3.1.

The preparation of outer-layer PUF shells coated inner-layered polyurea shells was demonstrated as following. 2.00 g urea, 0.50 g ammonium chloride and 0.50 g resorcinol were firstly dissolved in 60 ml DI water in a 250 ml beaker under agitation rate of 200 RPM. Afterwards, the pH value of the solution was adjusted to approximate 3.50 using NaOH and HCl solutions. After stabilization at 55 °C, microcapsules with inner-layered polyurea shells were introduced in systems. With the addition of 4.5 ml of formaldehyde solution (37 wt%), the polymerization of PUF resin started. After reaction for 20 min, the microcapsules suspension was rinsed and washed with DI water for 3 times before air dried for 12 h. The typical preparation process was shown in Figure 3.2.

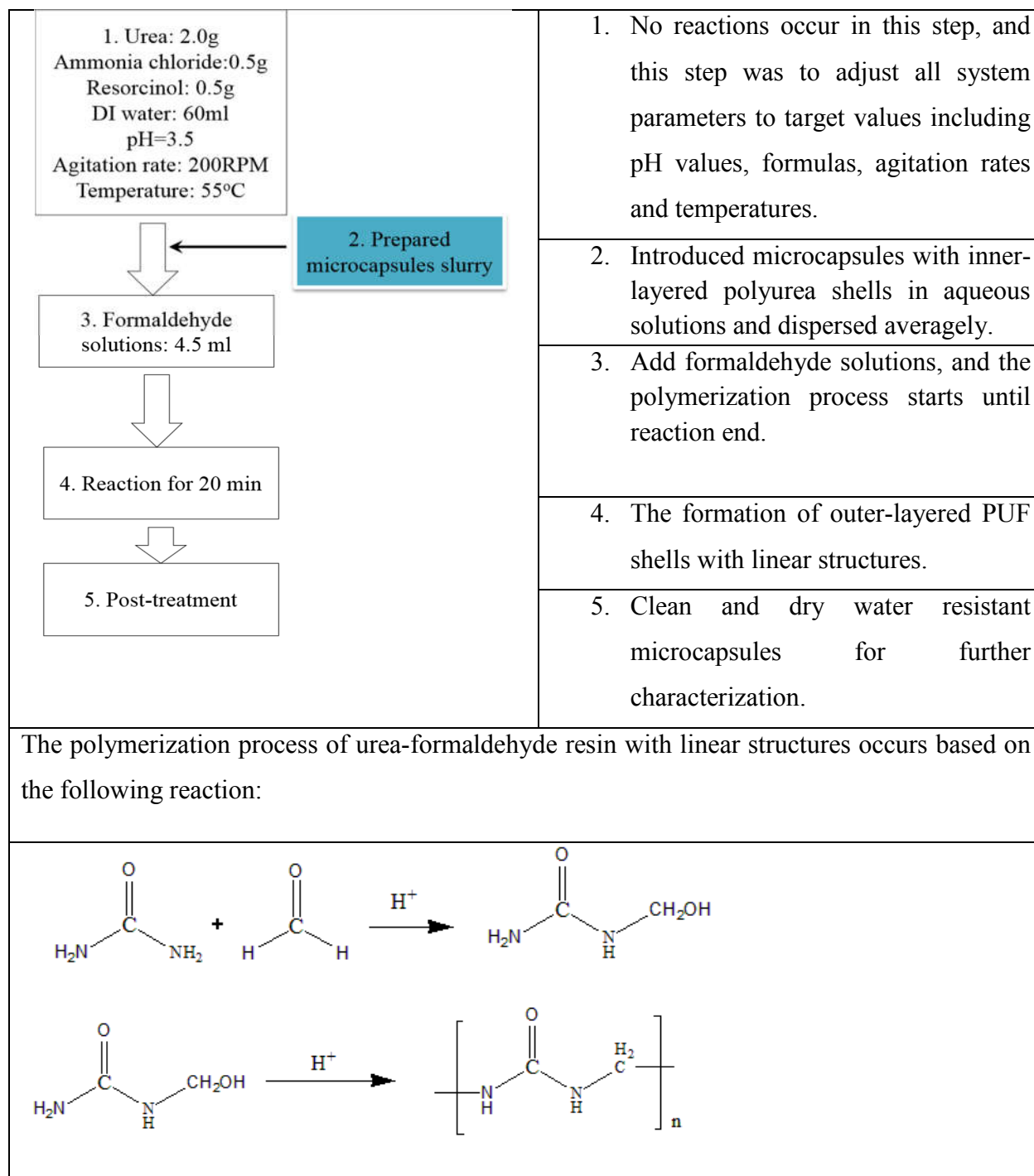


Figure 3.2 The second step of preparing water resistant microcapsules applied the rapid formation of PUF resins in acidic environments [146].

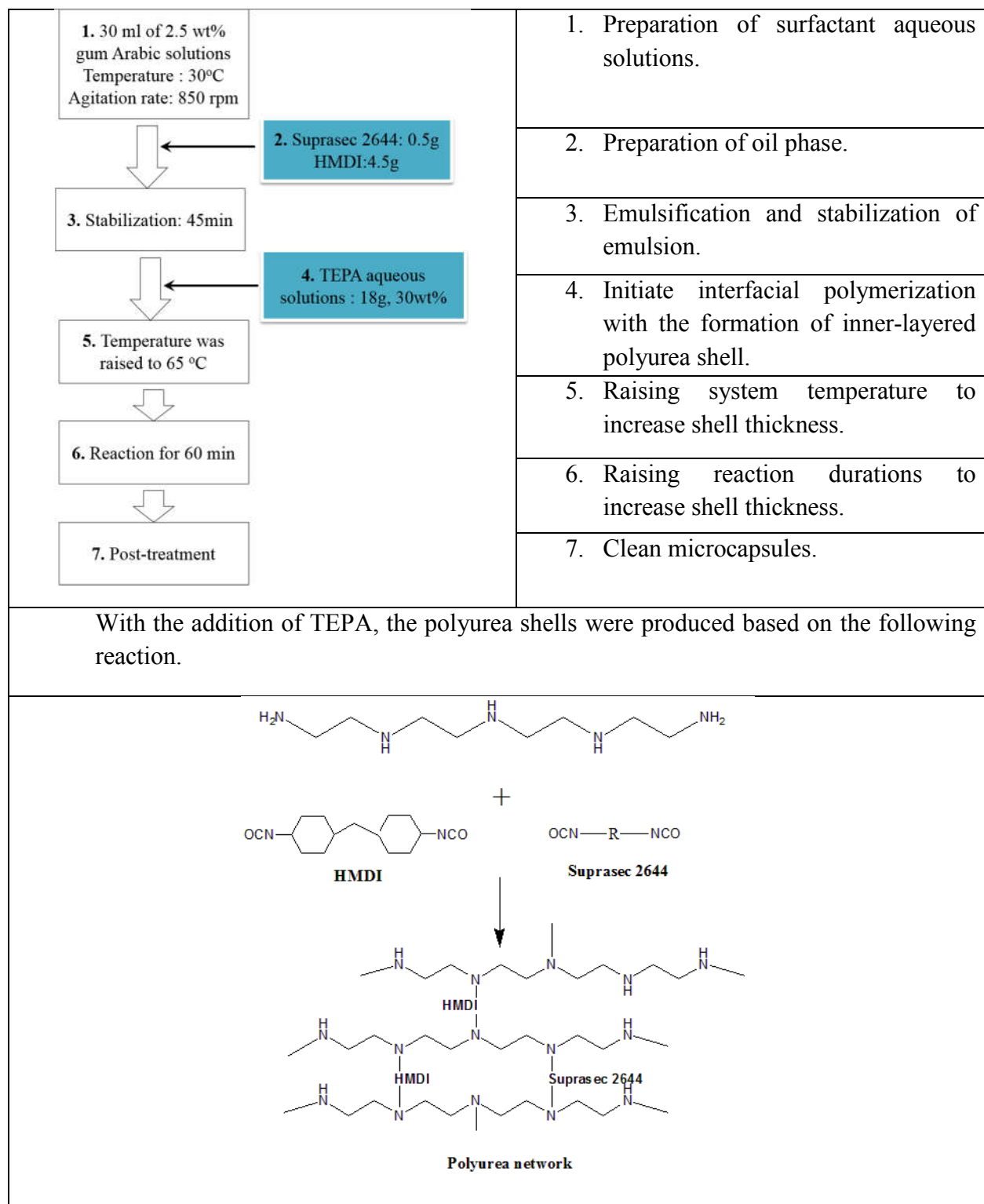


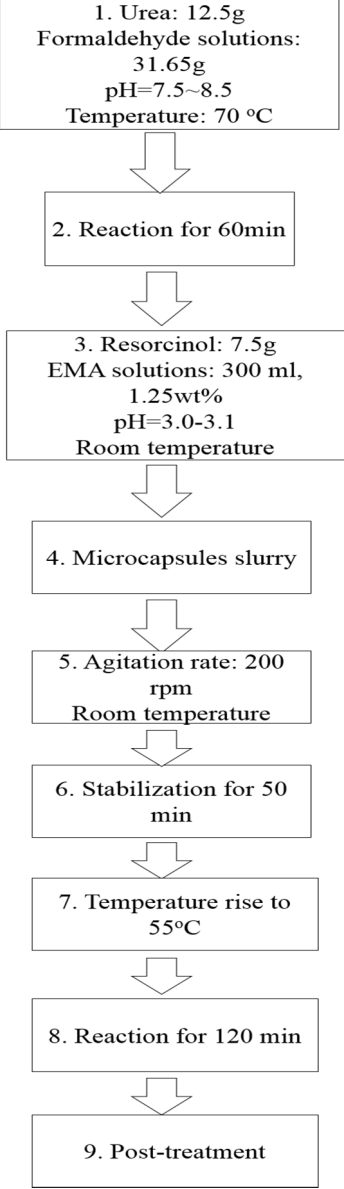
Figure 3.3 The first step to prepare double resistant microcapsules is the same with the first step of preparing water resistant microcapsules.

3.2.2 Synthesis of double-resistant microcapsules

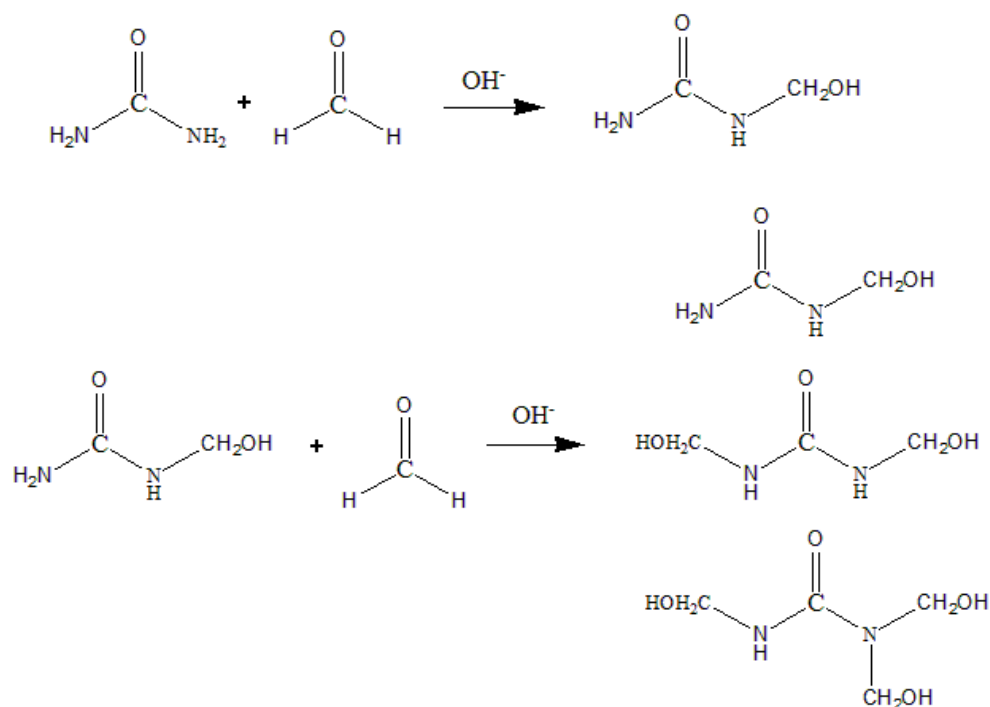
The synthesis of double-resistant microcapsules was divided into two steps. The first step is to prepare microcapsules with inner-layered polyurea shells, and it possesses the same procedure with the first step of preparing water resistant microcapsules, as shown in Figure 3.3. The second step is to cover outer-layered PUF shells with highly crosslinked structure on microcapsules with inner-layered polyurea shells. Herein, the reaction system was enlarged 5 times.

The preparation process of microcapsules with inner-layered polyurea shells was demonstrated in 3.2.1 and the diagram of preparation process was shown in Figure 3.3 without detailed demonstration. The second step of preparation of PUF shells with highly crosslinked structure was shown as following.

Urea-formaldehyde prepolymer was firstly synthesized by polymerizing 31.65g of formaldehyde aqueous solutions (37 wt%) with 12.5g of urea at pH value of 7.5~8.5 and temperature of 70 °C for 1h. Then the urea-formaldehyde prepolymer and 7.5g of resorcinol were dissolved in 300 ml of EMA aqueous solutions (1.25 wt%) as prepolymer aqueous solutions. Subsequently, the slurry of microcapsules with inner-layered polyurea shells was introduced in prepolymer aqueous solutions and the pH value of solutions was adjusted to 3.0. The mixture was then allowed to stabilize for 50 min at room temperature followed by elevating temperature to 55 °C. After 2h, the final slurry was rinsed with DI water for several times, and then air dried 12h for future characterization. The typical preparation procedure was shown in Figure 3.4.

 <pre> graph TD A["1. Urea: 12.5g Formaldehyde solutions: 31.65g pH=7.5~8.5 Temperature: 70 °C"] --> B["2. Reaction for 60min"] B --> C["3. Resorcinol: 7.5g EMA solutions: 300 ml, 1.25wt% pH=3.0-3.1 Room temperature"] C --> D["4. Microcapsules slurry"] D --> E["5. Agitation rate: 200 rpm Room temperature"] E --> F["6. Stabilization for 50 min"] F --> G["7. Temperature rise to 55°C"] G --> H["8. Reaction for 120 min"] H --> I["9. Post-treatment"] </pre>	<p>1 and 2: Preparation of Urea-formaldehyde prepolymer in alkaline environments.</p> <p>3. Mixing the prepolymer of Urea-formaldehyde resin with resorcinol and surfactant solutions, adjust pH values to target values.</p> <p>4. Add microcapsules with inner-layered polyurea shell in the aqueous solution of resin prepolymer</p> <p>5 and 6: the PUF resin was produced gradually and covered on the outer surface of microcapsules with inner-layered polyurea shells.</p> <p>7 and 8: the system temperature was raised, and the crosslink density of PUF resin increased gradually.</p> <p>9. Microcapsules were cleaned for further characterization.</p>
--------------------------------------------------------------------------------------------------------------------------------------------------------------------------------------------------------------------------------------------------------------------------------------------------------------------------------------------------------------------------------------------------------------------------------------------------------------------------------------------------------------------------------------------------------------------------------------------------------------------------------------------------------------------	----------------------------------------------------------------------------------------------------------------------------------------------------------------------------------------------------------------------------------------------------------------------------------------------------------------------------------------------------------------------------------------------------------------------------------------------------------------------------------------------------------------------------------------------------------------------------------------------------------------------------------------------------------------------

Preparation of urea-formaldehyde resin prepolymer in alkaline environments



The preparation of highly crosslinked PUF resin in acidic environments

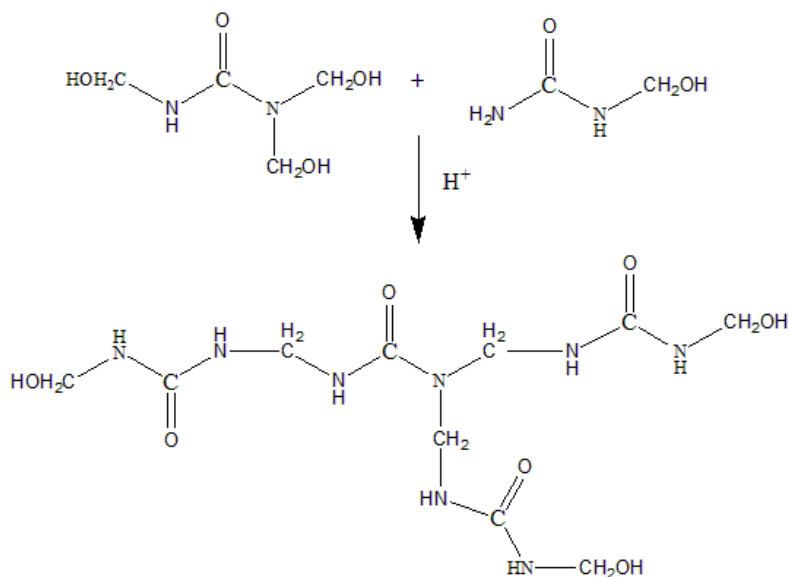


Figure 3.4 The second step of preparing double resistant microcapsules is to coat highly crosslinked PUF resin on microcapsules with inner-layered polyurea shells in acidic environments [147].

3.2.3 Synthesis of trifunctional microcapsules

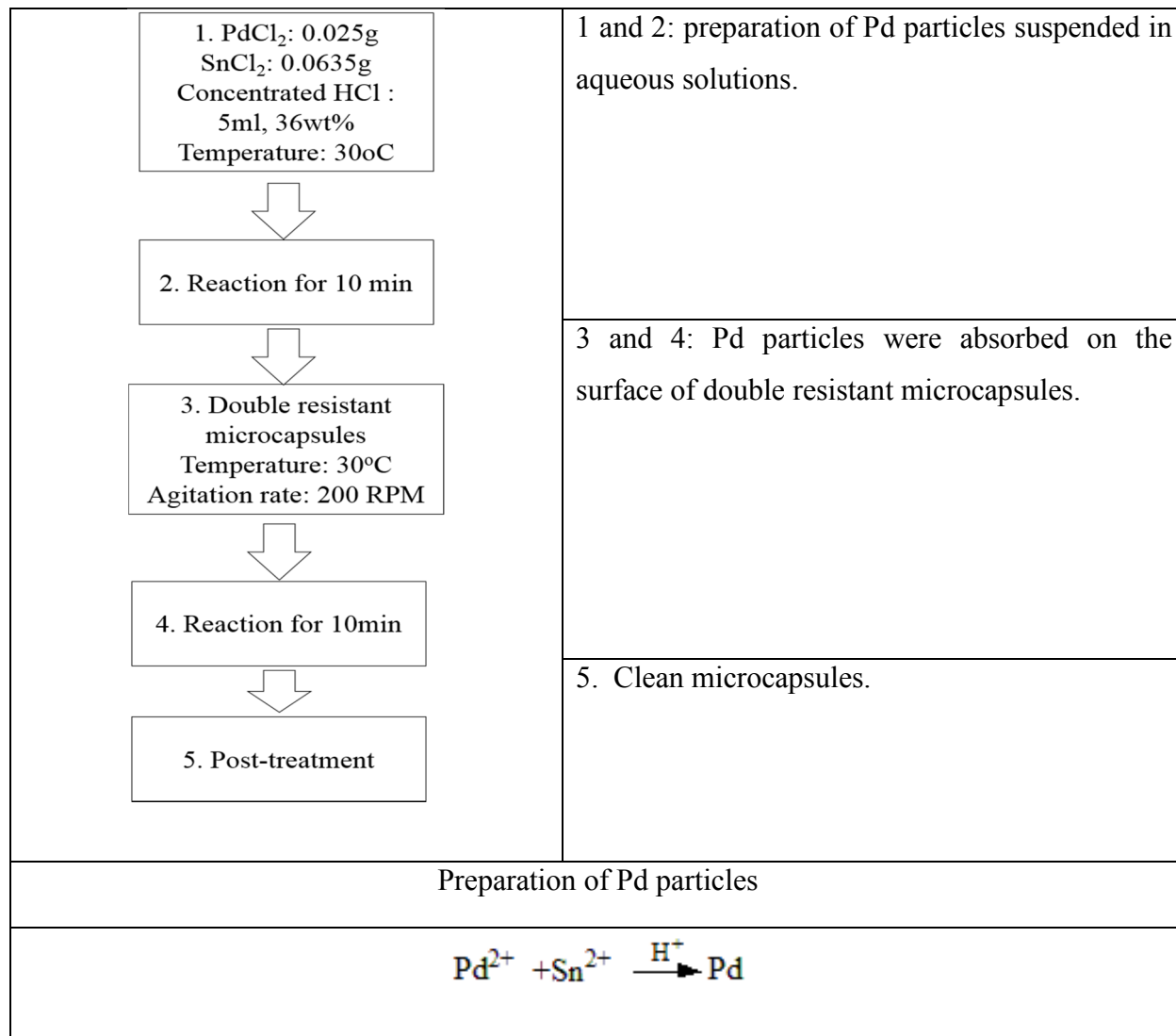


Figure 3.5 The preparation process of microcapsules with catalyst on the surface. The newly formed Pd particles were prepared by reducing Pd²⁺ with Sn²⁺.

The tri-functional microcapsules were synthesized by plating a layer of Nickel-P alloy covering double resistant microcapsules. The whole preparation process is divided into two steps. The first step is to deposit Palladium (Pd) particles as catalyst on the surface of double resistant microcapsules and the second step is to conduct chemical plating in plating solutions.

Firstly, the Pd particles were deposited on the surfaces of double resistant microcapsules. 0.025g of PdCl₂ was dissolved in 5 ml of concentrated HCl solution (36 wt%) in a 50 ml glass beaker, which was suspended in a water bath with temperature of 30 °C on a magnetic stirring apparatus. After complete dissolve of PdCl₂ in concentrated HCl solutions, 0.0635 g of SnCl₂ was introduced and allowed to react for 10 min with the formation of suspended Pd solutions, which was then added into double resistant microcapsules slurry at 30 °C under agitation rate of 200 RPM. After 10 min, the double resistant microcapsules with Pd on the surface were rinsed for several times for future plating process. The typical process was shown in Figure 3.5.

The second step was to plate a layer of Nickel-P alloy on the surface of double resistant microcapsules in plating solutions. Plating solutions were prepared by mixing uniformly 3.0g of nickel sulfate, 3.0g of sodium hypophosphite monohydrate, 2.0g of sodium acetate, 0.4g of malic acid, 2.0 ml of lactic acid, 1 droplet of Tergitol and 10 droplets of thiourea solutions (0.01g thiourea in 100 ml DI water). The pH value of plating solution was adjusted to 5.5 with triethanolamine, and then heated to 70 °C. Subsequently, microcapsules with catalyst were added into plating solutions and allowed to proceed for another 60 min. Finally, the microcapsules with metal shells were rinsed and washed for future characterization after air drying for 12 h. The formation process of Ni-P shell covering on the surface of double resistant microcapsules was shown as following:

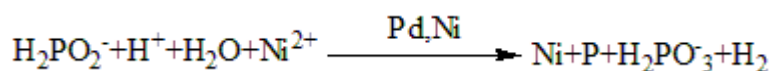


Figure 3.6 the formation progress of metal shell on the surface of double resistant microcapsules.

3.3 Characterization of microcapsules

The morphology, size and shell thickness of resultant microcapsules were observed through scanning electron microscope (FESEM, Joel, Model: JSM-7600F). The size distributions of the microcapsules were derived from the statistic of at least 150 individuals using ImageJ in SEM images. Microcapsules were mounted on conductive tape and some of them were ruptured with a razor blade to observe the core-shell structure.

Spectrophotometer (Varian 3100) was applied to obtain FTIR spectra curves of pure HMDI, Suprasec 2644, capsule core material, and organic capsule shells. Organic capsule shells can be obtained by flushing crushed microcapsules with acetone for several times, and the sedimentary shells within acetone can be used for FTIR test after dried. The range of applied spectrum was within 1000-4000 cm^{-1} . The composition of metal shells was determined through Energy Dispersive X-Ray Spectroscopy (EDX).

The core fraction of water resistant microcapsules was determined through TGA test. 10-20 mg of microcapsules were heated in nitrogen atmosphere at a rate of 10 $^{\circ}\text{C}/\text{min}$ from room temperature to 180 $^{\circ}\text{C}$ followed by 60 min of isothermal for complete evaporation of core material. Finally, the samples were heated to 600 $^{\circ}\text{C}$ for complete decomposition. The core fraction of capsules was derived by consideration of the weight loss of microcapsules and shell at 180 $^{\circ}\text{C}$. The calculation method was listed as following. The weight loss of core, shell and microcapsules from room temperature by 180 $^{\circ}\text{C}$ were defined as C_{core} , C_{shell} and $C_{microcapsules}$.

$$C_{shell} + C_{core} = C_{microcapsules} \quad (3.1)$$

$$\frac{C_{shell}}{1 - C_{core}} = 7.6\% \quad (3.2)$$

The core fractions of double resistant microcapsules and metal shell microcapsules were derived by titrating NCO contents of crushed microcapsules, and then converted into the weight of HMDI core, which possess stoichiometric relation with NCO functional groups. Certain amount of microcapsules were crushed firstly with two pieces of clean glass slides leaving released core materials and broken shell materials on the surface of glass slides, which are then flushed into a glass beaker with massive acetone. Subsequently, the NCO content within acetone solutions can be titrated according to ASTM D2572-97 and then converted into the weight of HMDI. The calculation method of HMDI was shown as following:

$$m_{(HMDI)} = 262.35 \times \frac{1}{2} \times n_{NCO} = 131.18 \times \frac{(V_{(blank)} - V) \times c_{(HCl)}}{2000} \quad (3.3)$$

$$Core\ fraction\ (wt\%) = \frac{m_{(HMDI)}}{m_{(microcapsules)}} \times 100\% \quad (3.4)$$

where $m_{(HMDI)}$ (g) is the weight of HMDI core. 262.35 is the equivalent weight of the HMDI. $V_{(blank)}$ (ml) and V (ml) are the volumes of the standard HCl (0.1M) aqueous solution consumed by the blank experiment and titration sample, respectively. $c_{(HCl)}$ is the normality of standard HCl (0.1 M) aqueous solution, core fraction (wt%) is the core fraction of microcapsules, and $m_{(microcapsules)}$ (g) are the masses of sample.

The thermal stability of final microcapsules was characterized by using TGA (Q500). 10-20 mg of microcapsules, shell materials, core materials and pure HMDI were heated from room temperature to 600 °C at a rate of 10 °Cmin⁻¹ within nitrogen atmosphere. The weight loss curves of samples were obtained as a function of temperature. The beginning decomposition temperature of samples was determined as the temperature when samples lose weight of 5 wt%.

3.4 Stability tests of microcapsules in water and organic solvents

The stability of resultant microcapsules in water and organic solvents was tested by immersing various types of microcapsules in different types of solvents for certain durations, and then characterized in terms of residual core fractions and morphology.

3.4.1 Water resistant test

Certain amount of microcapsules was soaked in ambient water at a concentration of 5 wt%. After designated durations (10 days and 20 days), the soaked microcapsules were rinsed with DI water for subsequent core fraction determination after air dried for 12h.

3.4.2 Organic solvents resistant test

Organic solvents including low-polar (hexane, xylene), medium polar (ethyl acetate) and polar (acetone) organic solvents were applied to measure the stability of resultant microcapsules including water resistant microcapsules, double resistant microcapsules and tri-functional microcapsules. The microcapsules were immersed in organic solvents for certain durations at designated concentrations. Subsequently, the conditioned microcapsules can be filtrated and washed, followed by characterization in terms of residual core fractions and morphology after air dried for 12h.

3.5 Mechanical property tests

The mechanical property test of samples can be divided into two parts. The first part is to test the micro-compression strength of individual microcapsule. And the second part is to test the compression strength of epoxy composites containing microcapsules at certain percentages.

3.5.1 Mechanical property of microcapsules

The compression strength of microcapsules was measured through published microsphere

compression experiments [39, 100]. The load was recorded by a load cell (FUTEK) with maximum load of 0.5 N and the applied loading rate for the stepper actuator (Physik Instrumente M-230S), which is controlled by a computer, was 2 $\mu\text{m/s}$. In addition, the diameter of microcapsules was measured by the images taken prior to the test. The shell strength can be calculated according to the following equation.

$$\delta_{max} = \frac{P_{max}}{\pi \left[\left(\frac{D_0}{2} \right)^2 - \left(\frac{D_i}{2} \right)^2 \right]} \quad (3.5)$$

where, σ_{max} is the normalized maximum strength; P_{max} is the maximum load; D_0 is the outer diameter of microcapsules; D_i is the inner diameter of microcapsules.

3.5.2 Compression test of epoxy composites containing microcapsules

The influence of microcapsules on matrix strength was characterized through compression strength of epoxy composite containing microcapsules at different concentrations. In comparison, the compression strength of pure epoxy samples was tested. Compression specimens were fabricated and tested according to ASTM-D695. The fabrication method of epoxy composites is different when double resistant microcapsules and trifunctional microcapsules are embedded in epoxy resin, respectively. Double resistant microcapsules were dispersed directly within formulated epoxy resin as multifunctional resin followed by degassing in vacuum to remove trapped bubbles. Subsequently, the multifunctional resins were added in silicone rubber mould for molding. The specimens were firstly cured at RT for 24h followed by another 24h at 35 $^{\circ}\text{C}$. When trifunctional microcapsules were dispersed in epoxy resin, the epoxy resin was required to pre-cure for 3h at room temperature followed by the addition of metal shell microcapsules. Subsequent curing process obeyed the same procedure with that of epoxy resin containing double resistant microcapsules. Instron machine (Instron 5500R) was applied to conduct the

compression test with loading speed of 1 mm/min.

3.6 Preparation and test of multifunctional composite coatings

The resultant microcapsules were dispersed in epoxy resin (Epilam 5015 and hardener 5014) at a concentration of 10 wt% to fabricate multifunctional composite coatings with embedded microcapsules. The fabrication method of composite coating is different when different microcapsules were embedded in epoxy resin. Double resistant microcapsules were dispersed directly within formulated epoxy resin as multifunctional resin followed by degassing in vacuum to remove trapped bubbles. When trifunctional microcapsules were dispersed in epoxy resin, the epoxy resin was required to pre-cure for 3h at room temperature followed by the addition of trifunctional microcapsules.

3.6.1 Preparation of anticorrosion coatings

Several pieces of steel panel ($50 \times 50 \times 5 \text{ mm}^3$) were firstly polished with sand paper and then washed with acetone to remove surficial impurities. Subsequently, multifunctional resins were coated uniformly on the surface of steel panel with final thickness within 300-400 μm after cured. After 24h at room temperature, self-healing specimens were ready for anticorrosion test. For comparison, specimens covered by pure epoxy resin were prepared as control specimens.

3.6.2 Evaluation of anticorrosion performance

Manual scratches were applied to the specimens followed by immersion in NaCl solutions (1M) for 24h for accelerated corrosion. Subsequently, the corrosion performance of self-healing specimens and control specimens can be recorded in term of pictures. And the detailed information within scratches was observed through SEM.

Besides SEM observation, self-healing process was also monitored by EIS experiments (Gamry

Reference 600 potentiostat) in electrolyte solutions (1 M Sodium Chloride solution). The detailed parameters were listed as following, swept frequency: 10^{-2} - 10^5 ; and AC amplitude: 20 mV.

3.6.3 Preparation of self-lubricating samples

To demonstrate the multi-functionality of smart resin, tribology sample was carried out in a PTFE cylindrical mold with diameters of 30 mm. After curing for 24h at room temperature, the multifunctional samples were allowed for post cure for another 24h at 35 °C. For comparison, samples prepared from pure epoxy resin were also fabricated.

3.6.4 Evaluation of self-lubricating performance

Before tribological test, the surfaces of self-lubricating samples were pre-polished using 800 grits to acquire stable surface conditions. The tribological properties of the samples were investigated using tribometers (Universal Tribometer Mod. UMT-3MT) by sliding a Cr6 steel ball with diameters of 4 mm against samples in a circular path of 3 mm for 8 hrs (28800 s) at three different sliding velocity (25 REV, 50 REV and 100 REV) under three different normal loads (3 N, 5 N and 10 N). The antiwear performance of resultant samples was characterized in terms of friction coefficient and wear loss of wear tracks. Wear width and wear depth as the important parameters of wear loss were measured using surface profilometry to obtain average value based 10 different points per wear track.

The surface morphology of wore samples was observed through SEM, and the topography were investigated using surface profilometry (Talyscan 150) with a diamond stylus of 4 μ m in diameter.

Chapter 4 Study of water resistant microcapsules

4.1 Motivation

Self-healing materials can be fabricated by dispersing uniformly microcapsules and catalyst (or the second component) within polymeric matrix. Along with the occurrence of crack within matrix, the embedded microcapsules can be easily broken, and release healing agent to fill damage areas. The healing agent meets the dispersed catalyst (or the second component) and then polymerizes into dense polymer film bonding cracked panels together. However, the property of polymer film depends largely on the correct stoichiometric ratio of two components. For better controllability and easy operation, one-component self-healing systems were developed and widely applied in anticorrosion coatings field. Typical one-component healing agents include linseed oil, UV-cured resin and isocyanates, which can polymerize rapidly under the action of surrounding oxygen, UV-light or moisture, respectively. Especially, isocyanates-based self-healing coatings attract increasing attentions due to satisfying anticorrosion performance. Isocyanates are highly reactive and can react rapidly with surrounding water molecules with the production of urea intermediate, which then polymerizes with isocyanates into polyurea film, as shown in Figure 4.1. Yang [1] firstly encapsulated successfully IPDI via interfacial polymerization between 1, 4-butanediol and MDI-based prepolymer in an oil/water system. Huang and Yang [2] presented satisfying anticorrosion performance of scratched self-healing coatings by embedding microcapsules containing HDI in epoxy coating. From then on, investigations focusing on shell properties of encapsulated isocyanates attract more and more attentions. Self-healing anticorrosion coatings are mostly applied in moist surroundings requiring embedded microcapsules to remain active during service life. Especially when embedded

microcapsules loading isocyanate as core materials, water-proof property of shell materials was even more important. Huang *et al.* [2] encapsulated HDI within polyurethane shell possessing poor stability in water, and the core fraction decrease to 0 wt% after 2 days immersion in ambient water. Besides, Yi *et al.* [9] use Pickering emulsion to encapsulate isocyanates which lost core material of 10 wt% after 4 days in ambient water. Nguyen *et al.* [143] improves stability of encapsulated isocyanates in water using fluorinated aromatic amine as cross-linker, and the core fraction of final microcapsules remain constant after 1 day in ambient water. Therefore, the preparation of microcapsules containing isocyanates remain active long-termly in moist environment is still in a high demand. Herein, water resistant microcapsules were fabricated successfully by combining interfacial and in situ polymerization method in an oil-in-water system, and resultant microcapsules possess great stability in water.

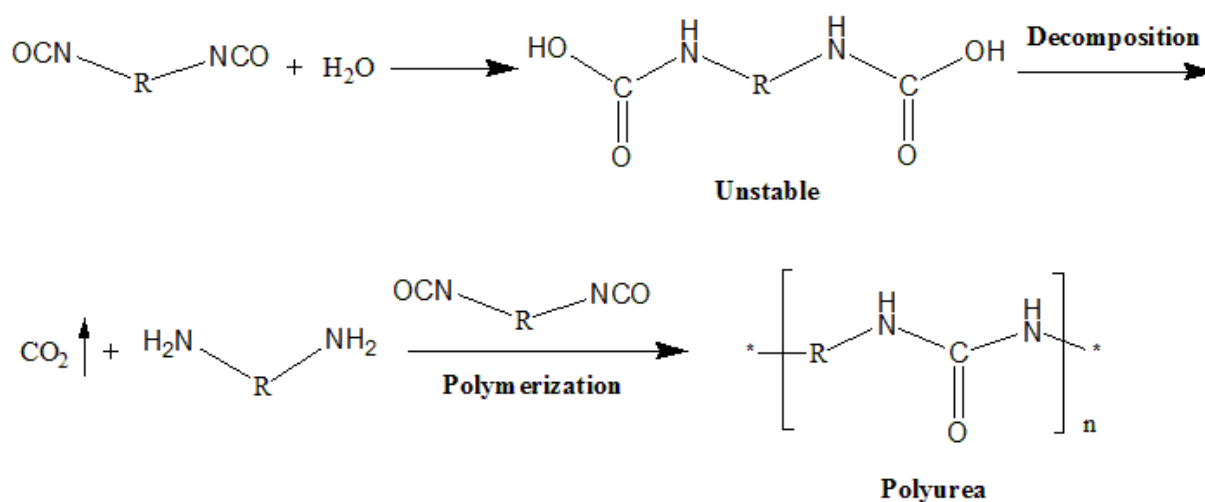


Figure 4.1 Reaction mechanism between isocyanate and water.

4.2 Overview of preparing water resistant microcapsules

The water resistant microcapsules were prepared by combining interfacial polymerization and modified in situ polymerization with shortened reaction durations. Interfacial polymerization was firstly applied to fabricate inner-layered polyurea shell, which was then coated by outer-layered PUF shell with linear structure via in situ polymerization. The preparation mechanism was shown in Figure 4.2.

4.2.1 Synthesis of water resistant microcapsules

The inner-layered polyurea shells were prepared via interfacial polymerization in an oil-in-water emulsion system. Firstly, the mixture of HMDI and Suprasec 2644 was emulsified into micro-droplets in surfactant solutions, and allowed to stabilize for certain durations. During the stabilization process, the NCO functional groups on the surface of liquid droplets can be consumed gradually by surrounding water. If the emulsification duration is insufficient, TEPA molecules will link different liquid droplets together by reacting with the NCO functional groups on different liquid droplets, resulting in serious aggregation. Therein, sufficient emulsification durations were required to prepare well-dispersed microcapsules. The individual liquid droplet was shown schematically in Figure 4.2a. When TEPA aqueous solution was introduced, the inner-layered polyurea wall was formed rapidly through the reaction between isocyanates (including Suprasec 2644 and HMDI) and TEPA molecules, as shown in Figure 4.2b. With increasing time, the TEPA molecules in aqueous phase diffused gradually into micro-droplets to thicken the shell, which can inversely retard the diffusion-in of TEPA molecules until equilibrium [148]. Simultaneously, reaction temperature was raised to increase polyurea shell thickness by softening polymeric shells and accelerate the diffusion of TEPA molecules. However, the newly formed inner-layered polyurea shell was still too soft to make microcapsules

collectable. Therefore, outer-layered PUF shells [146] were deposited on the surface of microcapsules with inner-layered polyurea shells for better collectability. In this step, reactants with high concentration and less oil-water ratio [85] were applied to accelerate the formation of outer-layered PUF shells, as shown in Figure 4.2c. The reactants concentration in our systems was nearly 5 times than that in traditional system [85]. In addition, lower oil-water ratio and higher beginning reaction temperature can also accelerate the formation of PUF shells. The short reaction durations can reduce the consumption of HMDI core by urea and water in aqueous solutions. After certain durations, water resistant microcapsules can be prepared successfully.

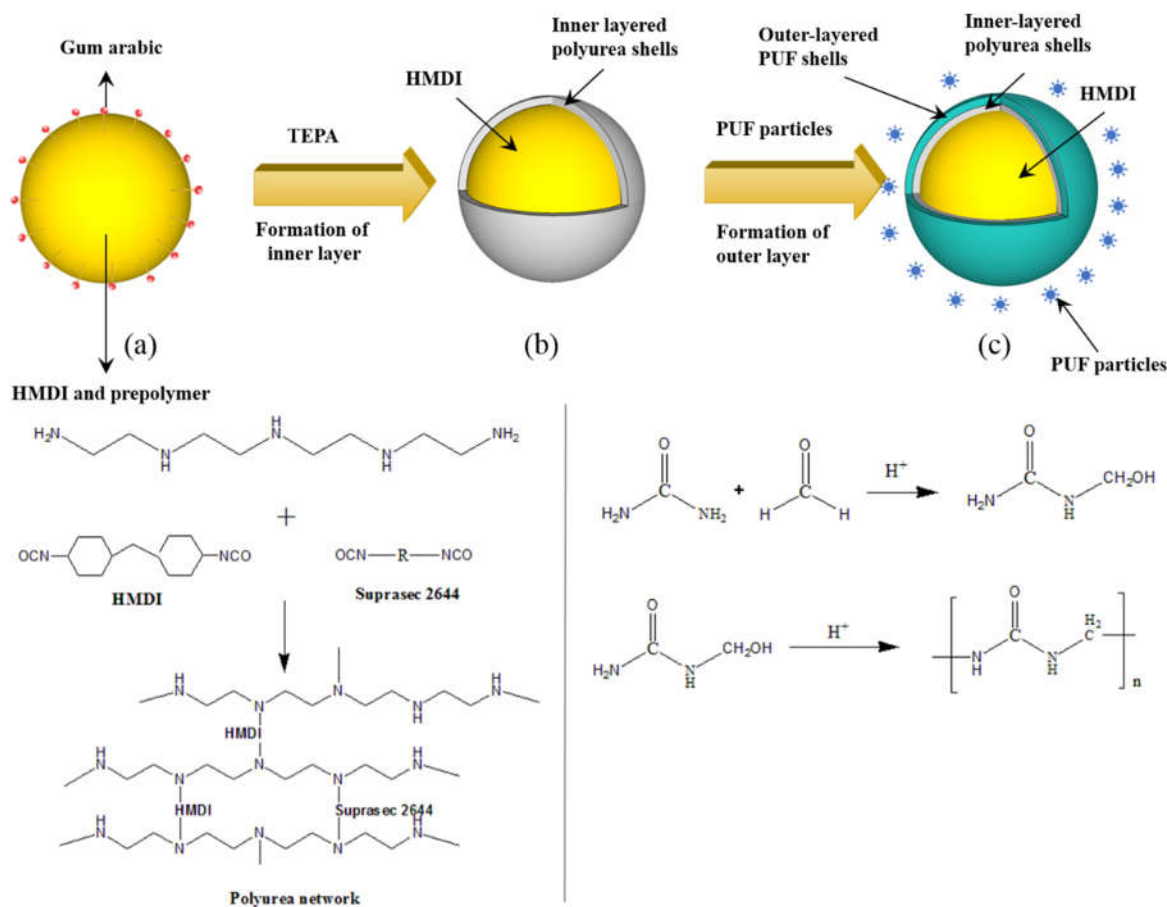


Figure 4.2 Schematic formation process of water resistant microcapsule.

4.2.2 The influence of agitation rate on water resistant microcapsules

The influence of agitation rate on water resistant microcapsules was investigated systematically, and characterized in terms of morphology and core fraction. Subsequently the optimum process was applied for future investigations.

On microcapsules diameter and shell thickness

The diameters of microcapsules affects obviously self-healing performance [149, 150], and it is controllable by agitation rate in emulsification process. As shown in Figure 4.3, the diameter of microcapsules decreases from $100.4 \pm 20.3 \mu\text{m}$ to $18.9 \pm 6.3 \mu\text{m}$ with the increase of agitation rate from 750 to 1450 RPM, which agrees with previous investigations [1, 85]. At higher agitation rate, smaller microcapsules were prepared from smaller oil droplets due to the stronger shear force. The average shell thickness of water resistant microcapsules as a function of agitation rate was also plotted in Figure 4.3. It is clear that the shell thickness reduced from $1.98 \pm 0.45 \mu\text{m}$ to $0.77 \pm 0.17 \mu\text{m}$ with the increase of agitation rate from 750 to 1450 RPM, which is in agree with prior investigation [149]. Finer oil droplets with larger specific interface area were generated under higher agitation rate. Based on constant total amount of TEPA, less TEPA was distributed averagely to every liquid droplet leading to thinner polyurea shell [151]. Besides, thinner outer-layered PUF shell can also be produced under higher agitation rates, corresponding to larger specific areas of microcapsules under constant PUF particles.

By consideration of both thinner polyurea shell and thinner PUF shell under higher agitation rates, it is reasonable that the shell thickness decreases gradually with the increase of agitation rate.

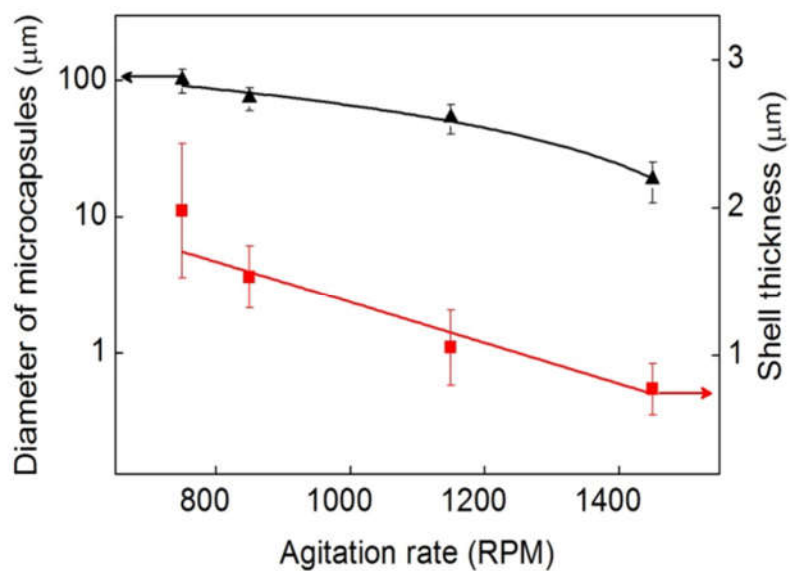


Figure 4.3 Diameter and shell thickness of microcapsules prepared at different agitation rates.

On core fractions

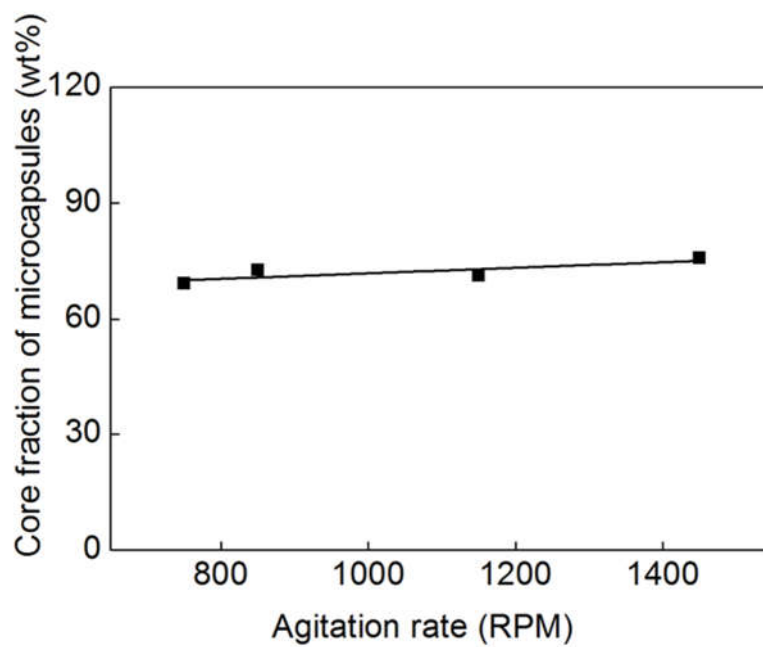


Figure 4.4 Core fraction of water resistant microcapsules prepared at different agitation rate.

Although microcapsules diameters and shell thickness varied significantly, the core fractions of water resistant microcapsules remain stable relatively at around 70 wt% when agitation rate was increased from 750 to 1450 RPM, as shown in Figure 4.4. The stable core fraction was mainly due to the excellent stability of shell in water, which can isolate efficiently water molecules during encapsulation process. In a typical run of synthesis, the microcapsules were obtained under the agitation rate of 850 RPM. The water resistant microcapsules had average diameter of $74.2 \pm 14.0 \mu\text{m}$ and shell thickness of $1.52 \pm 0.21 \mu\text{m}$.

Besides agitation rates, the mass of Suprasec 2644 also influence the core fractions of water resistant microcapsules. As shown in Figure 4.5, the core fractions of water resistant microcapsules decreased from 79.9 wt% to 61.9 wt% with the increase of the mass of Suprasec 2644 from 0.3 g to 1.2 g. More Suprasec 2644 in the oil phase signifies less fraction of HMDI. Finally, less HMDI was left when reaction process was finished. As shown in the inset pictures of Figure 4.5, more solid-state impurities existed in microcapsules when 1.2 g of Suprasec 2644 was applied. More Suprasec 2644 in micro-droplets could absorb more water molecules with the formation of more solids during encapsulation process. Suprasec 2644 was mainly made from MDI and polyol, both of which are slightly soluble in water resulting in more absorption of water molecules.

In addition, the water resistant microcapsules are not collectable when 0.3 g of Suprasec 2644 was used. Although the newly formed polyurea shells possess high crosslink density, the shells were too thin to make microcapsules collectable. This is because shells with higher crosslink density isolate more TEPA molecules, leading to the decrease of shell thickness.

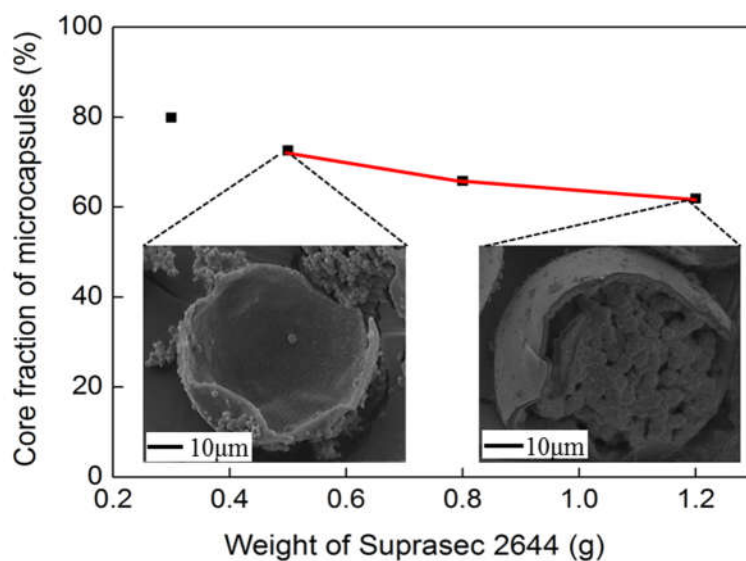


Figure 4.5 Core fractions of microcapsules prepared under different fractions of Suprasec 2644, and the inset pictures are the corresponding interior morphology of related microcapsules.

4.3 Characterization of water resistant microcapsules

4.3.1 Morphology of water resistant microcapsules

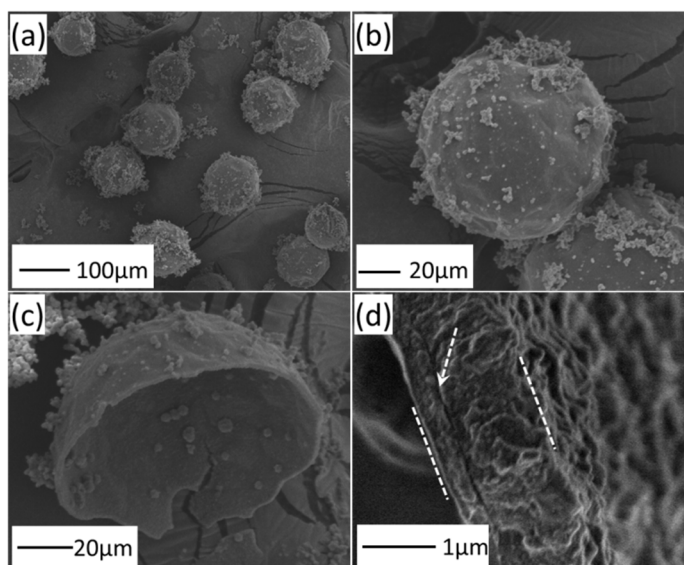


Figure 4.6 (a) Overview of water resistant microcapsules; (b) Morphology of single microcapsule; (c) Inner structure of microcapsules, and (d) Shell profile.

The morphology of water resistant microcapsules was observed through SEM, as presented in Figure 4.6. Figure 4.6a shows nearly spherical shaped microcapsules and related size distribution. Microcapsules have coarse outer surfaces (Figure 4.6b) resulted from the deposition of PUF particles [68]. The obvious core-shell structure with rare solid impurities adhering to the inner surface is presented in Figure 4.6c. The impurities are produced from the reaction between the diffused-in water and Suprasec 2644 [7]. The reason why the particles are not produced from the reaction between TEPA and Suprasec 2644 is that the activity of TEPA is very high, creating difficulty for TEPA molecules to diffuse in microcapsules in free status. Figure 4.6d provides the detailed profile of shell structure, double-layered structure. The shell with whole thickness of $1.5 \pm 0.21 \mu\text{m}$ is mainly composed of inner-layered shell of about $1.3 \mu\text{m}$ and outer-layered shell of about $0.2 \mu\text{m}$. The inner-layered shell is produced from the reaction between TEPA and isocyanates, whereas outer-layered shell is due to the deposition of PUF particles [85]. Final double-layered shells provide microcapsules enough mechanical strength for post processing and act as appropriate barriers to retard the attack of water molecules.

4.3.2 Chemical composition of water resistant microcapsules

The FTIR spectra curves of HMDI, core material, Suprasec 2644, shell material of water resistant microcapsules and processed shell material were shown in Figure 4.7. The processed shell material was obtained by immersing fresh shell material in TEPA aqueous solution (10 wt%) at room temperature for 3 days followed by air dried for 24h. The nearly identical spectrum curves of pure HMDI with core material indicated that HMDI was encapsulated successfully, while very small amount of Suprasec 2644 exists in core materials because the obscure signal peaks of phenyl group at 1641 cm^{-1} and 1540 cm^{-1} were still detected.

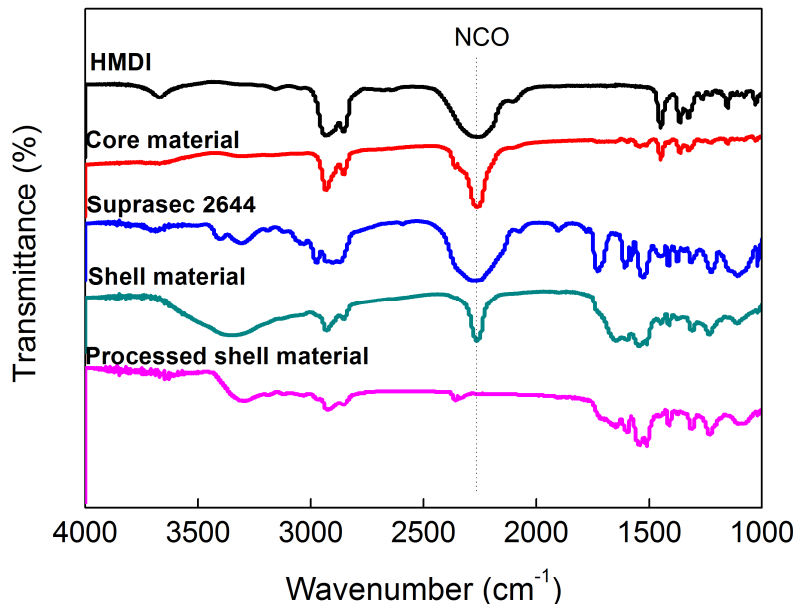


Figure 4.7 Comparison of FTIR spectrums of water resistant microcapsule's shell, processed shell materials, core materials, Suprasec 2644 and HMDI.

Most of the Suprasec 2644 within droplets was depleted by diffusion-in water molecules [7]. In the spectrum of fresh shell material, the characteristic signal of NCO stretch at 2269.5 cm^{-1} was detected and disappeared after treatment by TEPA solution. The NCO functional groups within fresh shell are protected short-termly by dense shell wall. However, the disappearance of this signal peak after shell being processed by TEPA aqueous solutions confirms the reactivity of NCO group.

4.3.3 Thermal property and core fraction of water resistant microcapsules

The weight loss curves of water resistant microcapsules, pure HMDI and shell material as a function of temperature are shown in Figure 4.8. In the curve, the water resistant microcapsules began to lose weight (defined as 5 % weight loss) at around $169\text{ }^{\circ}\text{C}$, and then experienced first major weight loss during the isothermal process at $180\text{ }^{\circ}\text{C}$, followed by a stable weight plateau until $200\text{ }^{\circ}\text{C}$. From then on, the microcapsules began second massive weight loss until $600\text{ }^{\circ}\text{C}$,

leaving slight coke residue. In the curve of shell materials, the beginning weight loss occurred at the isothermal process, and continued degrading massively from 200 °C until 600 °C, leaving coke residue of approximate 10 wt%. The pure HMDI began to lose weight at around 176 °C, and evaporated completely during isothermal process at 180 °C. The lower beginning weight loss temperature of water resistant microcapsules than pure HMDI is because of the loose shell structure and larger specific surface area of microcapsules, accelerating the evaporation of liquid core. During the isothermal process, water resistant microcapsules release all core materials resulting in subsequent weight plateau. The decomposition of shell materials includes two parts: those during isothermal process and major part at above 200 °C.

From RT to 180 °C, water resistant microcapsules lost weight approximate 75.3 wt% including all liquid core and partial shell materials, while the partial shell materials take 7.6 % of all shell materials from the TGA curve of shell materials.

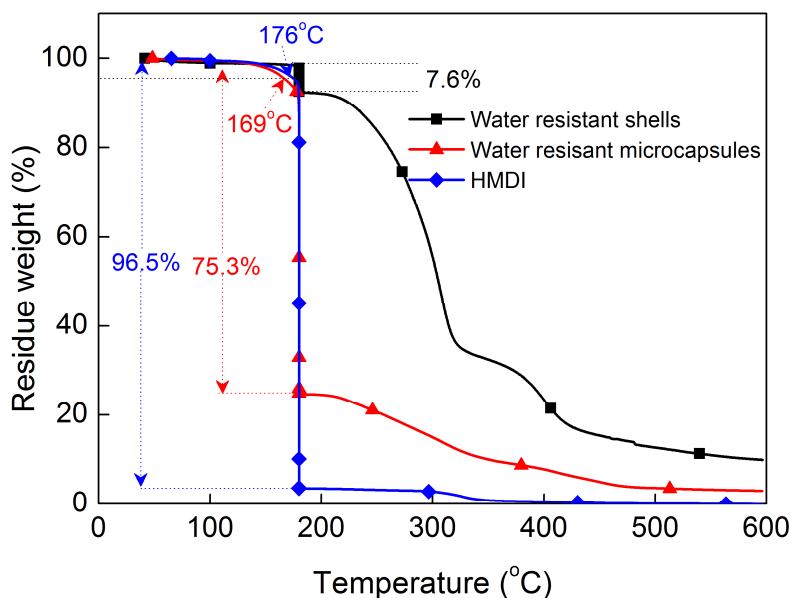


Figure 4.8 Thermal performances of water resistant microcapsules and constituent materials under heating procedure with isothermal process.

Therefore, the core fraction of water resistant microcapsules can be calculated according to following equations (Equation 4.1 and 4.2). The weight loss of core, shell and water resistant microcapsules from room temperature to 180 °C were defined as C_{core} , C_{shell} and $C_{microcapsules}$. The typical core fraction of water resistant microcapsules prepared under the agitation rate of 850 RPM was 72.3 wt%, which is less than theoretical value due to the existence of PUF particles on the surface of microcapsules.

$$C_{shell} + C_{core} = C_{microcapsules} \quad (4.1)$$

$$\frac{C_{shell}}{1 - C_{core}} = 7.6\% \quad (4.2)$$

4.4 Stability of water resistant microcapsules in water

4.4.1 Stability in aqueous solutions with various pH values

The influence of pH values on the stability of water resistant microcapsules was tested by immersing fresh microcapsules in aqueous solutions from acidity to alkalinity. After certain durations, the relative core fractions of residual microcapsules were obtained and presented as a function of immersion durations. As shown in Figure 4.9, the relative core fraction (residual/original core fraction) decreased gradually with immersion time in all solutions including NaCl solution (10 wt%), acid solution (pH=3) and alkaline solution (pH=11). The relative core fraction was 83.1 % after 24 days immersion in NaCl solution (10 wt%), 81 % in alkali solution (pH=11) and 78 % in acid solution (pH=3), respectively. Water molecules can diffuse continuously in and consume more HMDI core under longer immersion time. However, the great stability of shell materials at buffered pH values protects efficiently encapsulated

isocyanates, leaving massive residue after long-term immersion. The excellent stability of water resistant microcapsules in aqueous solutions extends greatly the service life of smart coatings.

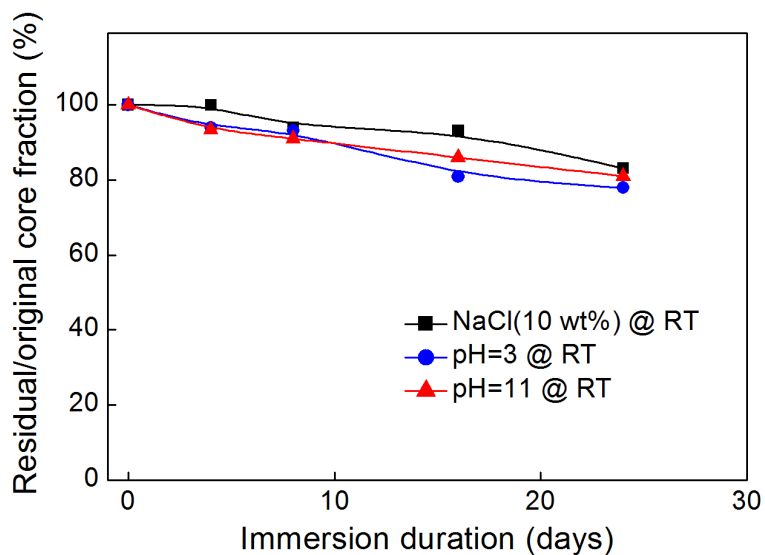


Figure 4.9 The relative core fractions (Residual/original core fraction) of water resistant microcapsules varied with durations after immersed in aqueous solutions with different pH values.

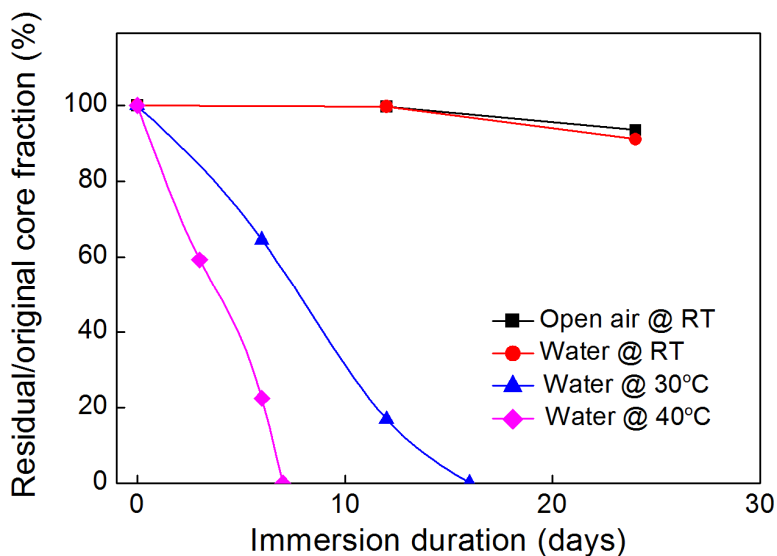


Figure 4.10 Relative core fractions of water resistant microcapsules varied with immersion durations after exposed in open air and water under different temperature.

4.4.2 Pot life

To assess the pot life of water resistant microcapsules, the fresh microcapsules were exposed to ambient open air and immersed in water with different temperatures, respectively. As shown in Figure 4.10, the relative core fraction keeps decreasing with time in humid air, and reached 93.5 % residue after 24 days. In addition, the core fraction of microcapsules in ambient water has the similar decrease trend with that in open air, and leaves 91.1 % residue after 24 days. There are more water molecules in water than in the open air. Hence, these water molecules will consume more HMDI core resulting in residue of less core materials. By comparing with published polyurea [7] or polyurethane [2] microcapsules, the unique shell structure of water resistant microcapsules contributes to the outstanding stability of microcapsules in moist environments. However, water resistant microcapsules showed compromised stability in warm water. The HMDI core was completely depleted after 16 days in 30 °C water and 7 days in 40 °C water. The reason why shorter service life of microcapsules in warm water is that higher temperature can accelerate the diffusion of water molecules and increase shell permeability [152].

4.4.3 Stability in organic solvents

Organic solvents including acetone, ethyl acetate and xylene were applied to examine the stability of water resistant microcapsules in organic solvents. After being immersed in organic solvents for certain period, the residual core fractions of water resistant microcapsules can be obtained through titration. As shown in Figure 4.11, the relative residue of core materials decreases gradually with immersion time. In xylene, relative residue of core materials decreases from 100% to 98% (0.5h), 93.4% (1h), 89.3% (3h), 58.3% (24h), 55.5% (72h) and 57.4 % (96h). In ethyl acetate, the relative residue of core fraction decreased from 100% to 44.73% (0.5h), 0% (1h) and 0 % (3h).

In acetone, the relative residue of core fraction decreased from 100% to 22.3% (0.5h), 0% (1h) and 0% (3h). Obviously, the release of core materials increases gradually with immersion duration and reached a platform after certain duration due to osmotic balance, and the formation duration of platform is related to solvents polarities. The formation durations of platform is longer when microcapsules were immersed in organic solvents with lower polarities. Besides, final microcapsules showed worse stability in organic solvents with higher polarities. When immersion duration was 0.5h, the relative residual of core materials was 98 % in xylene, 44.73% in ethyl acetate and 22.3% in acetone, respectively. Residual core fractions of microcapsules decreased obviously in organic solvents with higher polarities, because organic solvents with higher polarities possess stronger swelling capability to increase the mesh size of polymeric shell, resulting in more severe release of liquid core [7].

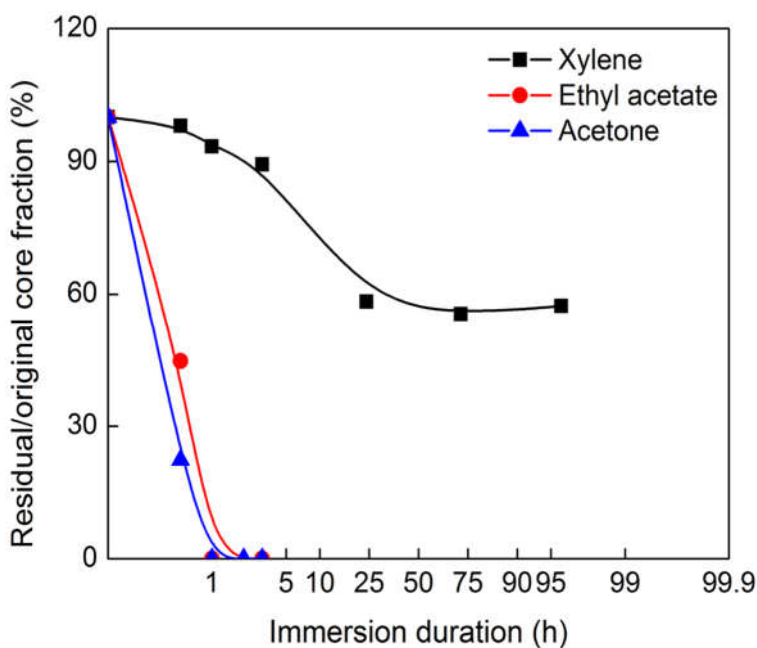


Figure 4.11 Stability of water resistant microcapsules in organic solvents.

4.5 Resistance mechanism of microcapsules to organic solvents

Normally, the thermosetting matrices swell through imbibition after being placed in organic solvents [153] and mesh size of network was enlarged accordingly with the swelling process [154]. The swelling ratio of polymer increases gradually with the increase of the polarity of organic solvents [155, 156]. Then the small solute molecules may diffuse across the swelling network according to free volume theory [157] until osmotic pressure balance. Therein, different mechanisms are provided depending on the polarities of solvents including non- or weakly polar organic solvents (Figure 4.12a), polar organic solvents (Figure 4.12b), and water (Figure 4.12c). When water resistant microcapsules that are immersed in weakly polar solvents like xylene (Figure 4.12a₁), the polymeric shells are hardly swelled (Figure 4.12a₂) and mesh size of polymeric network remain almost unchanged, resulting in little release of HMDI core (Figure 4.12a₃). With the increase of organic solvents polarities (Figure 4.12b₁), larger swelling ratio and thus larger mesh size (Figure 4.12b₂) of microcapsules shell aggravates the release of HMDI core (Figure 4.12b₃).

Water can hardly swell polyurea network due to physical incompatibility. However, water molecules can still pass through polymeric shell by interacting with H-bonds [158]. When water resistant microcapsules are immersed in water (Figure 4.12c₁), water molecules can diffuse inwards and react with HMDI core at the internal surface of shell (Figure 4.12c₂) to grow new polyurea shell, which thickens the shell (Figure 4.12c₃), and barrier property is improved accordingly with the depletion of HMDI.

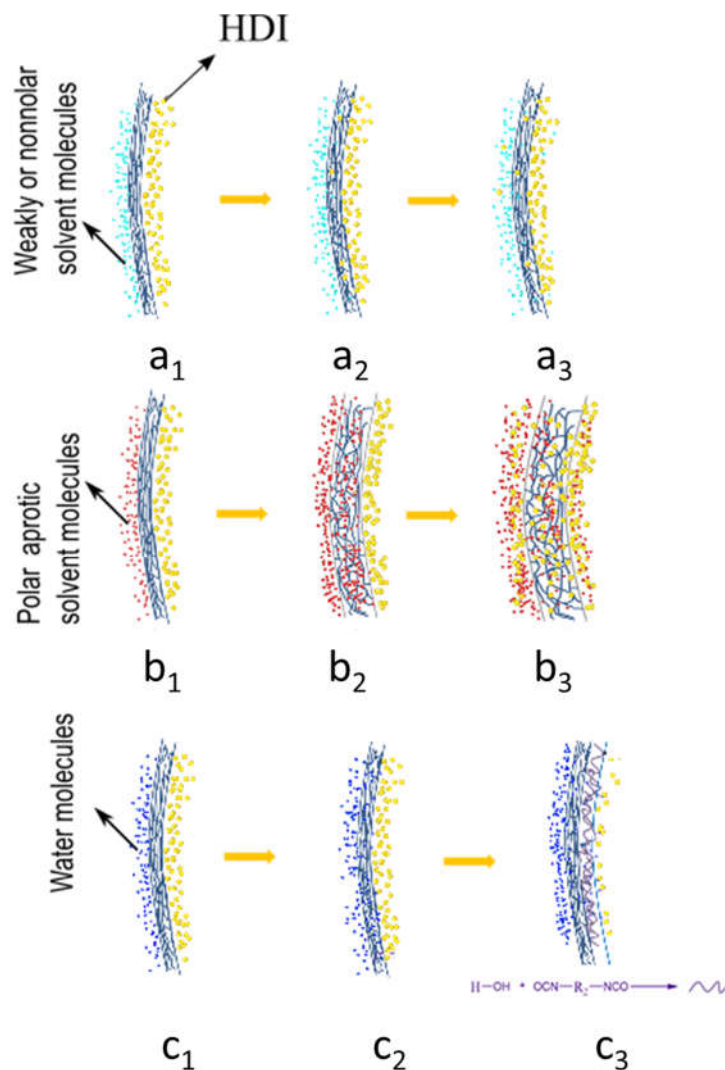


Figure 4.12 Schematic diagrams showing different release mechanisms of liquid core through shell after microcapsules immersion in weakly or nonpolar organic solvents (a), polar aprotic organic solvents (b), and ambient water (c).

4.6 Summary

Water resistant microcapsules with superior stability in aqueous solutions were successfully prepared by combining interfacial and in-situ polymerization. The achieved progress was presented as following:

1. The diameters of water resistant microcapsules decreased from 100 μm to 18 μm corresponding to the increase of agitation rate from 750 to 1450 RPM, and the shell thickness decreases from 2 μm to 0.7 μm . However, the core fractions remain stable relatively at around 70 wt%.
2. The final double-layered shell of water resistant microcapsules possesses superior stability in water. The relative residue of core fractions were beyond 90% after 24 days in both ambient water and open air, and stabilized at around 80% after 24 days exposure in acid and alkaline aqueous solutions. However, stability of water resistant microcapsules was inversed in warm water.
3. The resistance mechanisms of microcapsules to organic solvents and water were presented. In organic solvents, the surrounding organic solvents molecules swell and then increase the matrix size of polymeric shell resulting in the release of liquid core. Water resistant microcapsules showed worse stability in organic solvents with higher polarities. When microcapsules were immersed in water, the consumption of HMDI was mainly resulted from the diffusion-in of water and the diffusion velocity of water molecules was accelerated significantly under higher temperature.

Chapter 5 Study of double resistant microcapsules

5.1 Motivation

Until now, improving the stability of microcapsules containing isocyanates in water has achieved significant developments. Various reports were published to improve the stability of encapsulated isocyanates in moist environments. Yi *et al.* [9] used Pickering emulsion to introduce inorganic components within shells, improving successfully the stability of encapsulated IPDI in water. Nguyen *et al.* [143] improved the stability of encapsulated isocyanate in water by introducing fluorinated aromatic amine within shell. Although water resistant microcapsules containing HMDI have been fabricated successfully and show outstanding stability in water [159], poor stability of water resistant microcapsules in organic solvents still restrict their practical application.

In practical applications, organic solvents as diluents are widely applied in polymeric coatings for easy operation. Besides, anticorrosion coatings as the outmost layer of steel substrates are susceptible to corrosion from organic solvents during service life. Especially, polymeric liners on the inner surface of steel risers need to be immersed in crude oil for long term. The organic solvents require microcapsules in coatings to possess outstanding stability. Multiple methods are investigated to improve the stability of microcapsules in organic solvents including introduction of inorganic fillers, increasing cross-link density of shells or fabricating multiple-layered shells. Fan *et al.* [122] improve microcapsules barrier property by adding nano-clays into PUF shells. Wu *et al.* [136] encapsulated HDI in polyurea/silica hybrid shell with excellent stability in low-polar organic solvents. Wu *et al.* [8] encapsulated HDI within highly cross-linked PUF shells showing great stability in organic solvents. Kang *et al.* [137] coated microcapsules with a layer

of polydopamine to boost the stability of microcapsules in organic solvents. Sun *et al.* [7] encapsulated HDI within double-layered polyurea shells possessing outstanding stability in low-polar organic solvents. However, the encapsulated isocyanates possessing superior stability in both organic solvents and water still remain challenging, and in a high demand to date. The existing method can merely fabricate microcapsules with single advantage (excellent stability in organic solvents or water). Herein, we coated a layer of highly cross-linked PUF shell on microcapsules with inner-layered polyurea shell to prepare double-resistant microcapsules. This is the first time to prepare microcapsules containing isocyanates possessing superior stability in both water and organic solvents.

5.2 Overview of preparing double resistant microcapsules

The double-resistant microcapsules were synthesized by combining interfacial and in situ polymerization. Interfacial polymerization was applied to fabricate inner-layered polyurea shells, and in situ polymerization was applied to fabricate outer-layered highly cross-linked PUF shell on the surface of inner-layered polyurea shell.

Synthesis of microcapsules with inner-layered polyurea shells

The preparation process of microcapsules with inner-layered polyurea shells was the same with that of water resistant microcapsules, and it was introduced in Chapter 4. However, the preparation process of outer-layered PUF shell was different from PUF shell of water resistant microcapsules, and the overview of this part was shown in the following.

Preparation of outer-layered PUF shells covering inner-layered polyurea shells

Urea-formaldehyde prepolymer was firstly synthesized in alkaline environments [147]. In alkaline environments, the urea can react with formaldehyde with the formation of

monomethylol urea, dimethylol urea and trimethylol urea. Then, the newly prepared prepolymer and resorcinol were dissolved in EMA aqueous solutions. Subsequently, the slurry of microcapsules with inner-layered polyurea shells was introduced in prepolymer solutions and allowed to stabilize for certain durations. During the stabilization process, electronegative EMA molecules were absorbed steadily on the surface of electropositive polyurea microcapsules as protective layers. Subsequently, PUF resin with crosslinked structure [147] can be absorbed on the surface of microcapsules with inner-layered polyurea shells, and react with exposed amine functional groups. The PUF resin with crosslinked structure was prepared by reacting trimethylol urea with dimethylol urea or monomethylol urea. Over time, the PUF shells were formed gradually and linked tightly with inner-layered polyurea shell. After 2h, the final slurry was rinsed with DI water for several times, and then air dried 12h for future characterization. The outer-layered PUF shells with highly crosslinked structure [147] boost efficiently the stability of double resistant microcapsules in organic solvents. Finally, double resistant microcapsules possessing outstanding stability in both water and organic solvents were fabricated successfully.

5.3 Characterizations of double resistant microcapsules

5.3.1 Morphology of double resistant microcapsules

The morphology of double resistant microcapsules is presented in Figure 5.1. Figure 5.1a showed well-dispersed microcapsules with diameters of $79.7 \pm 21.5 \mu\text{m}$. Each microcapsule possesses smooth and dense outer surface, as shown in Figure 5.1b.

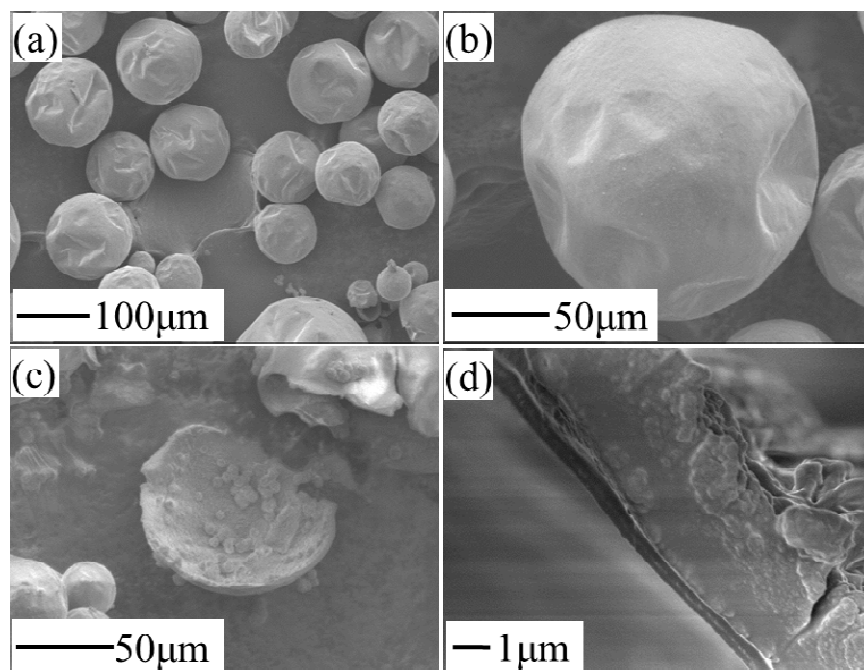


Figure 5.1 (a) Overview of double resistant microcapsules; (b) Morphology of single double resistant microcapsule; (c) Inner structure of double resistant microcapsule, and (d) Shell profile of double resistant microcapsules.

The interior of double resistant microcapsules displayed obvious core-shell structure with few solid impurities (Figure 5.1c), which is produced from the reaction between diffusion-in water and Suprasec 2644. Moreover, the cross-section profile of microcapsules shell showed obvious double-layered structure, whose thickness in total is around $3.8\ \mu\text{m}$ including outer-layered PUF shell of $387\pm40\ \text{nm}$ and inner-layered shell of $3.5\pm0.18\ \mu\text{m}$. The close link between outer-layered and inner-layered shell was due to the chemical bonding between PUF prepolymer and exposed amine functional groups on polyurea shells. However, some separations (Figure 5.1d) can still be observed between inner-layered and outer-layered shells resulting probably from the uneven deposition of PUF prepolymers.

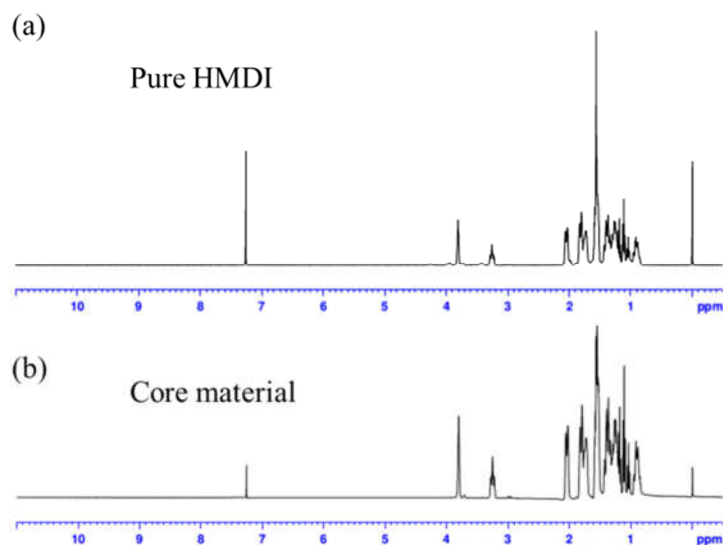


Figure 5.2 Comparison of ¹H-NMR spectras of pure HMDI (a) and core materials (b).

5.3.2 Chemical composition of core materials

The chemical composition of core material of double resistant microcapsules was determined by comparing the ¹H –NMR spectra curves of core materials with that of pure HMDI. As shown in Figure 5.2, the spectrum of core materials (Figure 5.2b) showed highly similar characteristics with pure HMDI (Figure 5.2a) proving that HMDI was encapsulated successfully.

5.3.3 Core fraction and thermal stability of double resistant microcapsules

The core fraction of double resistant microcapsules was obtained by titrating crushed microcapsules in acetone according to ASTM D2572-97. The NCO contents in acetone solutions can be titrated and then converted into the weight of HMDI (core materials) based on Equation 5.1. Subsequently, the core fractions of double resistant microcapsules can be calculated according to Equation 5.2. The obtained core fractions of microcapsules were 74.1±1.3 wt% which is highly close to theoretical value.

$$m_{(HMDI)} = 262.35 \times \frac{1}{2} \times n_{NCO} = 131.18 \times \frac{(V_{(blank)} - V) \times c_{(HCl)}}{2000} \quad (5.1)$$

$$Core \text{ fraction (wt\%)} = \frac{m_{(HMDI)}}{m_{(microcapsules)}} \times 100\% \quad (5.2)$$

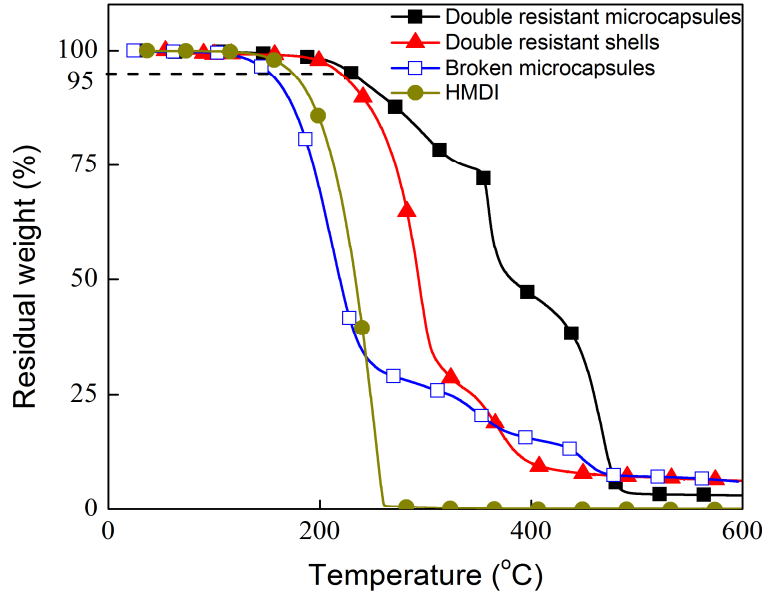


Figure 5.3 Thermal stability of double resistant microcapsules, shell, broken double resistant microcapsules and HMDI under heating procedure without isothermal process.

The thermal stability of double resistant microcapsules was tested by heating all materials including integrated double resistant microcapsules, shell materials, pure HMDI and broken double resistant microcapsules from room temperature to 600 °C at a rate of 10 °C min⁻¹ in Nitrogen atmosphere.

The weight loss curves of samples as a function of temperature are shown in Figure 5.3. The beginning decomposition temperature of materials was set as the temperature at 5 wt% weight loss. As shown in Figure 5.3, double resistant microcapsules begin to decompose at 230 °C, followed by massive weight loss including thermal decomposition of shell materials and

evaporation of core materials until 500 °C leaving nearly 3.5 wt% coke residue. Shell materials begin to decompose at 220 °C, and continue to decompose massively until 500 °C leaving coke residue around 7.2 wt%. Pure HMDI begin to evaporate at 174 °C until vanish completely at 260 °C. The beginning weight loss temperature of broken double resistant microcapsules was 153 °C due to evaporation of HMDI core followed by primary weight loss including the evaporation of HMDI core and thermal decomposition of shell until 500 °C leaving approximate 7.2 wt% coke residue. Double resistant microcapsules possess excellent thermal stability resulting from higher beginning decomposition temperature than shell material. When shell materials lose weight around 5 wt% (220 °C), integrated double resistant microcapsules lose weight approximate 3 wt% meaning that no serious damages occurred to shells structure resulting in little loss of core materials. In addition, microcapsules shells showed superior density to retard the release of HMDI vapor when environmental temperature is higher than boiling point (168 °C) of pure HMDI. Moreover, the lower beginning weight loss temperature (153 °C) of broken double resistant microcapsules than that of integrated double resistant microcapsules also demonstrates that microcapsules shell possess great thermal stability. More interestingly, microcapsules containing isocyanates possessing higher beginning decomposition temperature than shell materials were firstly reported, while liquid core were released massively from microcapsules before boiling point in previous publications [2, 7, 8, 134, 136].

5.4 Stability of double resistant microcapsules in organic solvents and water

5.4.1 Shell functions of double resistant microcapsules

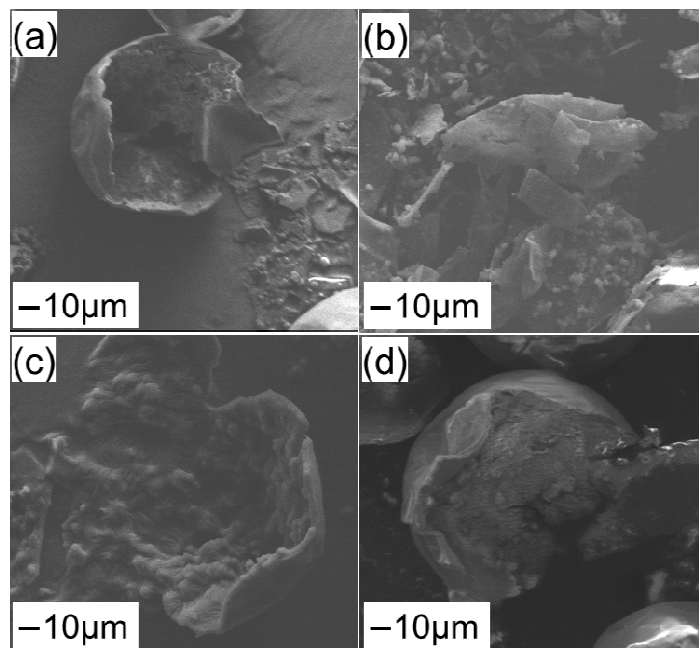


Figure 5.4 The morphologies of microcapsules with inner-layered polyurea shells (a, b) and double resistant microcapsules (c, d) after immersion in water (a, c) for 20 days and hexane (b, d) for 5 days.

Inner-layered polyurea shells and outer-layered PUF shells impart double resistant microcapsules diverse capabilities to resist harsh conditions. The shell functions of double resistant microcapsules were characterized by immersing microcapsules with inner-layered polyurea shells and double resistant microcapsules in related solvents for certain durations to observe the residual morphologies and core fractions.

The inner-layered polyurea shells provide double resistant microcapsules superior stability in water. Microcapsules with inner-layered polyurea shells were immersed in ambient water for 20 days and hexane for 5 days to test the functions of inner-layered polyurea shells. As shown in Figure 5.4a, microcapsules with inner-layered polyurea shell still remain hollow inner structures without overmuch solid impurity inside after 20 days in water due to water-proof polyurea shells, allowing little water diffused-in. In addition, the core fraction of microcapsules with inner-

layered polyurea shells decreases slightly from 91.6 ± 0.84 wt% to 73 ± 2.2 wt%. In comparison, the HDI core within polyurethane shells was depleted completely leaving solid inner structure after 48h immersion in ambient water [2]. Massive residue of core materials and hollow inner structure of microcapsules with inner-layered polyurea shells after long-term immersion in ambient water proves the superior stability of inner-layered polyurea shell in water. However, such single-layered polyurea shells resist poorly to hexane, which possesses lowest polarity and weakest infiltration capability. Microcapsules with inner-layered polyurea shells were soaked in hexane to test the stability in organic solvents. As shown in Figure 5.4b, microcapsules with inner-layered polyurea shells collapsed into debris along with complete loss of HMDI core after 5 days immersion in hexane. For better stability in organic solvents, outer-layered highly cross-linked PUF shells were coated covering microcapsules with inner-layered polyurea shells.

In order to test the functions of the outer-layered PUF shells, double resistant microcapsules were immersed in water for 20 days and hexane for 5 days, and characterized in terms of residual core fractions and morphologies. The outer-layered PUF shells impart double resistant microcapsules superior stability in organic solvents. Spherical double resistant microcapsules survive steadily without collapse (Figure 5.4d) and hold massive HMDI core, which decreased slightly from 74.1 ± 1.3 wt% to 72.2 ± 1.03 wt% after 5 days in hexane. Moreover, double resistant microcapsules still remain great stability in ambient water. As shown in Figure 5.4c, hollow inner structure of double-layered microcapsules without impurities were observed obviously, and core fraction decreased slightly from 74.1 ± 1.3 wt% to 69.6 ± 3.1 wt% after 20 days in ambient water. Therefore, it is reasonable to conclude that inner-layered polyurea shells provide double resistant microcapsules outstanding stability in water, and outer-layered PUF shells impart

microcapsules superior stability in organic solvents. Systematic characterizations of stability of double resistant microcapsules in water and organic solvents were presented in the following part.

5.4.2 Stability of double resistant microcapsules in water

Moist application environments of anticorrosion coating require embedded microcapsules to survive in water for long term. Especially when microcapsules containing isocyanates were applied, stability in water is particular important. When isocyanates based microcapsules were immersed in moist environments, surrounding water molecules can diffuse gradually in microcapsules and consume massive isocyanates core resulting in the failure of self-healing function. Stability of double resistant microcapsules in water were tested by soaking fresh microcapsules in ambient water for certain duration, and then characterized in terms of residual core fraction (Figure 5.5) and morphology of microcapsules (Figure 5.6). Figure 5.5 presents the residual core fractions of double resistant microcapsules as a function of immersion durations in water. The core fraction of double resistant microcapsules decreases slightly from 74.1 ± 1.26 wt% to 69.6 ± 3.1 wt% after 20 days in ambient water. The massive residue of HMDI core proves that microcapsules shells possess outstanding water-proof to isolate surrounding water molecules. Figure 5.6 showed the outer morphology (a) and inner structure (b) of double resistant microcapsules after 20 days in ambient water, respectively. Both smooth outer morphology (Figure 5.6a) and hollow inner structure (Figure 5.6b) remain highly similar with the fresh double resistant microcapsules, proving the great stability of double resistant microcapsules in ambient water.

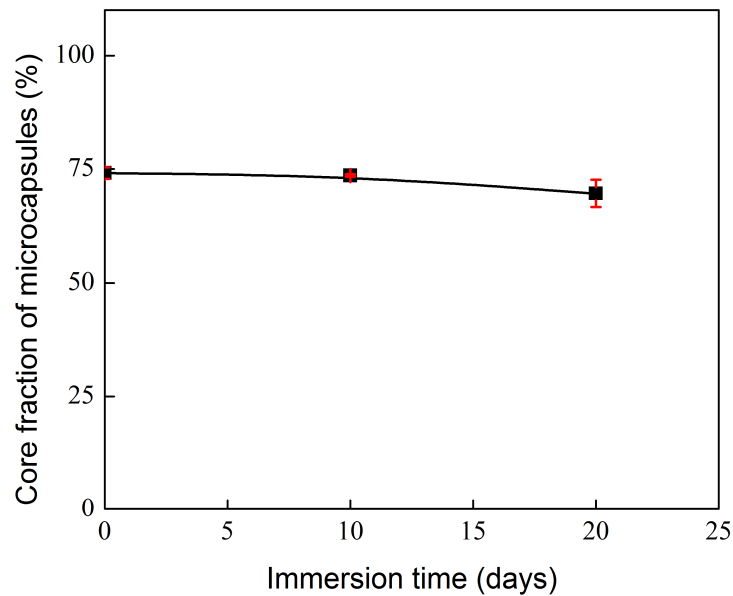


Figure 5.5 The residual core fraction of double resistant microcapsules as a function of immersion time in ambient water.

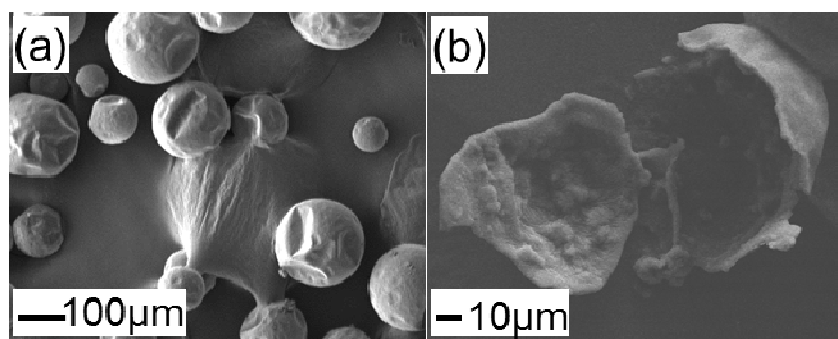


Figure 5.6 Morphology (a) and inner structure (b) of double resistant microcapsules after being immersed in ambient water for 20 days.

5.4.3 Stability of double resistant microcapsules in organic solvents

Stability in organic solvents renders the double resistant microcapsules with promising potential in practical applications. The stability of double resistant microcapsules in organic solvent is influenced by many factors including solvents polarities, immersion durations, microcapsules

size and concentration in organic solvents. Herein, batches of microcapsules with various diameters were soaked in organic solvents with different polarities at different concentrations for different durations, and then characterized in terms of residual core fractions and morphology.

Polarity of organic solvents

The polarities of organic solvents influence significantly on the stability of microcapsules. Double resistant microcapsules with standard diameters of $79.7 \pm 21.5 \mu\text{m}$ were soaked in ambient hexane (polar: 0), xylene (polar: 1.4) and ethyl acetate (polar: 5.3) at a concentration of 5 wt% for 5 days, 10 days, 20 days, and 30 days, respectively. In addition, the double resistant microcapsules were also immersed in acetone (polar: 7.0) for 1 day and 2 days to test the stability in highly polar organic solvents. The residual core fractions of double resistant microcapsules as a function of immersion durations in organic solvents were shown in Figure 5.7. Besides, Figure 5.8 a, b and c showed the morphology of double resistant microcapsules after 30 days in hexane, xylene and ethyl acetate, respectively. Figure 5.8d showed the morphology of double resistant microcapsules after 2 days in acetone.

Firstly, the residual core fractions of double resistant microcapsules decrease gradually with immersion durations, and then reached a platform after certain durations. The residual core fractions of microcapsules decreases gradually from $74.1 \pm 1.3 \text{ wt\%}$ to $72.2 \pm 1.03 \text{ wt\%}$, $72.2 \pm 0.24 \text{ wt\%}$, $71.06 \pm 0.33 \text{ wt\%}$, and $71 \pm 0.29 \text{ wt\%}$ in hexane, to $69.8 \pm 0.91 \text{ wt\%}$, $69.1 \pm 1.17 \text{ wt\%}$, $67.9 \pm 0.41 \text{ wt\%}$, and $67.7 \pm 1.12 \text{ wt\%}$ in xylene, and to $67.0 \pm 0.58 \text{ wt\%}$, $65.1 \pm 0.43 \text{ wt\%}$, $65.6 \pm 0.5 \text{ wt\%}$, and $65.5 \pm 1.35 \text{ wt\%}$ in ethyl acetate after immersion for 5 days, 10 days, 20 days, and 30 days, respectively. In organic solvents, the release of core materials decelerated gradually after 5 days with the formation of platform. The formation of platform was mainly due to the balance of

osmotic pressure between core part and surrounding organic solvents in agreement with previous publications [7]. In addition, organic solvents with higher polarities can induce more release of core materials under the same immersion conditions. As shown in Figure 5.7, residue of less core fractions can be observed when microcapsules were soaked in solvents with higher polarities under the same immersion durations. Organic solvents with higher polarities can swell polymeric shell more seriously resulting in larger mesh size of polymeric shells followed by more release of core materials [7]. Double resistant microcapsules in organic solvents with medium polarities can remain highly similar morphology with the fresh after 30 days in hexane (Figure 5.8a), xylene (Figure 5.8b), ethyl acetate (Figure 5.8c)). Comparing with severe shrinkage of microcapsules with poor stability in organic solvents [6], double resistant microcapsules possesses outstanding stability in organic solvents with medium or low polarities.

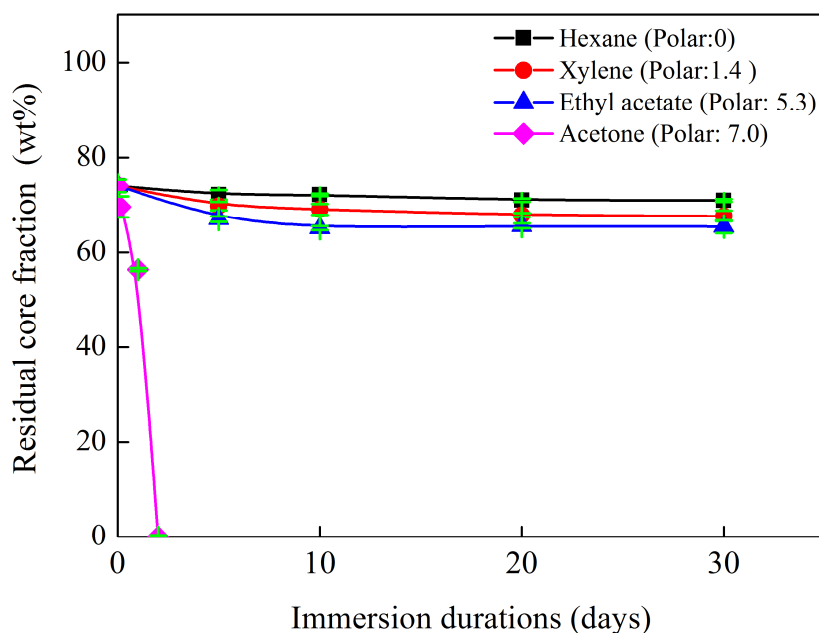


Figure 5.7 Stability of typical microcapsules in hexane, xylene, ethyl acetate and acetone.

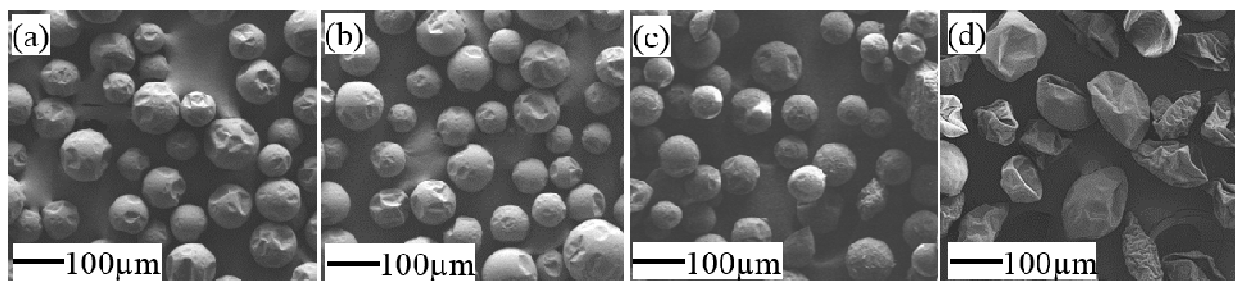


Figure 5.8 Morphology of microcapsules after 30 days in hexane (a), xylene (b) and ethyl acetate (c). (d) is the morphology of microcapsules after 2 days in acetone

In addition, when double resistant microcapsules were immersed in acetone (polar: 7.0), the residual core fractions decreased from 74.1 ± 1.3 wt% to 56.4 ± 0.32 wt%, and 0 wt% after 1 day and 2 days. Severe shrinkage occurs after 2 days in acetone, as shown in Figure 5.8d, demonstrating that double resistant microcapsules can still possess certain stability in organic solvents with high polarities.

Microcapsules size and concentration

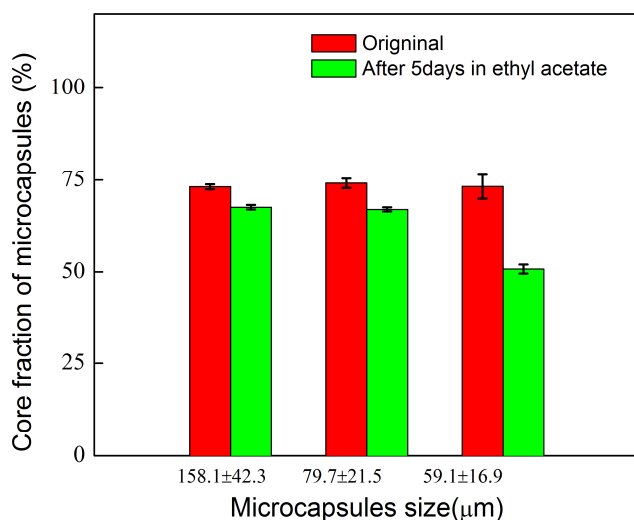


Figure 5.9 Core fractions of double resistant microcapsules with different size before and after immersion in ethyl acetate for 5 days.

Besides, microcapsules size and concentration also influence the stability in organic solvents. Increasing agitation rates (450 RPM, 650 RPM, 850 RPM) were applied to fabricate double resistant microcapsules with decreasing diameters ($158.1\pm42.3\ \mu\text{m}$, $79.7\pm21.5\ \mu\text{m}$, $59.1\pm16.9\ \mu\text{m}$). Microcapsules with different diameters were immersed in ambient ethyl acetate for 5 days at a concentration of 5 wt%, and then the residual core fraction can be obtained through titration. The core fractions of fresh double resistant microcapsules and those experiencing 5 days in ethyl acetate as a function of microcapsules size were shown in Figure 5.9.

Double resistant microcapsules with smaller sizes possess worse stability in ethyl acetate. As shown in Figure 5.9, the core fraction of microcapsules with diameters of $158.1\pm42.3\ \mu\text{m}$, $79.7\pm21.5\ \mu\text{m}$ and $59.1\pm16.9\ \mu\text{m}$ decreased from $73.16\pm0.68\ \text{wt}\%$ to $67.63\pm0.6\ \text{wt}\%$ ($158.1\pm42.3\ \mu\text{m}$), from $74.14\pm1.26\ \text{wt}\%$ to $67.04\pm0.58\ \text{wt}\%$ ($79.7\pm21.5\ \mu\text{m}$), and from $73.23\pm3.25\ \text{wt}\%$ to $50.74\pm1.24\ \text{wt}\%$ ($59.1\pm16.9\ \mu\text{m}$) after immersion in ethyl acetate for 5 days, respectively. The main reason was attributed that smaller microcapsules possess thinner outer-layered PUF shell. As shown in Figure 5.10, the thickness of outer-layered PUF shell was $422\pm36\ \text{nm}$ (a), $387\pm40\ \text{nm}$ (b), $309\pm27\ \text{nm}$ (c) corresponding to the diameter of microcapsules in $158.1\pm42.3\ \mu\text{m}$, $79.7\pm21.5\ \mu\text{m}$, $59.1\pm16.9\ \mu\text{m}$, respectively. The microcapsules with smaller diameters possess larger specific surface area resulting in the deposition of thinner outer-layered shell on inner-layered polyurea shells.

Besides size, the influence of concentration on the stability of microcapsules in organic solvents was also investigated systematically. Double resistant microcapsules with standard diameters of $79.7\pm21.5\ \mu\text{m}$ were immersed in ethyl acetate at different concentrations (2.5 wt%, 5 wt% and 10 wt%) for 5 days, and characterized in terms of residual core fraction. The residual core fractions of double resistant microcapsules as a function of concentration were shown in Figure

5.11. The residual core fractions of double resistant microcapsules after 5 days in ethyl acetate was 67.99 ± 0.8 wt%, 67 ± 0.58 wt% and 68.7 ± 0.09 wt% corresponding to the microcapsules concentrations of 2.5 wt%, 5 wt% and 10 wt%, respectively. Obviously, residual core fractions remain relatively stable under different concentrations.

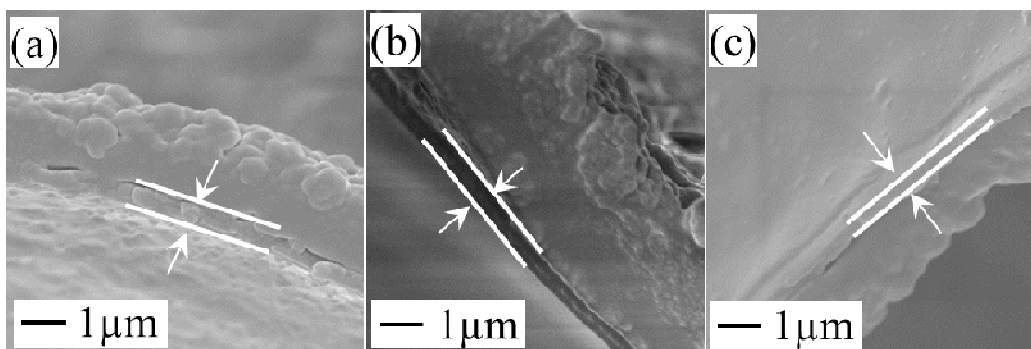


Figure 5.10 The thickness of outer-layered shell of microcapsules with diameters of 158.1 ± 42.3 μm (a), 79.7 ± 21.5 μm (b), 59.1 ± 16.9 μm (c).

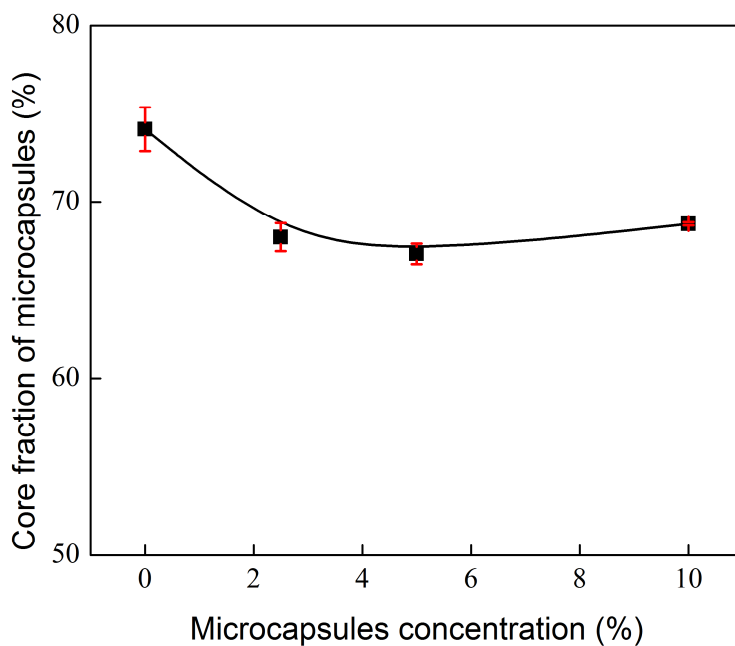


Figure 5.11 The influence of concentration on stability of microcapsules in ethyl acetate.

5.5 Summary

Double resistant microcapsules were fabricated successfully and showed outstanding stability in both water and organic solvents. The main conclusions were shown in the following:

1. Current method can avoid efficiently the aggregation of microcapsules when in situ polymerization method was applied to cover the polyurea shells.
2. Double resistant microcapsules possess superior thermal stability. HMDI core can be retained massively even when shell materials lost weight of 5 wt%.
3. The outer-layered PUF shells provide double resistant microcapsules excellent stability in organic solvent, and the inner-layered polyurea shells provides microcapsules superior stability in water.
4. Double resistant microcapsules showed worse stability in organic solvents with higher polarities. The release of core materials was increased gradually with immersion durations, while microcapsules concentrations in organic solvents influence slightly on final stability.

Chapter 6 Study of tri-functional microcapsules

6.1 Motivation

The introduction of microcapsules in polymeric matrix imparts matrix intelligent features including self-healing and self-lubricating functions. However, strength and modulus degradation of composites with microcapsules concentration is an unavoidable issue. Especially in coatings, modulus plays an important role in resisting external physical attacks. The fabrication of microcapsules with high shells strength possesses great potential in practical applications. The mechanical strength of microcapsules shells can be boosted through various techniques. Wang *et al.* [123] used oxygen plasma treated carbon nanotubes to improve micromechanical behavior of polyurea shell. Caruso *et al.* [124] improved PUF shell strength by increasing shell thickness. Zhang *et al.* [160] loaded liquid agents within hollow glass bubbles to improve mechanical behaviors of composites. However, current microcapsules still fail to stop the decrease of modulus in composites. Plating a layer of metal shell covering microcapsules was considered as an available method to improve shells strength. Metallic materials with outstanding mechanical strength and robustness can serve as ideal containers to preserve liquid agents. Traditional vacuum evaporation deposition method can merely coat microcapsules a layer of thin metal membrane with thickness in nano-scale, which can hardly withstand external collision and solvents corrosion [161]. Theoretically, chemical plating techniques are permissible to fabricate metal shells with tunable thickness and have been implemented successfully on such solid surface as, powders [162] and natural silk [163]. Recently, chemical plating technique was applied to microcapsules successfully. Patchan *et al.* [144] plated successfully a layer of Nickel

shell on polyurethane microcapsules. However, system characterizations of metal shell microcapsules were not shown yet. In addition, the plating solutions containing ammonia tends to consume massive isocyanates core. Herein, trifunctional microcapsules were fabricated successfully by plating a layer of Nickel shell on double-resistant microcapsules and displayed great stability in acetone. After trifunctional microcapsules being incorporated in epoxy matrix, the modulus of composites remains stable relatively with microcapsules concentration.

6.2 Overview of preparing trifunctional microcapsules

The trifunctional microcapsules were fabricated by plating chemically a layer of Nickel-P alloy covering double resistant microcapsules. The entire preparation process was divided into two steps. The first step is to deposit palladium (Pd) particles as catalyst on the surface of double resistant microcapsules and the second step was to initiate chemical plating in plating solutions.

The first step is to deposit Pd as catalyst on the surface of double resistant microcapsules. The Pd suspensions were prepared by reacting PdCl_2 with SnCl_2 in acid solutions. When SnCl_2 was added in PdCl_2 solutions, the Pd^{2+} cations can be reduced rapidly into Pd particles in aqueous solutions. Subsequently, slurry of newly prepared double resistant microcapsules was introduced in Pd suspensions and the Pd particles can be absorbed on the surface of microcapsules.

The second step is the conduct chemical plating on the surfaces of double resistant microcapsules under the catalysis of Pd. First of all, plating solutions were heated to target temperature. When double resistant microcapsules with catalyst was added into plating solutions, the Ni^{2+} cations in plating solutions were reduced immediately by sodium hypophosphite under the activation of Pd catalyst, with the formation of Nickel-P alloy surrounding Pd particles resulting in the deactivation of Pd particles. The freshly formed metal Nickel will serve as new catalyst to

activate subsequent chemical plating process, with the formation of metal shell on the surfaces of double resistant microcapsules. Metal shell was thickening gradually with reaction durations. After complete coverage of microcapsules by metal shells, the metal shell thickness continues to increase over durations. The surfactant in plating solution can eliminate hydrogen bubbles aggregating on shell surface for denser deposition of subsequent Nickel shell. After certain durations, the resultant trifunctional microcapsules with desired shell thickness can be prepared successfully.

6.3 Characterization of trifunctional microcapsules

6.3.1 Morphology of trifunctional microcapsules

The morphologies of trifunctional microcapsules were shown in Figure 6.1. Figure 6.1a show the overview of well-dispersed trifunctional microcapsules with diameters of $184.3 \pm 41.7 \mu\text{m}$ and related size distribution. Some small bumps (Figure 6.1b) were observed on the surface individual trifunctional microcapsule, and they were mainly produced from the uneven deposition of Nickel-P particles on the surfaces of double resistant microcapsules. The hollow inner structure (Figure 6.1c) of trifunctional microcapsules illustrates that the water and triethonamine molecules in plating solutions can hardly diffuse into the microcapsules to consume the inner HMDI during plating process, due to the excellent robustness of double resistant microcapsules. Moreover, the detailed information of cross-sectioned shells profile was shown in Figure 6.1d. The trifunctional shells with total thickness of $7.35 \pm 0.35 \mu\text{m}$ is a three-layered structure, which comprises of outer-layered metal shell with thickness of $5.52 \pm 0.21 \mu\text{m}$, medium-layered PUF shell with thickness of $369 \pm 21 \text{ nm}$, and inner-layered polyurea shell with thickness of $1.74 \pm 0.16 \mu\text{m}$.

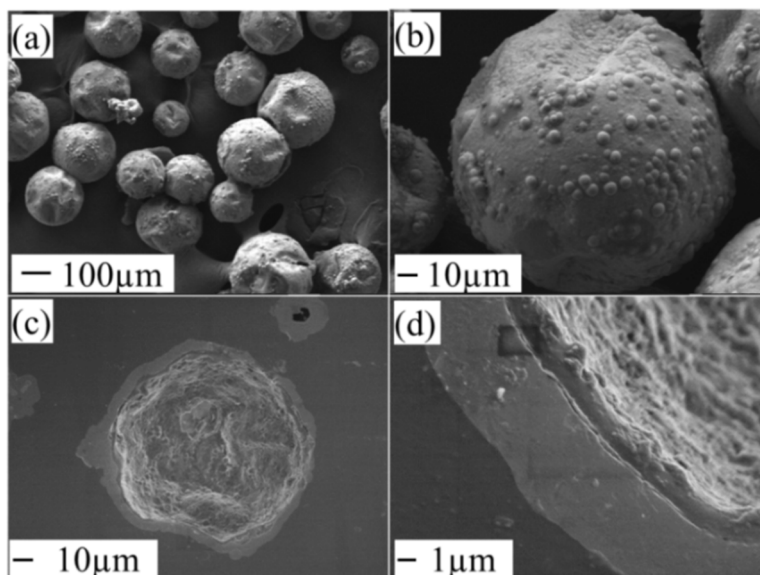


Figure 6.1 (a) Overview of trifunctional microcapsules; (b) Morphology of single trifunctional microcapsule; (c) Trifunctional microcapsules showed hollow inner structure; (d) The three-layered shell structure of trifunctional microcapsules.

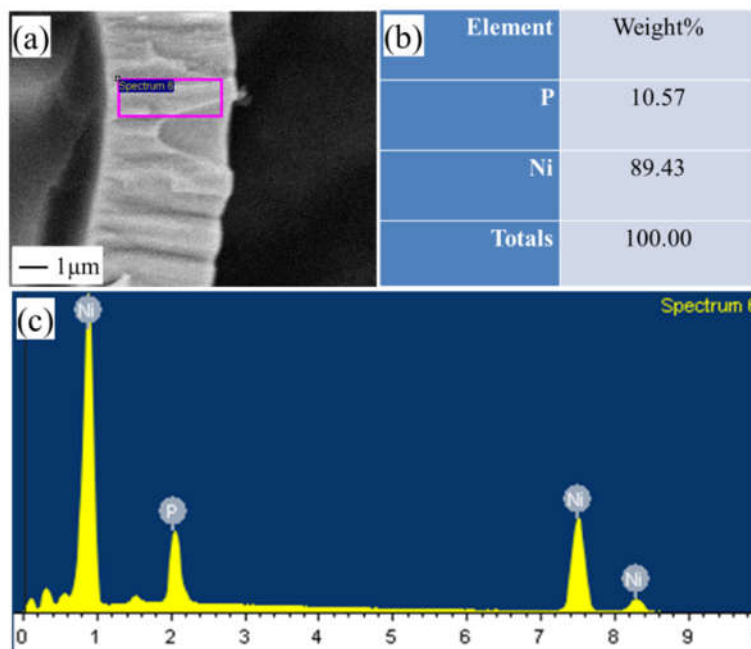


Figure 6.2 (a) The test area of metal shell; (b) Elements composition of metal shell, and (c) EDX spectrum of metal shell.

Moreover, the outer-layered metal shell was mainly comprised of Nickel-P alloy. The chemical composition of metal shell was determined through EDX analysis, as shown in Figure 6.2. The specific area on cross-section area of metal shell was chosen as target area (Figure 6.2a). The spectra curves of this area showed the existence of Nickel and P (Figure 6.2c) which consists of Nickel 89.4 wt% and Phosphorus 10.6 wt%.

6.3.2 Chemical determination of core materials

The chemical composition of core materials was determined by comparing the FTIR spectra curves of core materials with that of pure HMDI, as shown in Figure 6.3. The nearly identical curves of both substances demonstrate that HMDI was encapsulated successfully. In addition, the characteristic peak of NCO functional groups was presented in 2250 cm^{-1} .

6.3.3 Core fraction and thermal stability of trifunctional microcapsules

The core fraction of trifunctional microcapsules was determined by titrating crushed microcapsules to obtain NCO contents according to ASTM D2572-97, and then the NCO contents were converted into HMDI contents. The weight percentage of core materials was $22.4 \pm 0.6\text{ wt\%}$, and corresponding volume percentage was $73.1 \pm 1.9\%$, which is in agreement with theoretical values. The obvious difference between weight percentage and volume percentage was due to higher density of metal Nickel-P alloy (8.902 g/cm^3) than HMDI (1.07 g/cm^3).

The thermal stability of trifunctional microcapsules was tested by heating trifunctional microcapsules, shell materials of trifunctional microcapsules and pure HMDI from room temperature to $600\text{ }^{\circ}\text{C}$ at a rate of $10\text{ }^{\circ}\text{Cmin}^{-1}$ in Nitrogen atmosphere. The residual sample weight as a function of temperature was shown in Figure 6.4.

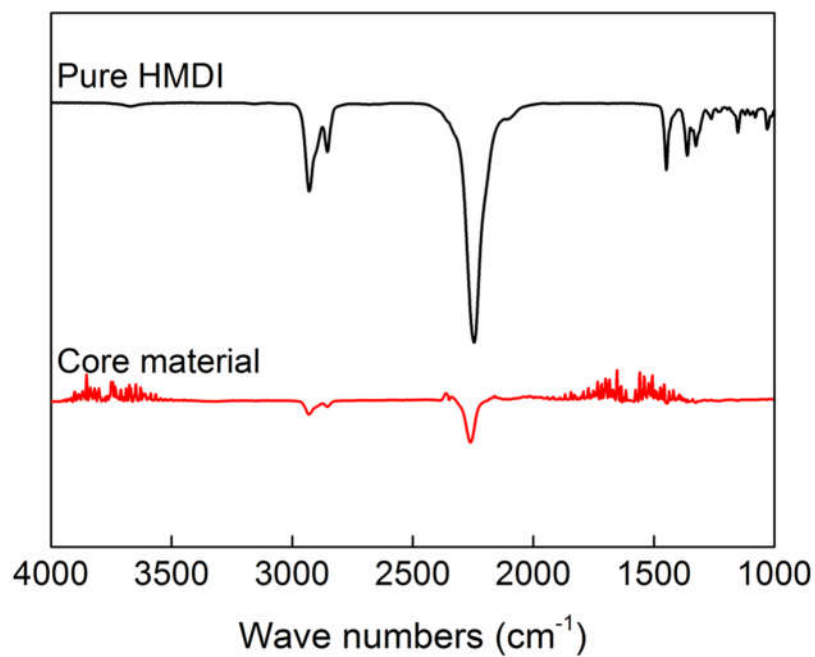


Figure 6.3 Comparison of FTIR curves of core materials and pure HMDI.

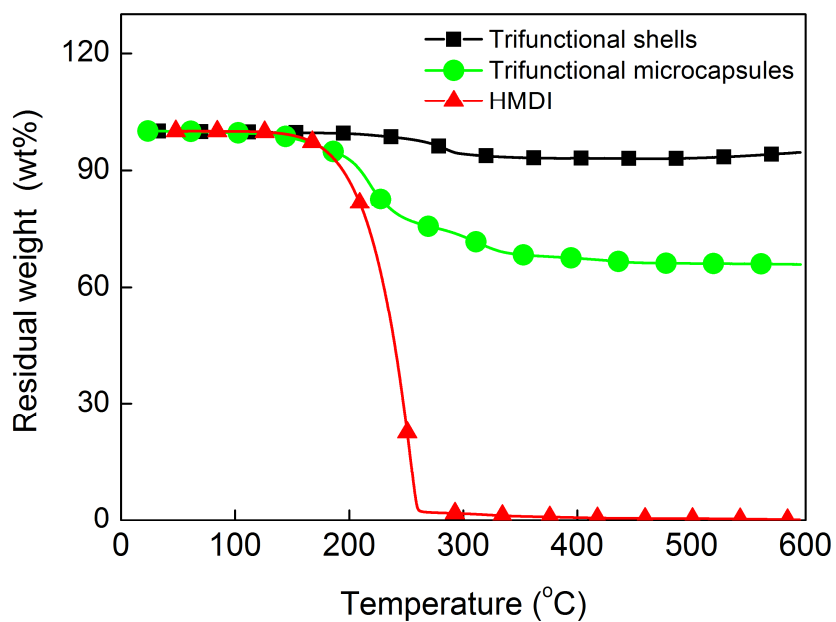


Figure 6.4 TGA weight loss curves of trifunctional shell materials, trifunctional microcapsules and pure HMDI as a function of temperature under heating procedure without isothermal process.

The shell materials remain nearly constant weight from room temperature to 250 °C. Subsequently, the shell materials begin to lose weight due to the thermal decomposition of organic constituents leaving metal constituents of 93 wt%. The trifunctional microcapsules begin to lose weight at around 180 °C due to the evaporation of HMDI core, followed by the decomposition of organic constituents of shell materials until 600 °C, leaving metal constituents of 66 wt%. Pure HMDI began to lose weight at around 180 °C, followed by the nearly vertical drop of samples weight due to massive evaporation of HMDI. The metal shell occupied around 66 wt% of trifunctional microcapsules providing great potential to improve microcapsules robustness and mechanical property.

6.4 Stability of trifunctional microcapsules in organic solvents and water

The stability of trifunctional microcapsules in organic solvents and water was tested by immersing trifunctional microcapsules in water and organic solvents for certain duration, and then characterized in terms of residual core fractions and morphologies.

6.4.1 Stability of trifunctional microcapsules in organic solvents

The trifunctional microcapsules were soaked in ambient hexane, xylene, ethyl acetate, and acetone for 10 days and 20 days, respectively. The residual core fractions of trifunctional microcapsules in different organic solvents as a function of immersion durations were shown in Figure 6.5. The shell morphology and inner structure of microcapsules after immersion in hexane (a₁, a₂), xylene (b₁, b₂), ethyl acetate (c₁, c₂) and acetone (d₁, d₂) were shown in Figure 6.6, respectively. As shown in Figure 6.5, the residual core fractions of trifunctional microcapsules decreased from 22.42±0.63 wt%, to 22.07±1.05 wt% (10 days) and 22.22±3.01 wt% (20 days) in hexane, to 23.65±1.01 wt% (10 days) and 21.05±1.00 wt% (20 days) in xylene, to 21.40±0.60 wt% (10 days) and 21.46±0.22 wt% (20 days) in ethyl acetate, and to 22.18±0.65 wt% (10 days) along

with 19.90 ± 0.69 wt% (20 days) in acetone, respectively. Obviously, the polarity of organic solvents influences little on the release of core materials. The residual core fractions of trifunctional microcapsules fluctuate slightly with immersion durations. Especially in acetone, the trifunctional microcapsules still remain highly stable without obvious decrease of core fractions. However, the isocyanates encapsulated in other shells were released massively in acetone within one hour [7, 8]. The outstanding stability of trifunctional microcapsules in acetone was due to dense structure of metal shell, which cannot be damaged by various organic solvents. After 20 days in organic solvents, all trifunctional microcapsules can remain constant morphologies and hollow inner structure, as shown in Figure 6.6.

The metal shell of trifunctional microcapsules can hardly be swelled by organic solvents, resulting in the stable core fraction of microcapsules. However, when microcapsules with polymeric shells were immersed in organic solvents, the polymeric shells can be swelled seriously resulting in massive release of core materials [7]. During swelling process, the mesh size of polymeric shells was enlarged by organic solvents resulting in the diffusion-out of liquid core. The metal shells can hardly be swelled by organic solvents.

6.4.2 Stability of trifunctional microcapsules in water

The stability of trifunctional microcapsules in water was tested by soaking microcapsules in ambient water for certain duration, and then characterized in terms of residual core fraction and morphologies.

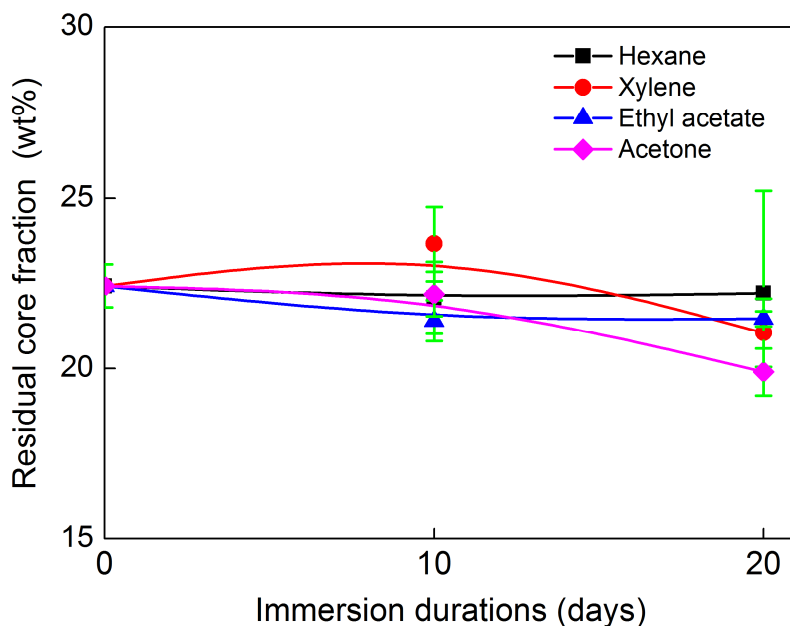


Figure 6.5 The residual core fraction of trifunctional microcapsules as a function of immersion durations after being immersed in hexane, xylene, ethyl acetate and acetone, respectively.

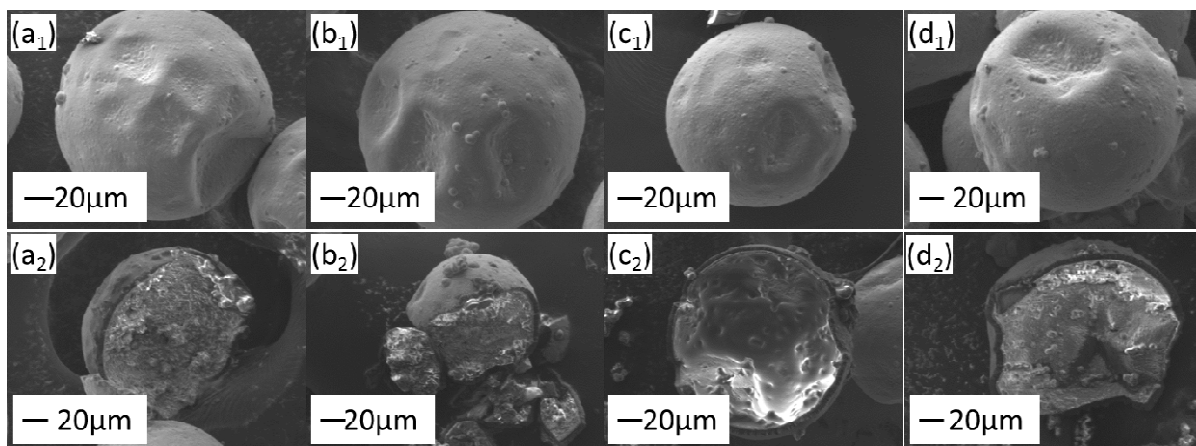


Figure 6.6 The outer morphology and inner structure of trifunctional microcapsules after being immersed in hexane (a₁, a₂), xylene (b₁, b₂), ethyl acetate (c₁, c₂) and acetone (d₁, d₂), respectively.

The residual core fractions of trifunctional microcapsules as a function of immersion durations in ambient water were shown in Figure 6.7. Figure 6.8 showed the morphologies and inner

structure of trifunctional microcapsules after 20 days in ambient water. The core fractions of trifunctional microcapsules decrease from 22.42 ± 0.63 wt% to 21.57 ± 0.23 wt% and 21.02 ± 0.74 wt%, when immersion durations were increased from 0 days, to 10 days and 20 days, respectively. The residual core fractions of trifunctional microcapsules fluctuated slightly with immersion durations in water, meaning that the plating solutions cannot impair the stability of trifunctional microcapsules in water. By comparing the stability of trifunctional microcapsules with that of double resistant microcapsules, it is reasonable to conclude that both types of microcapsules possess high stability in water. The final morphologies of trifunctional microcapsules after 20 days in ambient water still remain spherical (Figure 6.8a) and hollow inner structure (Figure 6.8b), proving that water cannot diffuse in microcapsules to consume HMDI core.

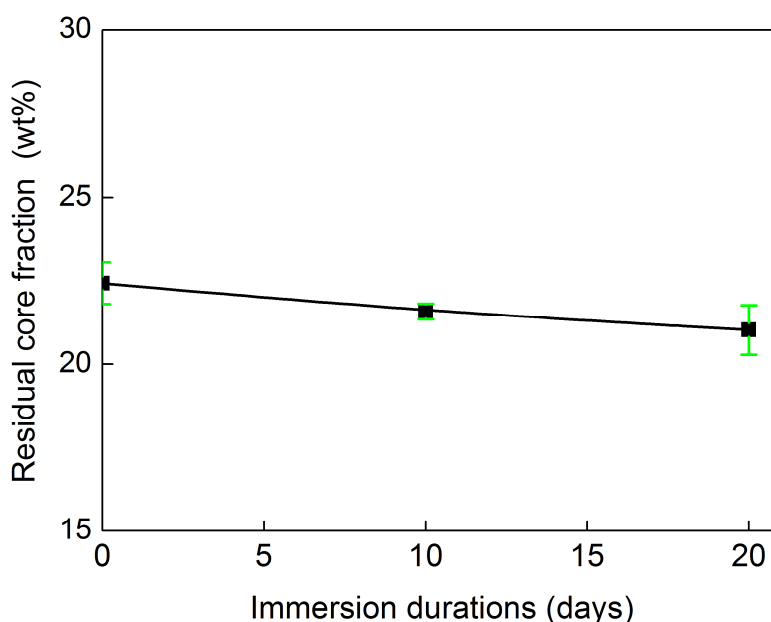


Figure 6.7 The residual core fraction of trifunctional microcapsules as a function of durations after being immersed in ambient water.

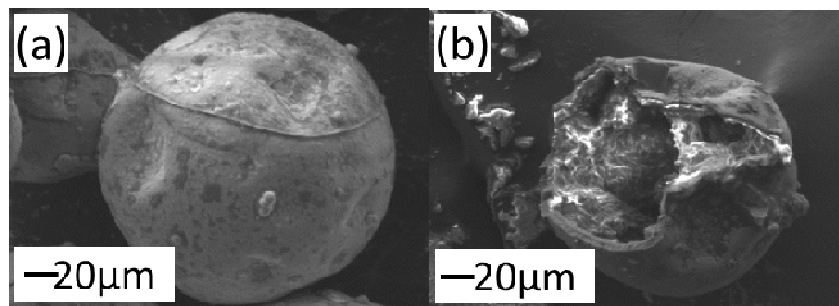


Figure 6.8 The outer morphology (a) and inner structure (b) of trifunctional microcapsules after being immersed in water for 20 days

6.5 Summary

Trifunctional microcapsules were fabricated successfully by plating a layer of metal shell on double resistant microcapsules. The main conclusions were shown in the following:

1. Current method can cover successfully a layer of metal shell on double-resistant with final thickness above 5 μm .
2. During the plating process, the encapsulated HMDI was consumed little in plating solutions, and the final core fractions of trifunctional microcapsules were above 70 v%.
3. The trifunctional microcapsules possess great stability in ambient water and organic solvents. After immersion in ambient water and organic solvents, the residual core fractions was remained as high as 90%. Especially, microcapsules remained constant core fractions after immersion in acetone for 20 days.

Chapter 7 Mechanical, anticorrosion and tribological performances of multifunctional composite coatings

7.1 Motivation

Our aim is to prepare a kind of multifunctional composite coating, which possesses both self-healing and self-lubricating functions, and it can be achieved by embedding microcapsules containing isocyanates in epoxy resin. We have fabricated successfully double-resistant microcapsules and tri-functional microcapsules containing HMDI as core. Double resistant microcapsules possess outstanding stability in ambient water and organic solvents with medium and low polarity, but weak mechanical properties. Plating a layer of metal shell covering double resistant microcapsules improved significantly shell strength. In order to investigate the influence of metal shell on self-healing and self-lubricating functions, detailed comparisons of double resistant microcapsules and trifunctional microcapsules were presented including mechanical properties, anticorrosion performance and tribological performance.

7.2 Mechanical properties of resultant microcapsules

The mechanical properties of microcapsules were characterized through two parts. The first part is to test mechanical strength of single microcapsules through published method. The second part is to measure the influence of microcapsules on the mechanical properties of epoxy matrix. Double resistant microcapsules and trifunctional microcapsules were dispersed in epoxy resin at certain concentrations, respectively, and the compressive strength and compressive modulus of composites can be obtained according to ASTM D695.

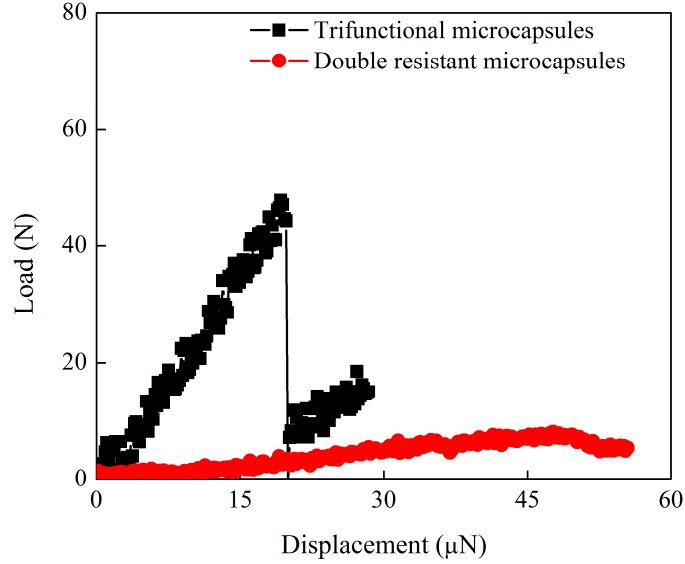


Figure 7.1 Typical load-displacement curves of double resistant microcapsules and trifunctional microcapsules.

7.2.1 Mechanical properties of shell materials

The micro-compressive apparatus were applied to measure the shell strength of double resistant microcapsules and tri-functional microcapsules according to the published method [160]. Figure 7.1 presents the load-displacement curves of double resistant microcapsules with diameters of 94.08 μm and trifunctional microcapsules with diameters of 99.14 μm.

The corresponding peak load of double resistant microcapsule was 7 mN, while the peak load of tri-functional microcapsules was 45 mN. Obviously, trifunctional microcapsules possess higher peak load than double resistant microcapsules due to the existence of metal shell.

In addition, the normalized shell strength (δ_{\max}) of microcapsules was calculated according to previous publication [1], and equation was shown in the following:

$$\delta_{max} = \frac{P_{max}}{\pi \left[\left(\frac{D_0}{2} \right)^2 - \left(\frac{D_i}{2} \right)^2 \right]} = \frac{P_{max}}{\pi t (D_0 - t)} \quad (7.1)$$

where P_{max} is the maximum load, D_0 is the outer diameter of microcapsules, D_i is the inner diameter of microcapsules, and t is the shell thickness of microcapsules.

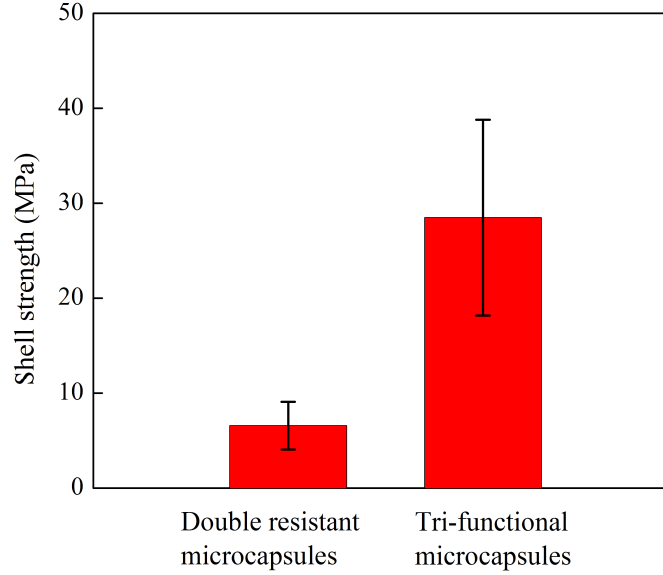


Figure 7.2 Normalized shell strength of double resistant microcapsules and trifunctional microcapsules.

Based on a total of 10 measurements, the statistic shell strengths of double resistant microcapsules and trifunctional microcapsules were 6.6±2.5 MPa and 28.5±10.3 MPa, respectively, as shown in Figure 7.2. Obviously, the shell strength of microcapsules was improved by 332% by covering a layer of metal shell on double resistant microcapsules due to the higher strength and modulus of metal materials.

7.2.2 Influence of microcapsules on mechanical properties of epoxy composites

Normally, higher microcapsules concentrations correspond to weaker mechanical strength of composites. In order to test the influence of resultant microcapsules on the mechanical properties

of composites, double-resistant microcapsules and trifunctional microcapsules were embedded in epoxy resin at different concentrations (10 wt%, 20 wt% and 30 wt%) and the composites were then tested according to ASTM-D695. The compressive strength and compressive modulus of composites were presented in Figure 7.3 and 7.4.

As shown in Figure 7.3, the composites show weaker compressive strength with the increase of microcapsules concentration. The compressive strength of composites containing double resistant microcapsules decreases from 100.98 ± 1.35 MPa to 72.23 ± 0.055 MPa, 55.03 ± 0.17 MPa, and 40.27 ± 0.025 MPa corresponding to the microcapsules concentrations increase from 0 wt% to 10 wt%, 20 wt% and 30 wt%, respectively. The compressive strength of composites containing trifunctional microcapsules decreases from 100.98 ± 1.35 MPa to 86.9 ± 0.71 MPa, 78.24 ± 0.39 MPa, and 69.42 ± 1.09 MPa when the concentrations of trifunctional microcapsules rose from 0 wt% to 10 wt%, 20 wt% and 30 wt%, respectively. The compressive strength of composites containing both microcapsules showed a decreasing trend with the increase of microcapsules concentrations. The microcapsules in composites were considered as a kind of flaws, and higher concentrations results in more flaws and weaker compressive strength. Although compressive strength of composites shows decreasing trends under higher microcapsules concentrations, epoxy composites containing tri-functional microcapsules still possess higher compressive strength than that containing double resistant microcapsules. The difference was magnified significantly with the increase of microcapsules concentrations. The main reason was that the metal shell of tri-functional microcapsules can improve efficiently the mechanical strength of microcapsules.

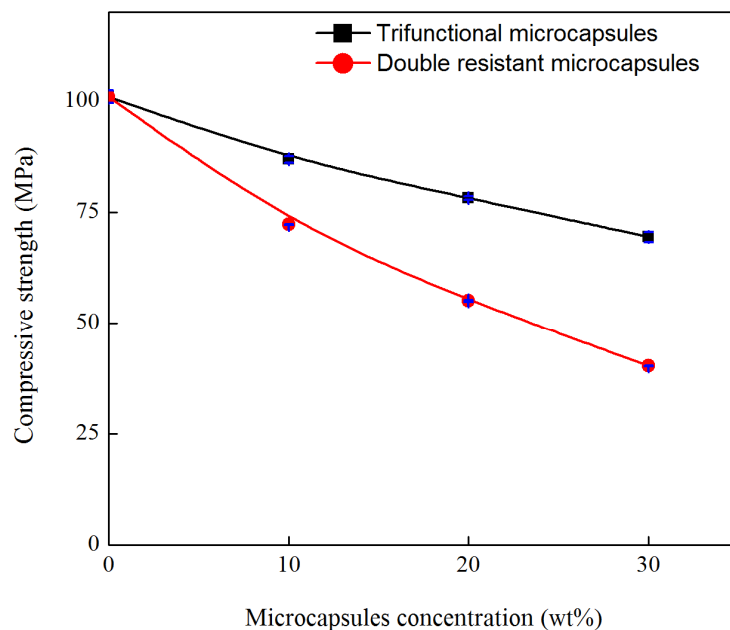


Figure 7.3 Compressive strength of composites containing double resistant microcapsules and trifunctional microcapsules as a function of microcapsules concentration.

Different from compressive strength, the compressive modulus of composites containing trifunctional microcapsules varied slightly with microcapsules concentrations. However, the compressive modulus of composites containing double resistant microcapsules still remains in decreasing trend. As shown in Figure 7.4, modulus of epoxy composites containing double-resistant microcapsules decreased from 2.54 ± 0.11 GPa, to 2.24 ± 0.05 GPa, 1.77 ± 0.04 GPa and 1.23 ± 0.04 GPa corresponding to the increase of microcapsules concentration from 0 wt% to 10 wt%, 20 wt%, and 30 wt%, respectively. When tri-functional microcapsules were introduced in epoxy matrix, the modulus of composites remain relatively stable around 2.54 ± 0.106 GPa, 2.53 ± 0.02 GPa, 2.54 ± 10^{-3} GPa and $2.36 \pm 5 \times 10^{-4}$ GPa with the increase of microcapsules concentration from 0 wt% to 10 wt%, 20 wt%, and 30 wt%, respectively.

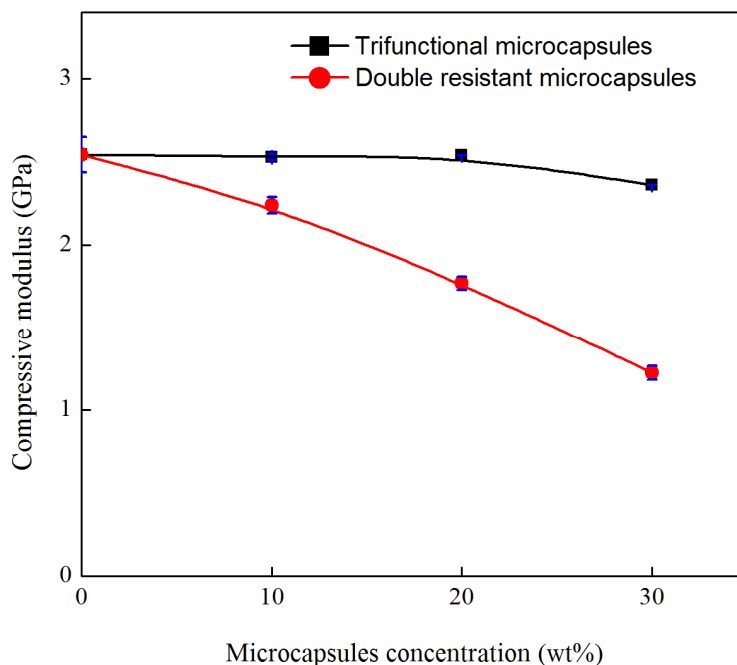


Figure 7.4 Compressive modulus of composites containing double resistant microcapsules and trifunctional microcapsules as a function of microcapsules concentration.

The main reason why composite containing trifunctional microcapsules remain stable compressive modulus was that metal shell possesses nearly identical modulus with epoxy matrix. The higher modulus of epoxy composites containing tri-functional microcapsules than those containing double-resistant microcapsules was due to the higher modulus of trifunctional microcapsules than double resistant microcapsules.

7.3 Influence of resultant microcapsules on anticorrosion performance of multifunctional composite coatings

In order to study the anticorrosion performance of resultant microcapsules, two types of microcapsules including double-resistant microcapsules and trifunctional microcapsules were dispersed in epoxy resin at a concentration of 10 wt%, and then covered uniformly on steel

panels as self-healing samples with final thickness around 300-400 μm after cure. For comparison, control samples were prepared by covering pure epoxy resin on steel panels.

7.3.1 Anticorrosion performance of self-healing coatings towards steel panels

After cure for 24h at ambient temperature, all specimens were scratched manually, then were immersed in salty water (1M) for accelerated corrosion. After 24h, the corrosion performances of specimens were shown in Figure 7.5. As shown in Figure 7.5a₁, severe corrosion occurs to control specimens because empty scratches (Figure 7.5a₂) within control coatings result in the direct exposure of steel substrates in corrosive environments. However, self-healing specimens containing double resistant microcapsules (Figure 7.5b₁) and tri-functional microcapsules (Figure 7.5c₁) were fully rust free after 24 h immersion in corrosive environments.

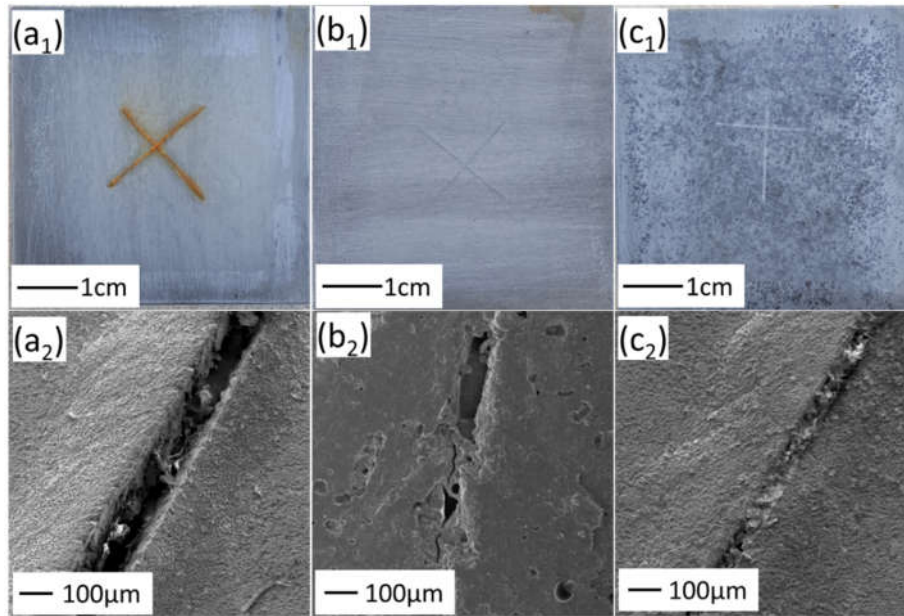


Figure 7.5 The corrosion performances and detailed information in scratches of coatings including control specimens (a₁, a₂), self-healing specimens containing double resistant microcapsules (b₁, b₂), and self-healing specimens containing trifunctional microcapsules (c₁, c₂).

The main reason was that the released HMDI from broken microcapsules polymerized with surrounding moisture into polyurea membrane to seal the scratches, as shown in Figure 7.5b₂ and c₂. The polyurea films within scratches of self-healing specimens isolate efficiently corrosive environments to keep the steel substrates free of rust.

7.3.2 Self-healing anticorrosion process monitored by EIS

The anticorrosion processes of self-healing specimens were further characterized through Electrochemical Impedance Spectroscopy (EIS) based on published model (Figure 7.6a) and equivalent circuit (Figure 7.6b) [145]. The obtained healing resistance (R_{healing}) from equivalent circuits can supply detailed information about the self-healing process at scratched area. Figure 7.7a presents R_{healing} of self-healing specimens containing double resistant microcapsules varied with corrosion durations, while Figure 7.7b shows R_{healing} of self-healing specimens containing tri-functional microcapsules varied with immersion durations.

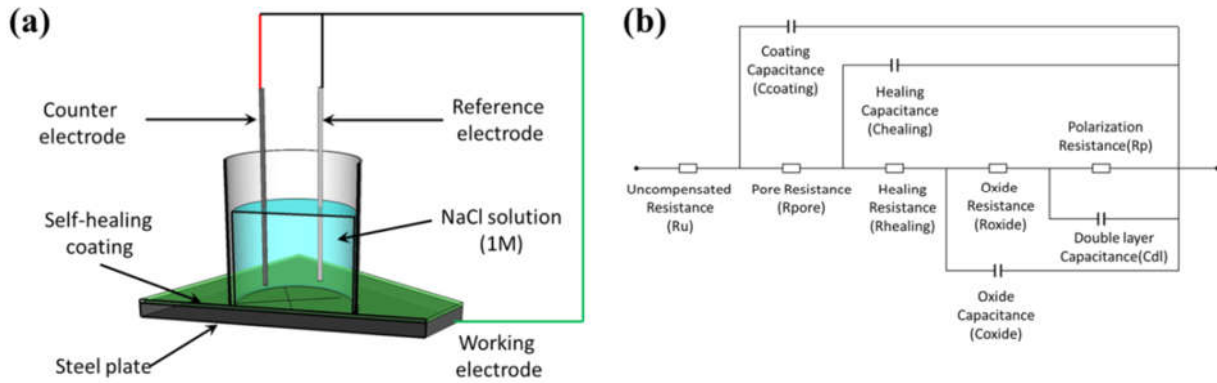


Figure 7.6 (a) The schematic picture of EIS experiment model; (b) The equivalent circuit applied to obtain the resistance due to healing (R_{healing}) by curve fitting.

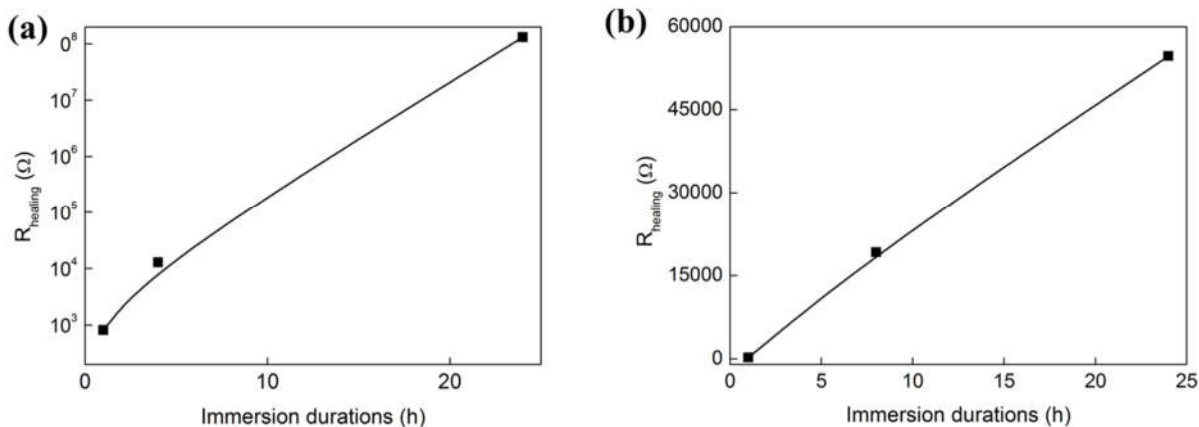


Figure 7.7 The healing resistance (R_{healing}) of scratched self-healing coating containing double resistance microcapsules (a) and trifunctional microcapsules (b) as a function of immersion durations.

As shown in Figure 7.7a, the R_{healing} of scratched self-healing coating containing double resistant microcapsules increases from 815Ω to $1.28 \times 10^4 \Omega$ and $1.32 \times 10^8 \Omega$, while R_{healing} (Figure 7.7b) of that containing tri-functional microcapsules rises from 261.4Ω to $1.92 \times 10^4 \Omega$ and $5.47 \times 10^4 \Omega$ when immersion duration in NaCl solutions extends from 1h to 4h, and 24h, respectively. The higher R_{healing} under longer immersion time means that more healing agent was polymerized in the scratched area resulting in the increase of electrical resistance at scratched area.

7.4 Tribology performance

Self-lubricating samples including pure epoxy, composites containing 10 wt% of double-resistant microcapsules (Composites DR-10 wt%), composites containing 10 wt% of tri-functional microcapsules (Composites Tri-10wt%) and composites containing 30 wt% of tri-functional microcapsules (Composites Tri-30wt%) were conducted tribological test to obtain the influence of microcapsules on friction performance of epoxy composites. The tribological experiments were conducted by sliding against a Cr6 steel ball in diameter of 4 mm for 8 h at various sliding rates (25 REV, 50 REV and 100 REV) under different normal loads (3 N, 5 N

and 10 N). The final tribological properties of samples were characterized in terms of friction coefficient and wear loss.

7.4.1 The influence of normal loads on tribology of epoxy composites

Three normal loads (3 N, 5 N and 10 N) were applied to tribological experiments of pure epoxy samples, composites DR-10wt%, composites Tri-10wt% and composites Tri-30wt% at sliding rate of 50 REV and wear duration was set as 8 hrs. The friction coefficients of related samples as a function of wear durations were shown in Figure 7.8. The average value of friction coefficient between 10000 s and 28800 s was set as the friction coefficient of samples.

Influence of normal loads on friction coefficient

Figure 7.8 presents the friction coefficients of pure epoxy samples (a), composites Tri-10wt% (b), composites Tri-30wt% (c) and composites DR-10wt% (d) as a function of friction durations. Except composites DR-10wt%, the friction coefficients of other samples increase firstly until balance. At the beginning of friction process, the smooth surface of steel ball was firstly roughened by samples resulting in gradual increase of friction coefficient until balance. Normally, the steel ball can be roughened more easily under higher normal loads resulting in shorter duration to reach balance. For composites DR-10wt%, the embedded double resistant microcapsules can be easily broken and released massive liquid core as lubricant resulting in the sudden balance of friction coefficient at the beginning of friction process. After balance, the friction coefficient of samples increase slightly over durations due to the increase of contact interface, which tends to increase the mechanical interlocking between two mating surfaces [164, 165]. In addition, the tribolayer of pure epoxy samples, composites Tri-10wt%, composites Tri-

30wt% can be observed obviously from the wear track, as shown in Figure 7.9 (a₁, b₁, c₁)(3N), (a₂, b₂, c₂)(5N) and (a₃, b₃, c₃)(10N).

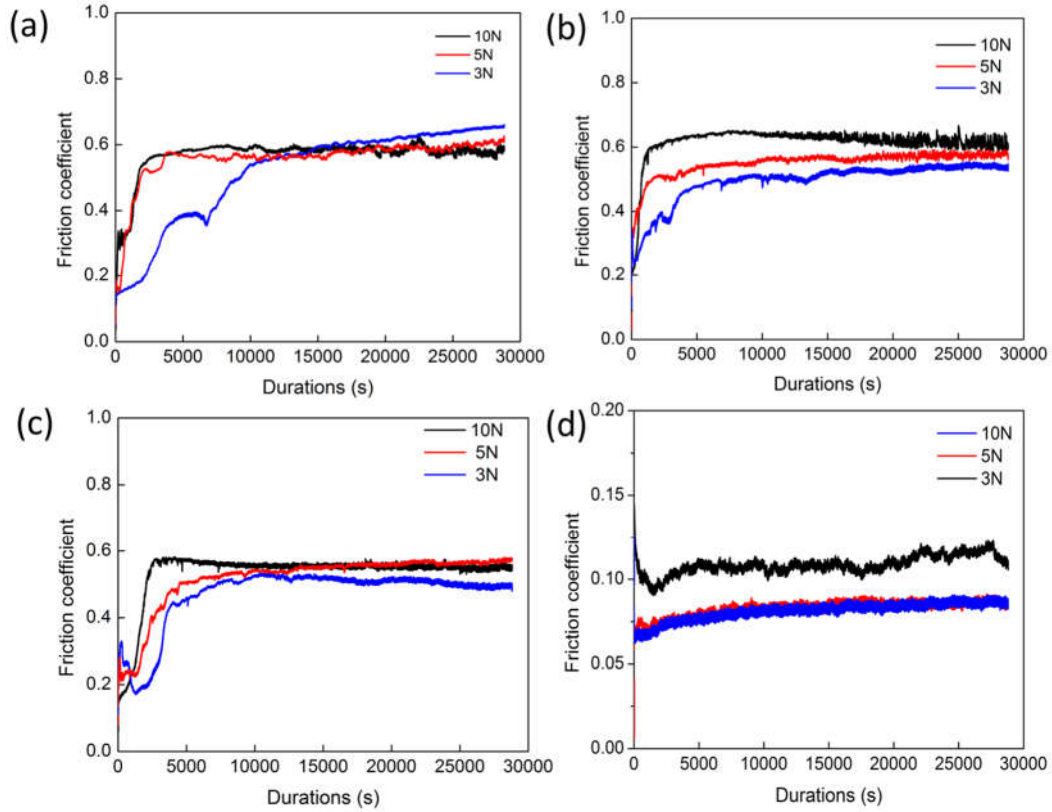


Figure 7.8 Friction coefficient of samples as a function of durations under different normal loads (3N, 5N, and 10N) at sliding velocity of 50 REV. (a) Pure epoxy samples; (b) Composites Tri-10wt%; (c) Composites Tri-30wt%, and (d) composites DR-10wt%.

However, tribolayer was not observed on the wear track of composites DR-10wt% due to the existence of massive liquid lubricant, as shown in Figure 7.9, d₁ (3N), d₂ (5N) and d₃ (10N). When liquid HMDI was released from broken double resistant microcapsules onto the wear track, the friction process were retarded and less debris was produced. The tribolayer was mainly made from compacted wear debris on the wear track. Therefore, it is reasonable to observe the disappearance of tribolayer on the wear track of composites DR-10wt%.

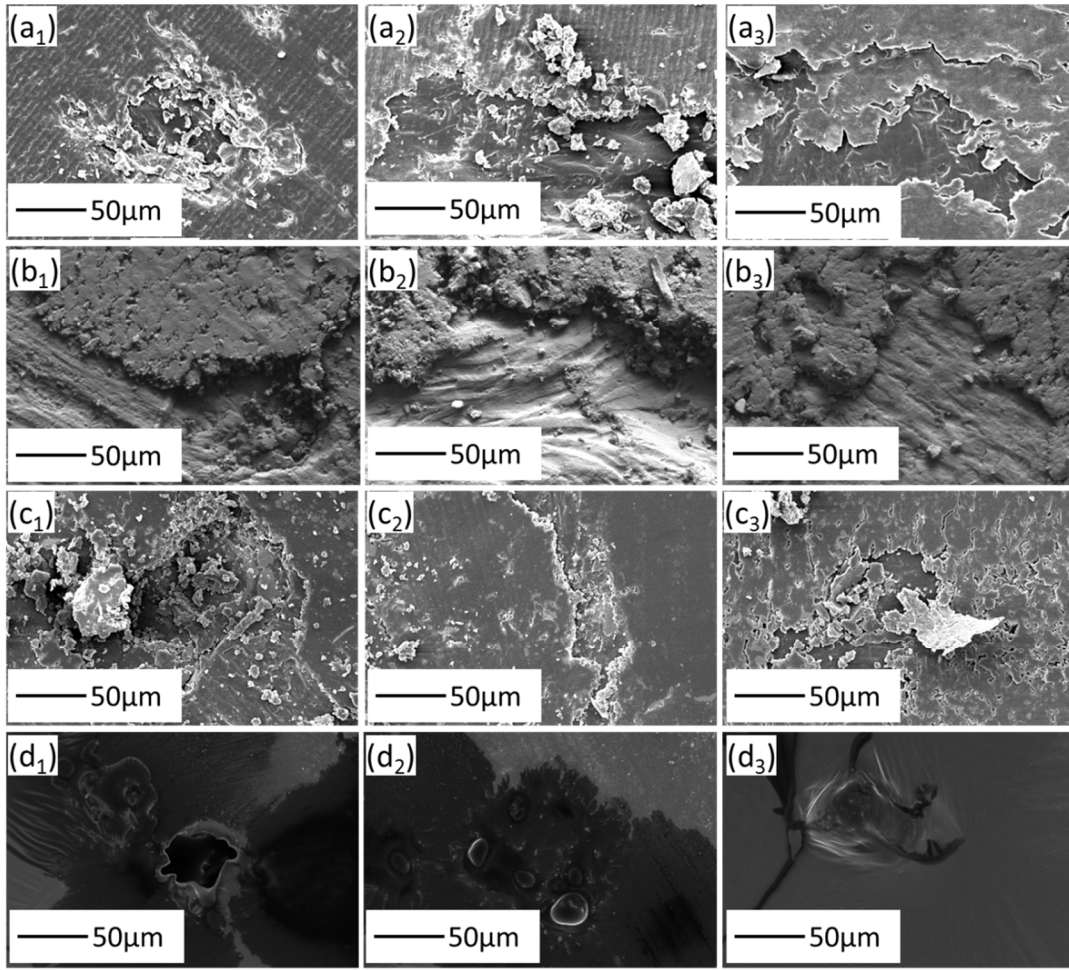


Figure 7.9 The detailed morphology of the wear track of pure epoxy samples (a), composites Tri-10wt% (b), composites Tri-30wt% (c) and composites DR-10wt% (d) under normal loads of 3N (a_1 , b_1 , c_1 and d_1), 5N (a_2 , b_2 , c_2 and d_2) and 10N (a_3 , b_3 , c_3 and d_3).

Influence of load on friction coefficient of composites

The friction coefficient of different samples containing pure epoxy samples, composites DR-10 wt%, composites Tri-10 wt% and composites Tri-30 wt% shows different trends under increasing normal loads, as shown in Figure 7.10. The friction coefficient of pure epoxy samples decrease slightly from 0.6085 to 0.5819 and 0.5837 when normal loads increase from 3N to 5N and 10N, respectively. Under higher normal load, the formed tribolayer on the wear track of pure

epoxy samples can be compacted more seriously. The more compact tribolayer is somewhat harder to lower the friction by lessening the contact between the rubbing surfaces. The friction coefficients of composites Tri-10 wt% increase from 0.525 to 0.569 and 0.623 when normal loads were increased from 3 N to 5 N and 10 N, respectively. Although more liquid core can be released onto wear track to decrease friction coefficient under higher normal loads, the existing metal shell tends to increase friction coefficient by increasing adhesion wear [84]. More metal shell can be worn into powder covering on the track under higher normal loads. When the concentration of tri-functional microcapsules concentration was increased to 30 wt%, the friction coefficient of composites fluctuated slightly under normal loads from 3 N to 5 N and 10 N, respectively. The friction coefficients of composites Tri-30 wt% increased from 0.5104 to 0.5569 when normal load was increased from 3 N to 5 N. Under higher load, more metal debris was produced to increase friction coefficient. However, the friction coefficients of composites Tri-30 wt% were levelled around 0.55 (from 0.5569 (5 N) to 0.5525 (10 N)) when normal load increases from 5 N to 10 N. Although more adhesion wear occurs to increase friction coefficient, some beneficial factors still exist to decrease friction coefficient. The first factor is that more microcapsules can be broken to release more liquid HMDI as lubricant under higher loads. The second reason is that the formed tribolayer on the track was more compact under higher load, and harder surface is favorable to decrease friction coefficient by decreasing contact interface. The friction coefficient of composites DR-10 wt% displayed a decreasing trend. The final friction coefficients decreased from 0.1105 to 0.0856 and 0.08418 when normal load was raised from 3 N to 5 N and 10 N, respectively. Under higher loads, more microcapsules can be broken to release more HMDI core as lubricant to decrease friction coefficients.

The shell materials of microcapsules influence significantly on the friction coefficient of composites. When embedded microcapsules possess polymeric shell materials, the microcapsules can be easily broken and release liquid HMDI core as lubricant to decrease friction coefficient. Comparing with pure epoxy samples, the friction coefficient of composites containing double resistant microcapsules decreased by 81.8% (3 N), 85.3% (5 N) and 85.6% (10 N) under different normal loads, respectively. When embedded microcapsules in epoxy composites possess metal shell, decrease of friction coefficient was not as obvious as that of composites containing double resistant microcapsules. The friction coefficient of composites containing metal shell microcapsules fluctuates obviously under different normal loads, when trifunctional microcapsules were embedded into epoxy resin at a concentration of 10 wt%. The friction coefficient of composite Tri-10wt% decreased by 13.3 %, 3.4% and -6.7% comparing with pure epoxy samples, under normal loads increasing from 3 N to 5 N and 10 N, respectively. When normal load is 10 N, the friction coefficient of composites Tri-10wt% decreases by 6.7% than \ pure epoxy samples. The main reason is that the existing metal shell powder tends to increase friction coefficient resulting in inefficient lubrication of liquid core. Even when the concentration of tri-functional microcapsules increased from 10 wt% to 30 wt%, the friction coefficient of composites was improved very slightly, as shown in Figure 7.10. Therefore, it is reasonable to conclude that the metal shell influence negatively on the lubricating performance of microcapsules in epoxy matrix.

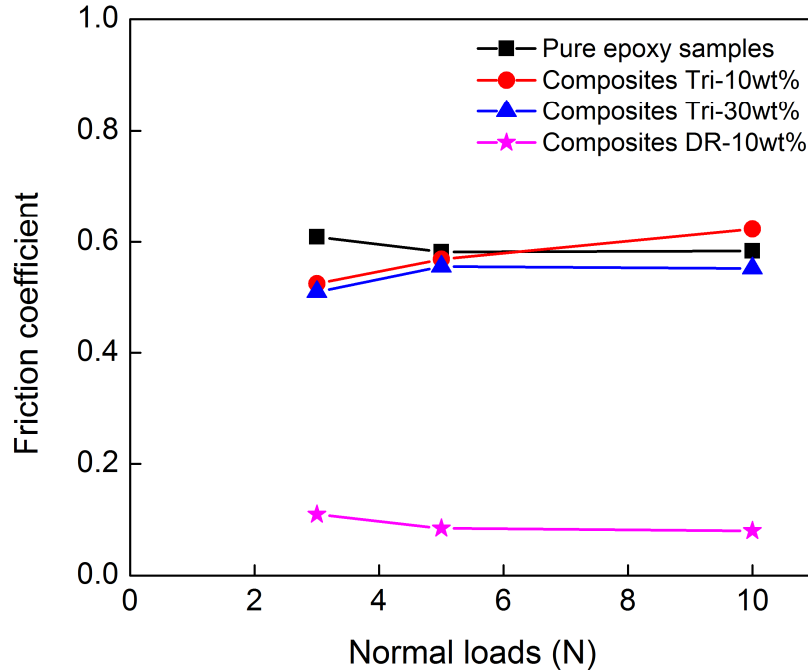


Figure 7.10 The friction coefficient of pure epoxy samples, composites Tri-10wt%, composites Tri-30wt% and composites DR-10wt% as a function of normal loads (3 N, 5 N and 10 N).

Influence of normal loads on wear loss of composites

Besides friction efficient, wear loss of composites including pure epoxy samples, composites DR-10 wt%, composites Tri-10 wt%, and composites Tri-30 wt% was influenced insignificantly by normal loads, and the wear loss was characterized in terms of wear width and wear depth, as shown in Figure 7.12 and Figure 7.13. The wear width and wear depth are obtained from the surface topographies of wear track, and a typical topographies (a) and profile (b) of wear track (pure epoxy samples, 5 N, 50 REV) were shown in Figure 7.11. From the surface topographies (Figure 7.11a) of wear track, the wear width and wear depth can be obtained, as shown in Figure 7.11b.

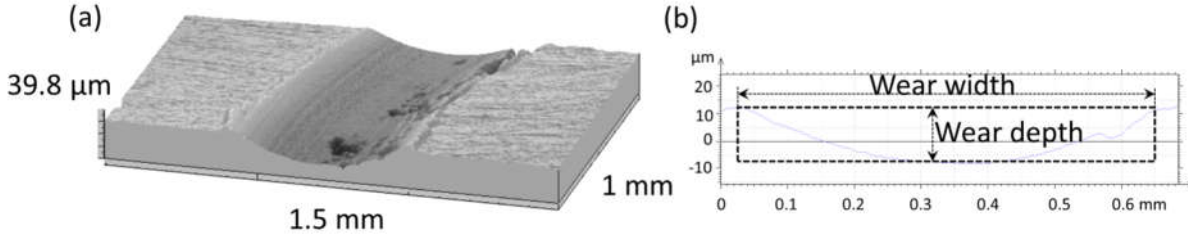


Figure 7.11 (a) The topography of wear track of pure epoxy samples (5 N, 50 REV); (b) Profile of related wear track.

Figure 7.12 showed that wear width varied as a function of normal loads under sliding velocity of 50 REV. Obviously, the wear widths of all samples increase gradually under higher normal loads. When normal load increases from 3 N to 5 N and 10 N, the wear width of samples increase from 0.62 ± 0.05 mm to 1 ± 0.06 mm and 1.57 ± 0.12 mm (pure epoxy samples); from 0.68 ± 0.05 mm to 0.94 ± 0.04 mm and 2 ± 0.07 mm (composites Tri-10 wt%); from 0.64 ± 0.03 mm to 0.9 ± 0.05 mm and 1.47 ± 0.18 mm (composites Tri-30 wt%); from 0.4 ± 0.06 mm, 0.43 ± 0.1 mm and 0.8 ± 0.05 mm (composites DR-10 wt%), respectively. Figure 7.13 presents that the wear depth of samples also increase gradually under higher normal loads. When normal loads increase from 3 N to 5 N and 10 N, the wear depth of samples increase from 17.84 ± 2.44 μm to 58.2 ± 4.22 μm and 180.55 ± 27.54 μm (pure epoxy samples); from 20.5 ± 2.77 μm to 58.56 ± 9.94 μm and 236.2 ± 16.82 μm (composites Tri-10 wt%); from 4.02 ± 0.54 μm to 50.55 ± 9.7 μm and 159.87 ± 34.95 μm (composites Tri-30wt%); and from 1.09 ± 0.41 μm to 5.8 ± 3.03 μm and 26.6 ± 3.48 μm (composites DR-10 wt%), respectively. The main reason why wear width and wear depth increase under higher normal loads was because higher friction force was produced under higher normal loads to aggravate the wear of matrix. The existence of metal shell in microcapsules aggravates wear loss of composites. When trifunctional microcapsules were embedded into epoxy matrix at a concentration of 10 wt%, the wear loss including wear width

and wear depth of composites was higher than those of pure epoxy samples. The main reason was that the embedded trifunctional microcapsules decreased the strength of epoxy matrix resulting in the increase of wear loss [166]. Although released HMDI can serve as lubricant to decrease wear, the existence of metal shell tends to increase friction coefficient resulting in more wear loss [84]. The concentration of trifunctional microcapsules influences slightly on the wear loss of composites. When concentration of trifunctional microcapsules in epoxy matrix was increased from 10 wt% to 30 wt%, the wear loss was improved slightly. The double resistant microcapsules possess outstanding self-lubricating performance in epoxy resin. When double resistant microcapsules were introduced in epoxy matrix at a concentration of 10 wt%, the wear loss of composites decreased very obviously. Comparing with pure epoxy samples, the wear width of composites DR-10wt% decreased by 35%, 57% and 49%, and the wear depth decreased by 98.3%, 90% and 85% when normal load increased from 3 N to 5 N and 10 N, respectively. The double resistant microcapsules can be damaged easily and released massive liquid core as lubricant during wear process. Residual broken microcapsules can still be observed in Figure 7.9 d_1 (3 N), d_2 (5 N) and d_3 (10 N). However, comparing to composites DR-10wt%, the wear width and wear depth of composites Tri-10wt% was increased very obviously under the same normal loads. Even when the concentration of trifunctional microcapsules was elevated from 10 wt% to 30 wt%, the wear loss of composites-30 wt% was improved slightly and still larger than that of composites DR-10wt%. The main reason is that metal shells tend to increase friction coefficient [84].

Therefore, it is reasonable to conclude that double resistant microcapsules possess excellent self-lubricating function to retard the wear of composites, while the trifunctional microcapsules influence slightly on the wear performance of composites due to the existence of metal shell.

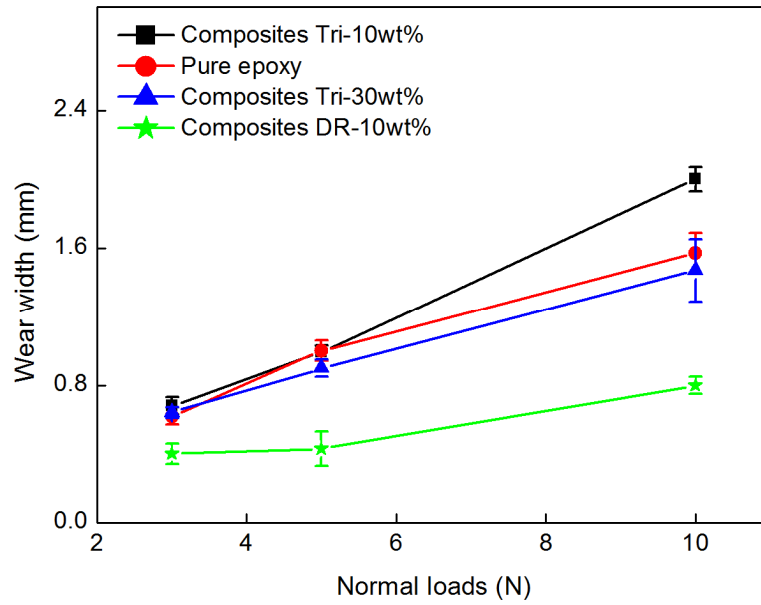


Figure 7.12 The wear width of pure epoxy samples, composites Tri-10wt%, composites Tri-30wt% and composites DR-10wt% as a function of normal loads (3 N, 5 N and 10 N).

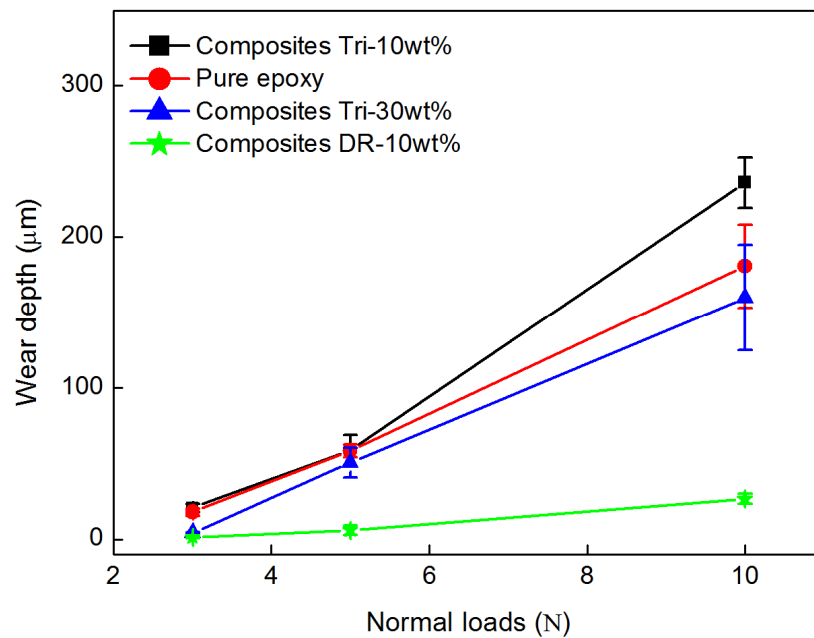


Figure 7.13 The wear depth of pure epoxy samples, composites Tri-10wt%, composites Tri-30wt% and composites DR-10wt% as a function of normal loads (3 N, 5 N and 10 N).

7.4.2 The influence of sliding velocities on tribology of epoxy composites

Besides normal loads, sliding velocities also influence significantly on the friction coefficient and wear loss of pure epoxy. Composites containing pure epoxy samples, composites tri-10wt%, composites tri-30wt% and composites DR-10wt% were tested at increasing sliding velocities of 25 REV, 50 REV and 100 REV for 8 hrs under normal load of 5 N. The tribological performances of samples were characterized in terms of friction coefficient and wear loss.

Influence of sliding velocities on friction coefficient of composites

Figure 7.14 showed the friction coefficient of pure epoxy samples (a), composites Tri-10wt% (b), composites Tri-30wt% (c) and composites DR-10wt% (d) as a function of friction durations at different sliding velocities (25 REV, 50 REV and 100 REV). Except composites DR-10wt%, the friction coefficients of other samples reach stable gradually because the steel ball was roughened gradually with friction durations. Faster sliding velocities corresponds faster formation of stable friction coefficient. However, the friction coefficient of composites DR-10wt% remain stable at the beginning of friction process. The main reason was that double resistant microcapsules can be broken easily and release massive liquid core as lubricant at the beginning of friction process. The lubricants keeps the friction coefficient of composites DR-10wt% at a low value. After balance, the friction coefficients of all samples increase slightly over durations due to bigger contact interface, which was increased gradually with wear depth and wear width. More mechanical interlock will be produced under bigger contact interface resulting in the increase of friction coefficient.

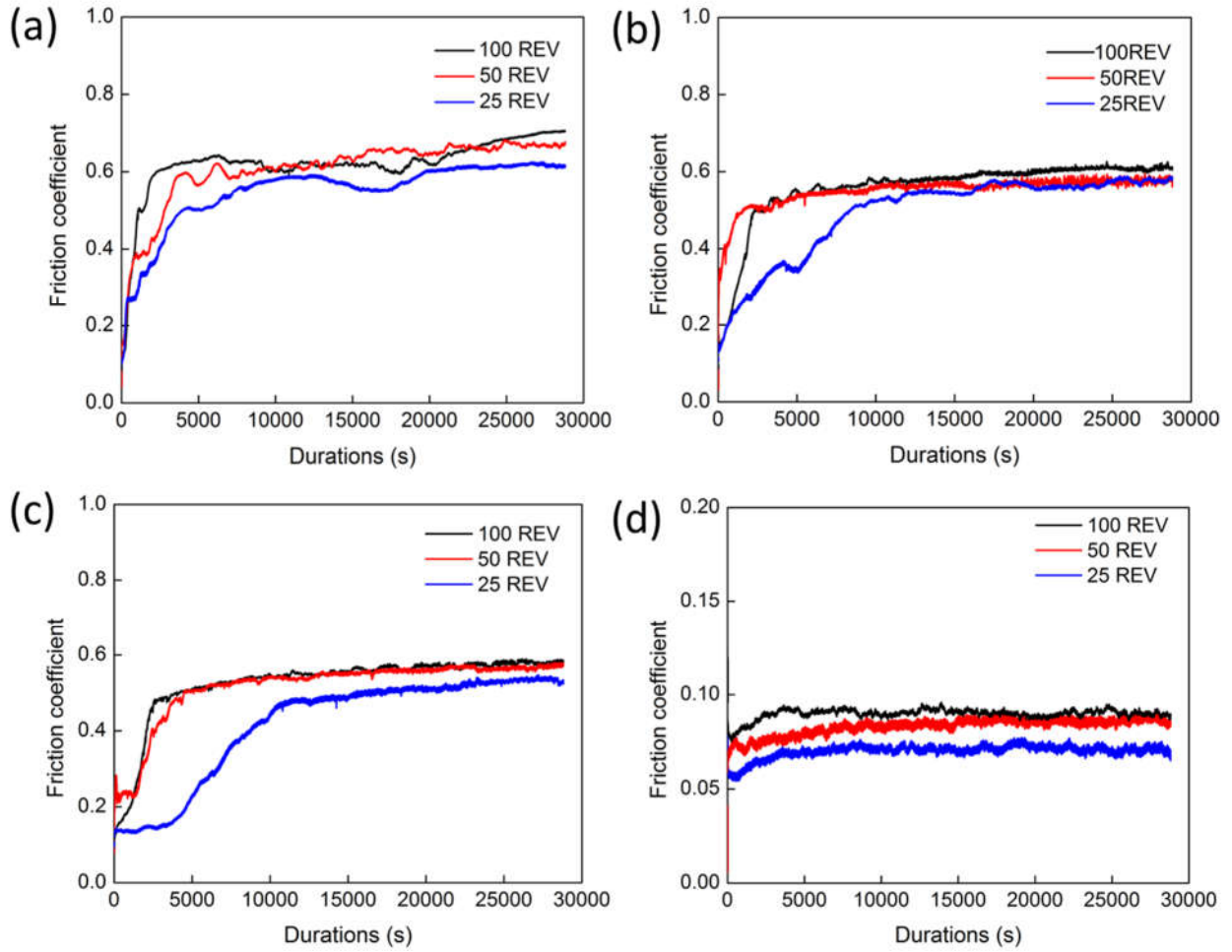


Figure 7.14 Friction coefficient of pure epoxy samples (a), composites Tri-10wt% (b), composites Tri-30wt% (c) and composites DR-10wt% (d) as a function of durations under normal load of 5 N at sliding rates of 25 REV, 50 REV and 100 REV.

The formed tribolayer of pure epoxy samples (a), composites Tri-10wt% (b), and composites Tri-30wt% on the track at sliding velocities of 25 REV (a_1, b_1, c_1), 50 REV (a_2, b_2, c_2) and 100 REV (a_3, b_3, c_3) can be observed from Figure 7.15. However, the tribolayer cannot be formed on the wear track of composites DR-10wt%, as shown in Figure 7.15 (d_1, d_2 and d_3), because massive liquid core can be released as lubricant to retard the formation of tribolayer.

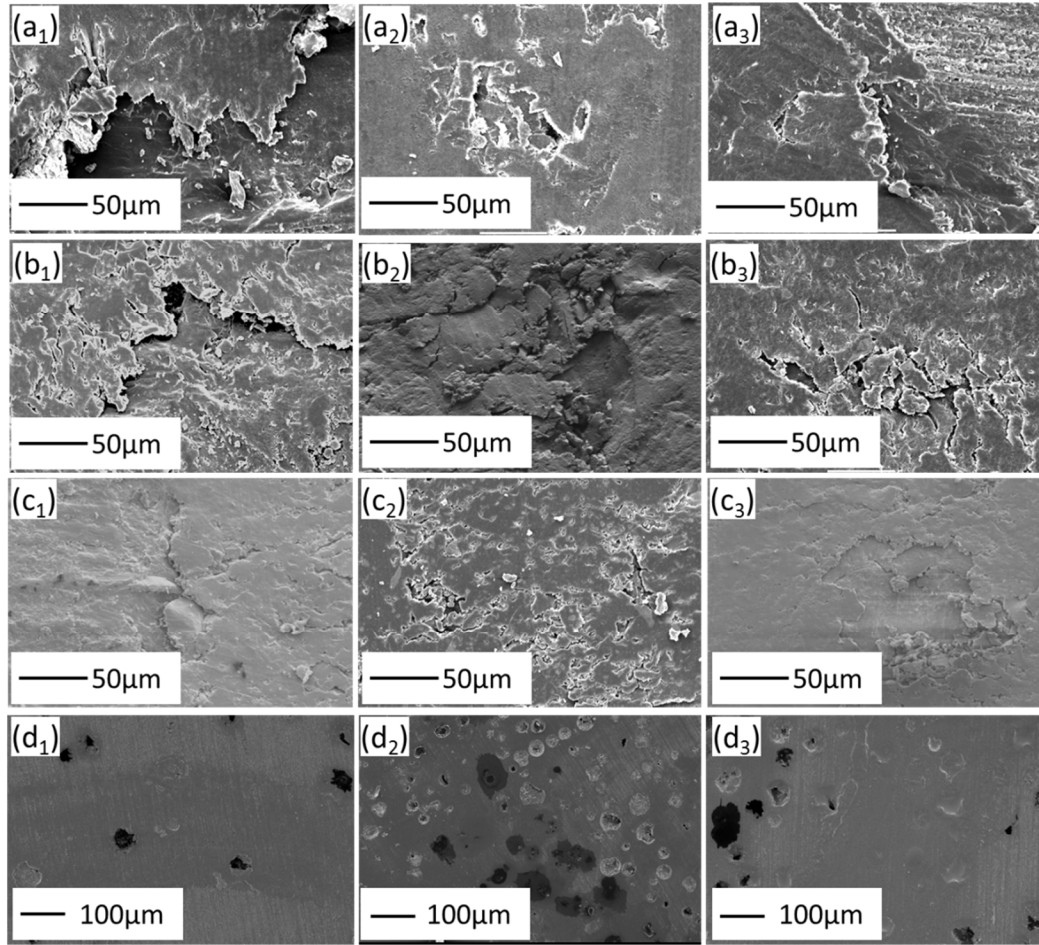


Figure 7.15 The detailed morphology of the wear track of pure epoxy samples (a), composites Tri-10wt% (b), composites Tri-30wt% (c) and composites DR-10wt% (d) at sliding rate of 25 REV (a₁, b₁, c₁ and d₁), 50 REV (a₂, b₂, c₂ and d₂) and 100 REV (a₃, b₃, c₃ and d₃).

Influence of sliding velocities on friction coefficient of composites

Samples containing pure epoxy samples, composites Tri-10wt%, composites Tri-30wt% and composites DR-10wt% were applied to tribological test under normal loads of 5N for 8 hrs at increasing sliding velocities (25 REV, 50 REV and 100 REV). The average value of friction coefficient from 10000s to the end was set as the friction coefficient of samples. The friction coefficients of all samples increase slightly under different sliding velocities, as shown in Figure

7.16. When sliding velocities increases from 25 REV to 50 REV and 100 REV, the friction coefficients of pure epoxy samples increase from 0.5917 to 0.582 and 0.672, the friction coefficient of composites Tri-10wt% increase slightly from 0.559 to 0.569 and 0.596, the friction coefficient of composites 30 wt% still increase from 0.507 to 0.557 and 0.566, and the friction coefficient of composites DR-10wt% also increases slightly from 0.071 to 0.086 and 0.09. The increase of friction coefficient was mainly because larger contact interfaces were produced under higher sliding velocities resulting in the increase of mechanical interlock and friction coefficient. In addition, more serious adhesion wear can be produced under faster sliding velocities due to the formation of friction heat.

The trifunctional microcapsules influences slightly on the friction coefficient of composites. When the concentration of tri-functional microcapsules was 10 wt%, the friction coefficient of composites Tri-10wt% decreased by 5.6% (25 REV), 2.2% (50 REV), and 11.3% (100 REV) under different sliding velocities comparing with pure epoxy samples. The minor decrease of friction coefficient of composites Tri-10wt% was mainly because the metal shell of trifunctional microcapsules increases the friction coefficient of matrix after being worn into powder. In addition, the concentration of trifunctional microcapsules influences slightly on the self-lubricating performance of composites. When concentration of tri-functional microcapsules increases from 10 wt% to 30 wt%, the friction coefficient of composites Tri-30wt% decreased by 9.3% (25 REV), 2.1% (50 REV) and 5% (100 REV) under different sliding velocities comparing to pure epoxy samples. Although more liquid core can be released under higher concentrations of trifunctional microcapsules, more metal powder can also be produced resulting in the increase of friction coefficient [84].

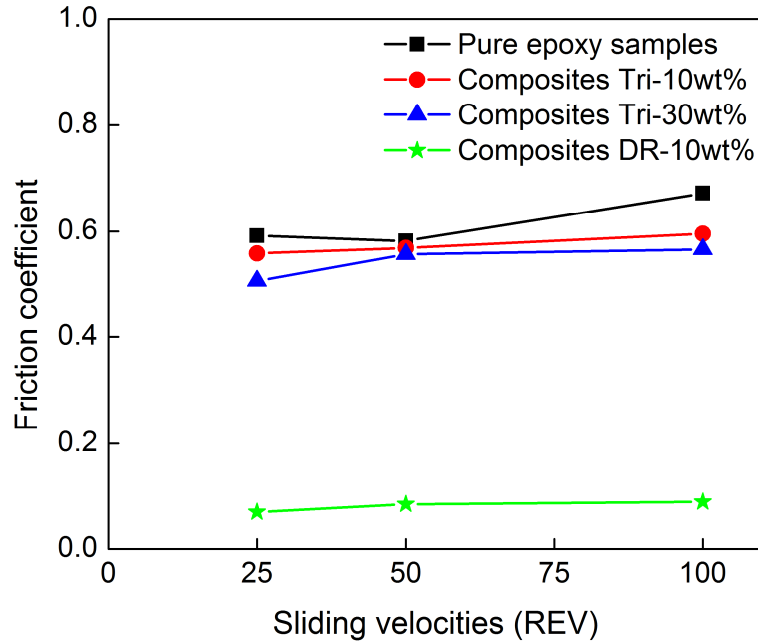


Figure 7.16 The friction coefficient of pure epoxy samples, composites Tri-10wt%, composites Tri-30wt% and composites DR-10wt% as a function of sliding velocities (25 REV, 50 REV and 100 REV).

In comparison, double resistant microcapsules possess outstanding self-lubricating performance towards epoxy matrix. The friction coefficients of composites DR-10wt% decrease by 88 % (25 REV), 85.3 % (50 REV) and 86.5 % (100 REV) under different sliding velocities, comparing with pure epoxy samples. Obviously, the released HMDI as lubricant can decrease efficiently friction coefficient. Comparing with trifunctional microcapsules, double resistant microcapsules possess better self-lubricating performance.

Influence of sliding velocity on wear loss of composites

Besides friction efficient, sliding velocities also influence significantly on the wear loss of composites including pure epoxy samples, composites DR-10 wt%, composites Tri-10 wt%, and composites Tri-30 wt%, and the wear loss was characterized in terms of wear width and wear depth, as shown in Figure 7.17 and 7.18.

Figure 7.17 shows the wear width of samples as a function of sliding velocities. The wear width of samples increases under higher velocities. As shown in Figure 7.17, the wear width of samples increases from 0.87 ± 0.04 mm to 1 ± 0.06 mm and 1.21 ± 0.04 mm (pure epoxy samples), from 0.86 ± 0.06 mm to 0.94 ± 0.9 mm and 1.29 ± 0.04 mm (Composites Tri-10wt%), from 0.81 ± 0.03 mm to 0.9 ± 0.05 mm and 1.16 ± 0.05 mm (Composites Tri-30wt%), along with from 0.35 ± 0.03 mm to 0.43 ± 0.1 mm and 0.45 ± 0.13 mm (Composites DR-10wt%) when sliding velocities increase from 25 REV to 50 REV and 100 REV, respectively. In addition, the wear depth of samples also increases under faster sliding velocities. As shown in Figure 7.18, the wear depth of samples increases from 46.3 ± 5.4 μ m to 58.2 ± 4.2 μ m and 99.2 ± 8.3 μ m (pure epoxy samples), from 40.7 ± 2.7 μ m to 58.6 ± 9.9 μ m and 99.3 ± 7.3 μ m (Composites Tri-10wt%), from 35.4 ± 2.4 μ m to 50.6 ± 9.7 μ m and 92.2 ± 11.2 μ m (Composites Tri-30wt%), along with from 2.97 ± 0.92 μ m to 5.8 ± 3 μ m and 8.9 ± 4.4 μ m (Composites DR-10wt%) when sliding velocities increase from 25 REV to 50 REV and 100 REV, respectively. The reason why wear loss increase with sliding velocities is that more severe wear occurs to samples under higher sliding velocities. The addition of trifunctional microcapsules influences slightly on the wear loss of composites. When trifunctional microcapsules were added in epoxy resin at a concentration of 10 wt%, the wear loss including wear width and wear depth of composites Tri-10wt% was almost the same with that of pure epoxy samples. Although trifunctional microcapsules can release liquid core as lubricant, the metal shell of trifunctional microcapsules tends to increase the friction coefficient of composites after being wore into powders. In addition, the trifunctional microcapsules decrease the strength of composites resulting in the increase of wear loss. When trifunctional microcapsules concentration was increased to 30 wt%, the wear loss of composites was improved slightly. Comparing with composites Tri-10wt%, the wear width of composites Tri-

30wt% decreased by 5.8% (25 REV), 4.2% (50 REV), and 10.1% (100 REV), while the depth decreased by 13% (25 REV), 13.6% (50 REV), and 0.1% (100 REV), respectively. The marginal decrease of wear loss was mainly because more liquid core was released under higher microcapsules concentrations resulting in better lubricating properties.

Composites containing double resistant microcapsules presented the lowest wear loss. Comparing with pure epoxy samples, the wear width of composites DR-10wt% decreased by 59.8% (25 REV), 57% (50 REV) and 62.8%, while the wear depth decreased by 93.6% (25 REV), 90% (50 REV) and 90.3% (100 REV), respectively. Such obvious decrease of wear loss was mainly due to the release of massive liquid core as lubricant was released.

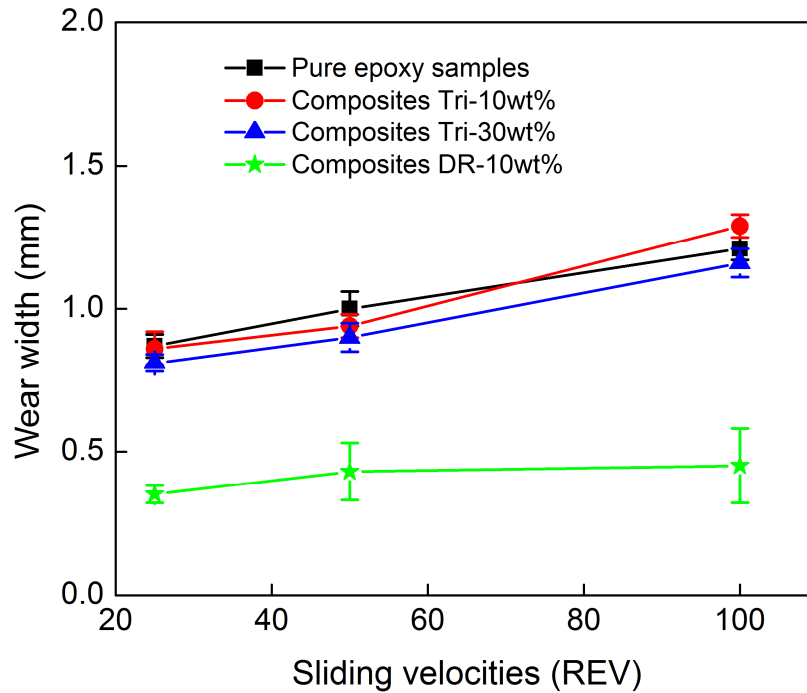


Figure 7.17 The wear width of pure epoxy samples, composites Tri-10wt%, composites Tri-30wt% and composites DR-10wt% as a function of sliding velocities (25 REV, 50 REV and 100 REV).

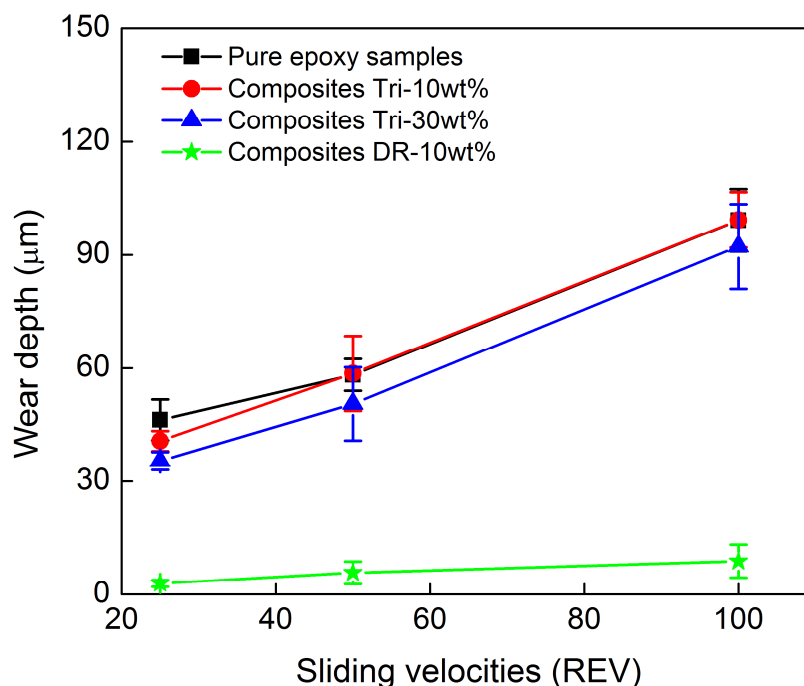


Figure 7.18 The wear depth of pure epoxy samples, composites Tri-10wt%, composites Tri-30wt% and composites DR-10wt% as a function of sliding velocities (25 REV, 50 REV and 100 REV).

Therefore, it is reasonable to conclude that trifunctional microcapsules possess poor self-lubricating performance in epoxy matrix, while double resistant microcapsules possess great self-lubricating performance in epoxy matrix.

7.5 Summary

1. The trifunctional microcapsules possess higher shell strength than double resistant microcapsules due to the existence of metal shell. Shell strength influence significantly on the mechanical properties of polymeric matrix. The compressive strength of epoxy composites containing trifunctional microcapsules was higher than that of composites containing double resistant microcapsules under the same concentrations. In addition, the compressive modulus of composite remains stable relatively with the increase of

trifunctional microcapsules concentration, while it decreases with the increase of double resistant microcapsules concentration.

2. Both double resistant microcapsules and trifunctional microcapsules in epoxy coating possess outstanding anticorrosion performance towards steel panels. Moreover, the EIS test results of both scratched coatings prove the occurrence of self-healing process.
3. Double resistant microcapsules possess excellent self-lubricating performance in composite coating. Comparing with pure epoxy samples, the friction coefficient of composites containing double resistant microcapsules of 10 wt% decreased by higher than 80% under various normal loads and sliding velocities, which the friction coefficient of composites containing trifunctional microcapsules of 10 wt% decreased by less than 10%. Moreover, the increase of trifunctional microcapsules concentration influences slightly on the friction coefficient and wear loss of composites under different conditions.

Chapter 8 Conclusions and future work

8.1 Conclusions

Two types of microcapsules including double resistant microcapsules and trifunctional microcapsules were fabricated successfully. Double resistant microcapsules possessing outstanding stability in both water and organics solvents were successfully fabricated. In order to improve shell strength of double resistant microcapsules, a layer of metal shell was covered on the surface of double resistant microcapsules as trifunctional microcapsules. In addition, multifunctional coatings possess both self-healing and self-lubricating functions were fabricated successfully by embedding microcapsules in epoxy coatings. Both double resistant microcapsules and trifunctional microcapsules show superior self-healing anticorrosion performance in epoxy coating. Comparing with the excellent self-lubricating performance of double resistant microcapsules, trifunctional microcapsules showed poor self-lubricating performance due to the existence of metals shell.

Water resistant microcapsules were synthesized firstly by combining interfacial polymerization and in situ polymerization. By adjusting agitation rate from 750 RPM to 1450 RPM, the diameters of water resistant microcapsules varied from 100 μm to 18 μm , while shell thickness decreased from 2 μm to 0.7 μm . However, the core fractions of water resistant microcapsules remain stable relatively at around 70 wt%. The water resistant microcapsules showed outstanding stability in moist environments. The relative residue of core fraction was beyond 90% after 24 days in ambient water and open air, respectively. The residual core fractions of water resistant microcapsules were more than 80% after 24 days in acid or alkaline water solutions. However, water resistant microcapsules showed poor stability in organic solvents.

The microcapsules possessing excellent stabilities in both water and organic solvents were fabricated successfully and named as double resistant microcapsules. The double resistant microcapsules possess total shell thickness of 3.8 μm , diameters of $79.7\pm 21.5 \mu\text{m}$, and typical core fraction of $74\pm 1.3 \text{ wt}\%$. Double microcapsules possess higher beginning weight loss temperature (230°C) than that of shell materials (220°C). In addition, double resistant microcapsules presented great stability in both ambient water and organic solvents. The relative residue of core fractions was higher than 90% after 20 days in ambient water and was beyond 90% after 30 days in ambient hexane, xylene and ethyl acetate, respectively. Double resistant microcapsules with bigger size possess better stability in organic solvents, and double resistant microcapsules showed worse stability in organic solvents with higher polarities. However, concentration of double resistant microcapsules in organic solvents influence slightly on final stability.

In order to improve the shell strength of double resistant microcapsules, chemical plating techniques were applied successfully to cover a layer of metal shell on double resistant microcapsules for the fabrication of trifunctional microcapsules. The shell thickness of trifunctional microcapsules was $5.52\pm 0.21 \mu\text{m}$. The core fraction of trifunctional microcapsules was $22.42\pm 0.63 \text{ wt}\%$ corresponding to volume percentage of $73.1\pm 1.89 \%$. The trifunctional microcapsules showed outstanding stability in both water and organic solvents. The relative residues of trifunctional microcapsules were beyond 90% after 20 days in ambient water and 30 days in organic solvents. More interestingly, the trifunctional microcapsules possess great stability in acetone, and the relative residue of core fraction was higher than 90% after 20 days in acetone.

The influence of metal shell on microcapsules and composites was investigated systematically by comparing double resistant microcapsules with trifunctional microcapsules including shell strength, influence of microcapsules on the mechanical properties of epoxy matrix, anticorrosion performance and self-lubricating performance. Metal shell improved successfully the shell strength of double resistant microcapsules. The shell strength of double resistant microcapsules was 6.6 ± 2.5 MPa, while that of trifunctional microcapsules was 28.5 ± 10.3 MPa. The compressive strengths of composites containing both microcapsules decrease with the increase of microcapsules concentrations. However, the composites containing trifunctional microcapsules possess higher compressive strength than those containing double resistant microcapsules. In addition, the compressive modulus of composites containing trifunctional microcapsules remain stable relatively with microcapsules concentration, while that of composites containing double resistant microcapsules decrease obviously with microcapsules concentration. Both double resistant microcapsules and trifunctional microcapsules showed superior self-healing anticorrosion performance in coatings. However, the self-lubricating performances of multifunctional coatings containing different microcapsules perform differently. Comparing with pure epoxy samples, the friction coefficient of composites containing double resistant microcapsules decrease obviously under different normal loads and sliding velocities, while that of composites containing trifunctional microcapsules decrease slightly, because the existing metal shell tend to increase friction coefficient of composites after being worn into powder

8.2 Future work

Although multifunctional coating with both anticorrosion and self-lubricating functions have been fabricated successfully, further studies are still needed to improve current shortages:

1. In our investigations, HMDI was encapsulated successfully in various shells. Extending the core materials from isocyanates to other available healing agents possess great potential in the practical application.
2. Although trifunctional microcapsules possess outstanding stability in water, organic solvents and excellent mechanical strength, high density of metal shell is unfavorable for easy dispersion in polymeric coatings. Finding a method to decrease microcapsules density is important for better practical application.
3. Plating a layer of metal shell covering double resistance microcapsules can improve efficiently mechanical strength of microcapsules shells. However, the existing metal shell can retard the self-lubricating performance of microcapsules. Therefore, it is necessary to find a new inorganic as shell materials, to improve shell strength and self-lubricating performance of microcapsules.

References

1. J. L. Yang, M. W. Keller, J. S. Moore, S. R. White and N. R. Sottos, *Microencapsulation of Isocyanates for Self-Healing Polymers*, *Macromolecules*, 2008, **41**, 9650-9655.
2. M. Huang and J. Yang, Facile microencapsulation of HDI for self-healing anticorrosion coatings, *Journal of Material Chemistry*, 2011, **21**, 11123-11130.
3. M. W. Keller, K. Hampton and B. McLaury, *Self-healing of erosion damage in a polymer coating*, *Wear*, 2013, **307**, 218-225.
4. N. Khun, D. Sun, M. Huang, J. Yang and C. Yue, *Wear resistant epoxy composites with diisocyanate-based self-healing functionality*, *Wear*, 2014, **313**, 19-28.
5. N. Khun, H. Zhang, J. Yang and E. Liu, *Tribological performance of silicone composite coatings filled with wax-containing microcapsules*, *Wear*, 2012, **296**, 575-582.
6. M. Huang, *One-part self-healing anticorrosive coatings via microencapsulation of reactive agents*, Nanyang technological university, phd thesis, 2013.
7. D. Sun, J. An, G. Wu and J. Yang, *Double-layered reactive microcapsules with excellent thermal and non-polar solvents resistance for self-healing coatings*, *Journal of Materials Chemistry A*, 2015, **3**, 4435-4444.
8. G. Wu, J. An, X. Z. Tang, Y. Xiang and J. Yang, *A versatile approach towards multifunctional robust microcapsules with tunable, restorable, and solvent - proof superhydrophobicity for self - healing and self - cleaning coatings*, *Advanced Functional Materials*, 2014, **24**, 6751-6761.
9. H. Yi, Y. Yang, X. Gu, J. Huang and C. Wang, *Multilayer composite microcapsules synthesized by Pickering emulsion templates and their application in self-healing coating*, *Journal of Materials Chemistry A*, 2015, **3**, 13749-13757.

10. R. Herrington and K. Hock, *Flexible polyurethane foams*, 1997: Dow Chemical.
11. A. Popoola, O. Olorunniwo, O. Ige and M. A. (Ed.), *Corrosion resistance through the application of anti-corrosion coatings, Developments in Corrosion Protection, Intech, 2014, Pretoria, South Africa*
12. F. Fragata, R. P. Salai, C. Amorim and E. Almeida, *Compatibility and incompatibility in anticorrosive painting: The particular case of maintenance painting*, Progress in Organic Coatings, 2006, **56**, 257-268.
13. M. Pandey and M. Nessim, *Reliability-based inspection of post-tensioned concrete slabs*, Canadian Journal of Civil Engineering, 1996, **23**, 242-249.
14. H. Humble, *Cathodic Protection of Steel Piling In Sea Water*, Corrosion, 1949, **5**, 292-302.
15. A. Husain, O. Al-Shamah and A. Abduljaleel, *Investigation of marine environmental related deterioration of coal tar epoxy paint on tubular steel pilings*, Desalination, 2004, **166**, 295-304.
16. Z. Zhou, L. Wang, F. Wang, H. Zhang, Y. Liu and S. Xu, *Formation and corrosion behavior of Fe-based amorphous metallic coatings by HVOF thermal spraying*, Surface and Coatings Technology, 2009, **204**, 563-570.
17. S. F. Liu, *Low temperature plasma enhanced CVD ceramic coating process for metal, alloy and ceramic materials*, 2002, US6482476 B1, US patent.
18. D. Chaliampalias, G. Vourlias, N. Pistofidis, E. Pavlidou, A. Stergiou, G. Stergioudis, E. K. Polychroniadis and D. Tsipas, *Deposition of zinc coatings with fluidized bed technique*, Materials Letters, 2007, **61**, 223-226.

19. W. D. Munz, *Large-scale manufacturing of nanoscale multilayered hard coatings deposited by cathodic arc/unbalanced magnetron sputtering*, Mrs Bulletin, 2003, **28**, 173-179.
20. A. Kalendová, *Effects of particle sizes and shapes of zinc metal on the properties of anticorrosive coatings*, Progress in Organic Coatings, 2003, **46**, 324-332.
21. W. Funke, *How organic coating systems protect against corrosion*, 1986: ACS Publications, Washington, US.
22. D. J. Penney, J. H. Sullivan and D. A. Worsley, *Investigation into the effects of metallic coating thickness on the corrosion properties of Zn–Al alloy galvanising coatings*, Corrosion Science, 2007, **49**, 1321-1339.
23. Z. Panossian, L. Mariaca, M. Morcillo, S. Flores, J. Rocha, J. Pena, F. Herrera, F. Corvo, M. Sanchez and O. Rincon, *Steel cathodic protection afforded by zinc, aluminium and zinc/aluminium alloy coatings in the atmosphere*, Surface and Coatings Technology, 2005, **190**, 244-248.
24. A. Barnoush and H. Vehoff, *Recent developments in the study of hydrogen embrittlement: hydrogen effect on dislocation nucleation*, Acta Materialia, 2010, **58**, 5274-5285.
25. P. Pedferri, *Cathodic protection and cathodic prevention*, Construction and Building Materials, 1996, **10**, 391-402.
26. A. Zhirnov, S. Karimova, L. Ovsyannikova and O. Gubenko, *New protective coatings for replacing cadmium coatings on steel parts*, Metal science and heat treatment, 2003, **45**, 23-25.
27. H. Royle, *Toxicity of chromic acid in the chromium plating industry* Environmental research, 1975, **10**, 39-53.

28. J. Gardea-Torresdey, J. Gonzalez, K. Tiemann, O. Rodriguez and G. Gamez, *Phytofiltration of hazardous cadmium, chromium, lead and zinc ions by biomass of Medicago sativa (Alfalfa)*, Journal of Hazardous Materials, 1998, **57**, 29-39.
29. J. W. Bibber, *Corrosion resistant aluminum coating composition*, 1988, US4755224A, US patent.
30. G. J. L., *Method of indium coating metallic articles*, 1968, US3389060A, US patent.
31. J. C. Lynn, W. R. Warke and P. Gordon, *Solid metal-induced embrittlement of steel*, Materials Science and Engineering, 1975, **18**, 51-62.
32. M. Mitchell and M. Summers, *How to select zinc silicate primers*, Protective Coating of European Journal, 2001, **12**, 77-89.
33. M. Thouless, *Cracking and delamination of coatings*, Journal of Vacuum Science & Technology A: Vacuum, Surfaces, and Films, 1991, **9**, 2510-2515.
34. M. J. Mitchell, presented in part at the 14th International Corrosion Conference, Cape Town, South Africa, 09.26-10.01, 1999.
35. H. Undrum, *Superior protection-silicate and epoxy zinc primers*, Surface Coatings Australia, 2007, **44**, 14.
36. M. Guglielmi, *Sol-gel coatings on metals*, Journal of sol-gel science and technology, 1997, **8**, 443-449.
37. R. Ballard, J. Williams, J. Njus, B. Kiland and M. Soucek, *Inorganic-organic hybrid coatings with mixed metal oxides*, European polymer journal, 2001, **37**, 381-398.
38. G. Schottner, *Hybrid sol-gel-derived polymers: applications of multifunctional materials*, Chemistry of Materials, 2001, **13**, 3422-3435.

39. S. Messaddeq, S. H. Pulcinelli, C. V. Santilli, A. C. Guastaldi and Y. Messaddeq, *Microstructure and corrosion resistance of inorganic-organic (ZrO₂-PMMA) hybrid coating on stainless steel*, Journal of Non-Crystalline Solids, 1999, **247**, 164-170.
40. A. Forsgren, *Corrosion control through organic coatings*, 2006: CRC Press, Boca Raton, US.
41. A. e. Tiwari, L. Hihara and J. Rawlins, *Intelligent coatings for corrosion control*, 2015: Elsevier Inc, Waltham, US.
42. T. Ross and J. Wolstenholme, *Anti-corrosion properties of zinc dust paints*, Corrosion Science, 1977, **17**, 341-351.
43. C. H. Hare, M. Steele and S. P. Collins, *Zinc loadings, cathodic protection, and post-cathodic protective mechanisms in organic zinc-rich metal primers*, Journal of Protective Coatings and Linings, 2001, **18**, 54-77.
44. S. Faidi, J. Scantlebury, P. Bullivant, N. Whittle and R. Savin, *An electrochemical study of zinc-containing epoxy coatings on mild steel*, Corrosion Science, 1993, **35**, 1319-1328.
45. D. Pereira, J. Scantlebury, M. Ferreira and M. Almeida, *The application of electrochemical measurements to the study and behaviour of zinc-rich coatings*, Corrosion Science, 1990, **30**, 1135-1147.
46. C. Gervasi, A. Di Sarli, E. Cavalcanti, O. Ferraz, E. Bucharsky, S. Real and J. Vilche, *The corrosion protection of steel in sea water using zinc-rich alkyd paints. An assessment of the pigment-content effect by EIS*, Corrosion Science, 1994, **36**, 1963-1972.
47. A. Baczoni and F. Molnár, *Advanced Examination of Zinc Rich Primers with Thermodielectric Spectroscopy*, Acta Polytechnica Hungarica, 2011, **8**, 43-51.

48. K. Schaefer and A. Miszczyk, *Improvement of electrochemical action of zinc-rich paints by addition of nanoparticulate zinc*, Corrosion Science, 2013, **66**, 380-391.
49. N. Arianpouya, M. Shishesaz, M. Arianpouya and M. Nematollahi, *Evaluation of synergistic effect of nanozinc/nanoclay additives on the corrosion performance of zinc-rich polyurethane nanocomposite coatings using electrochemical properties and salt spray testing*, Surface and Coatings Technology, 2013, **216**, 199-206.
50. J. Vilche, E. Bucharsky and C. Giudice, *Application of EIS and SEM to evaluate the influence of pigment shape and content in ZRP formulations on the corrosion prevention of naval steel*, Corrosion Science, 2002, **44**, 1287-1309.
51. L. Zhang, A. Ma, J. Jiang, D. Song, J. Chen and D. Yang, *Anti-corrosion performance of waterborne Zn-rich coating with modified silicon-based vehicle and lamellar Zn (Al) pigments*, Progress in Natural Science: Materials International, 2012, **22**, 326-333.
52. R. Twite and G. Bierwagen, *Review of alternatives to chromate for corrosion protection of aluminum aerospace alloys*, Progress in Organic Coatings, 1998, **33**, 91-100.
53. E. Joussein, S. Petit, J. Churchman, B. Theng, D. Righi and B. Delvaux, *Halloysite clay minerals—a review*, Clay Minerals, 2005, **40**, 383-426.
54. E. Abdullayev, R. Price, D. Shchukin and Y. Lvov, *Halloysite tubes as nanocontainers for anticorrosion coating with benzotriazole*, Acs Applied Materials & Interfaces, 2009, **1**, 1437-1443.
55. Z. Zheng, X. Huang, M. Schenderlein, D. Borisova, R. Cao, H. Möhwald and D. Shchukin, *Self - Healing and Antifouling Multifunctional Coatings Based on pH and Sulfide Ion Sensitive Nanocontainers*, Advanced Functional Materials, 2013, **23**, 3307-3314.

56. D. Grigoriev, R. Miller, D. Shchukin and H. Möhwald, *Interfacial assembly of partially hydrophobic silica nanoparticles induced by ultrasonic treatment*, *Small*, 2007, **3**, 665-671.
57. A. Latnikova, D. O. Grigoriev, H. Möhwald and D. G. Shchukin, *Capsules made of cross-linked polymers and liquid core: possible morphologies and their estimation on the basis of hansen solubility parameters*, *The Journal of Physical Chemistry C*, 2012, **116**, 8181-8187.
58. M. L. Zheludkevich, D. G. Shchukin, K. A. Yasakau, H. Möhwald and M. G. Ferreira, *Anticorrosion coatings with self-healing effect based on nanocontainers impregnated with corrosion inhibitor*, *Chemistry of Materials*, 2007, **19**, 402-411.
59. D. Borisova, H. Möhwald and D. G. Shchukin, *Influence of embedded nanocontainers on the efficiency of active anticorrosive coatings for aluminum alloys part I: influence of nanocontainer concentration*, *Acs Applied Materials & Interfaces*, 2012, **4**, 2931-2939.
60. D. W. DeBerry, *Modification of the electrochemical and corrosion behavior of stainless steels with an electroactive coating*, *Journal of the Electrochemical Society*, 1985, **132**, 1022-1026.
61. N. Gospodinova and L. Terlemezyan, *Conducting polymers prepared by oxidative polymerization: polyaniline*, *Progress in Polymer Science*, 1998, **23**, 1443-1484.
62. G. Ćirić-Marjanović, *Recent advances in polyaniline composites with metals, metalloids and nonmetals*, *Synthetic Metals*, 2013, **170**, 31-56.
63. U. Riaz, C. Nwaoha and S. Ashraf, *Recent advances in corrosion protective composite coatings based on conducting polymers and natural resource derived polymers*, *Progress in Organic Coatings*, 2014, **77**, 743-756.

64. M. Oliveira, J. Moraes and R. Faez, *Impedance studies of poly (methylmethacrylate-co-acrylic acid) doped polyaniline films on aluminum alloy*, Progress in Organic Coatings, 2009, **65**, 348-356.
65. A. J. Dominis, G. M. Spinks and G. G. Wallace, *Comparison of polyaniline primers prepared with different dopants for corrosion protection of steel*, Progress in Organic Coatings, 2003, **48**, 43-49.
66. D. Kowalski, M. Ueda and T. Ohtsuka, *Corrosion protection of steel by bi-layered polypyrrole doped with molybdophosphate and naphthalenedisulfonate anions*, Corrosion Science, 2007, **49**, 1635-1644.
67. G. Bereket and E. Hür, *The corrosion protection of mild steel by single layered polypyrrole and multilayered polypyrrole/poly (5-amino-1-naphthol) coatings*, Progress in Organic Coatings, 2009, **65**, 116-124.
68. G. Kousik, S. Pitchumani and N. Renganathan, *Electrochemical characterization of polythiophene-coated steel*, Progress in Organic Coatings, 2001, **43**, 286-291.
69. C. Ocampo, E. Armelin, F. Liesa, C. Alemán, X. Ramis and J. I. Iribarren, *Application of a polythiophene derivative as anticorrosive additive for paints*, Progress in Organic Coatings, 2005, **53**, 217-224.
70. A. Michalik and M. Rohwerder, *Conducting polymers for corrosion protection: a critical view*, Zeitschrift für Physikalische Chemie, 2005, **219**, 1547-1559.
71. T. Tüken, G. Tansuğ, B. Yazıcı and M. Erbil, *Poly (N-methyl pyrrole) and its copolymer with pyrrole for mild steel protection*, Surface and Coatings Technology, 2007, **202**, 146-154.

72. İ. Çakmakcı, B. Duran and G. Bereket, *Influence of electrochemically prepared poly (pyrrole-co-N-methyl pyrrole) and poly (pyrrole)/poly (N-methyl pyrrole) composites on corrosion behavior of copper in acidic medium*, Progress in Organic Coatings, 2013, **76**, 70-77.
73. J.-C. Lacroix, J.-L. Camalet, S. Aeiyaç, K. Chane-Ching, J. Petitjean, E. Chauveau and P.-C. Lacaze, *Aniline electropolymerization on mild steel and zinc in a two-step process*, Journal of Electroanalytical Chemistry, 2000, **481**, 76-81.
74. J. O. Iroh, Y. Zhu, K. Shah, K. Levine, R. Rajagopalan, T. Uyar, M. Donley, R. Mantz, J. Johnson and N. N. Voevodin, *Electrochemical synthesis: a novel technique for processing multi-functional coatings*, Progress in Organic Coatings, 2003, **47**, 365-375.
75. Y.-Z. Long, M.-M. Li, C. Gu, M. Wan, J.-L. Duvail, Z. Liu and Z. Fan, *Recent advances in synthesis, physical properties and applications of conducting polymer nanotubes and nanofibers*, Progress in Polymer Science, 2011, **36**, 1415-1442.
76. Y. Guo and Y. Zhou, *Polyaniline nanofibers fabricated by electrochemical polymerization: A mechanistic study*, European Polymer Journal, 2007, **43**, 2292-2297.
77. S. H. Cho, S. R. White and P. V. Braun, *Self - healing polymer coatings*, Advanced Materials, 2009, **21**, 645-649.
78. C. Suryanarayana, K. C. Rao and D. Kumar, *Preparation and characterization of microcapsules containing linseed oil and its use in self-healing coatings*, Progress in Organic Coatings, 2008, **63**, 72-78.
79. J. Lee, *Introduction to offshore pipelines and risers. Primera edition*, 2009: Self-published, Houston.

80. C. P. Sparks, *Fundamentals of marine riser mechanics: basic principles and simplified analyses*, 2007: PennWell Books, Tulsa, US.
81. D. Sawyer., Post-2003 talk about ODP is on the rise, JOI/USSAC Newsletter, 1996, **9**, 1-28.
82. Z. Tan, P. Quiggin and T. Sheldrake, *Time domain simulation of the 3D bending hysteresis behavior of an unbonded flexible riser*, Journal of Offshore Mechanics and Arctic Engineering, 2009, **131**, 031301.
83. G. Stachowiak and A. W. Batchelor, *Engineering tribology*, 2013: Butterworth-Heinemann, Boston, US.
84. S. Bahadur and D. Gong, *The action of fillers in the modification of the tribological behavior of polymers*, Wear, 1992, **158**, 41-59.
85. E. N. Brown, M. R. Kessler, N. R. Sottos and S. R. White, *In situ poly(urea-formaldehyde) microencapsulation of dicyclopentadiene*, Journal of Microencapsulation, 2003, **20**, 719-730.
86. G. West and J. Senior, High temperature plastics bearing compositions, Tribology, 1973, **6**, 269-275.
87. Z. Z. Zhang, W. M. Liu and Q. J. Xue, *Effects of various kinds of fillers on the tribological behavior of polytetrafluoroethylene composites under dry and oil - lubricated conditions*, Journal of Applied Polymer Science, 2001, **80**, 1891-1897.
88. Q. B. Guo, K. T. Lau, B. F. Zheng, M. Z. Rong and M. Q. Zhang, *Imparting Ultra-Low Friction and Wear Rate to Epoxy by the Incorporation of Microencapsulated Lubricant*, Macromolecular Materials and Engineering, 2009, **294**, 20-24.

89. K. Thanawala, N. Mutneja, A. S. Khanna and R. K. S. Raman, *Development of Self-Healing Coatings Based on Linseed Oil as Autonomous Repairing Agent for Corrosion Resistance*, Materials, 2014, **7**, 7324-7338.
90. M. Samadzadeh, S. H. Boura, M. Peikari, A. Ashrafi and M. Kasiriha, *Tung oil: An autonomous repairing agent for self-healing epoxy coatings*, Progress in Organic Coatings, 2011, **70**, 383-387.
91. B. Mistry, N. Patel, S. Sahoo and S. Jauhari, *Experimental and quantum chemical studies on corrosion inhibition performance of quinoline derivatives for MS in 1N HCl*, Bulletin of Materials Science, 2012, **35**, 459-469.
92. R.-C. Zeng, Z.-G. Liu, F. Zhang, S.-Q. Li, H.-Z. Cui and E.-H. Han, *Corrosion of molybdate intercalated hydrotalcite coating on AZ31 Mg alloy*, Journal of Materials Chemistry A, 2014, **2**, 13049-13057.
93. J. Tedim, M. Zheludkevich, A. Salak, A. Lisenkov and M. Ferreira, *Nanostructured LDH-container layer with active protection functionality*, Journal of Materials Chemistry, 2011, **21**, 15464-15470.
94. X. K. D. Hillewaere, R. F. A. Teixeira, L. T. T. Nguyen, J. A. Ramos, H. Rahier and F. E. Du Prez, *Autonomous Self-Healing of Epoxy Thermosets with Thiol-Isocyanate Chemistry*, Advanced Functional Materials, 2014, **24**, 5575-5583.
95. D. Zhao, M. Z. Wang, Q. C. Wu, X. Zhou and X. W. Ge, *Microencapsulation of UV-Curable Self-healing Agent for Smart Anticorrosive Coating*, Chinese Journal of Chemical Physics, 2014, **27**, 607-615.

96. S. H. Cho, H. M. Andersson, S. R. White, N. R. Sottos and P. V. Braun, *Polydimethylsiloxane-Based Self-Healing Materials*, *Advanced Materials*, 2006, **18**, 997-1000.
97. M. W. Keller, S. R. White and N. R. Sottos, *A Self-Healing Poly(Dimethyl Siloxane) Elastomer*, *Advanced Functional Materials*, 2007, **17**, 2399-2404.
98. M. Huang, H. Zhang and J. Yang, *Synthesis of organic silane microcapsules for self-healing corrosion resistant polymer coatings*, *Corrosion Science*, 2012, **65**, 561-566.
99. Y. K. Song and C. M. Chung, *Repeatable self-healing of a microcapsule-type protective coating*, *Polymer Chemistry*, 2013, **4**, 4940-4947.
100. S. H. Boura, M. Peikari, A. Ashrafi and M. Samadzadeh, *Self-healing ability and adhesion strength of capsule embedded coatings-Micro and nano sized capsules containing linseed oil*, *Progress in Organic Coatings*, 2012, **75**, 292-300.
101. E. M. Fayyad, M. A. Almaadeed and A. Jones, *Encapsulation of Tung Oil for Self-Healing Coatings in Corrosion Applications*, *Science of Advanced Materials*, 2015, **7**, 2628-2638.
102. S. A. El-Maksoud, *The influence of some Arylazobenzoyl acetonitrile derivatives on the behaviour of carbon steel in acidic media*, *Applied Surface Science*, 2003, **206**, 129-136.
103. A. A. Abd-Elaal, I. Aiad, S. M. Shaban, S. M. Tawfik and A. Sayed, *Synthesis and evaluation of some triazole derivatives as corrosion inhibitors and biocides*, *Journal of Surfactants and Detergents*, 2014, **17**, 483-491.
104. M. Lebrini, F. Bentiss, H. Vezin and M. Lagrenée, *Inhibiting effects of some oxadiazole derivatives on the corrosion of mild steel in perchloric acid solution*, *Applied Surface Science*, 2005, **252**, 950-958.

105. R. A. Hameed, H. Al-Shafey, A. Abul Magd and H. Shehata, *Pyrazole derivatives as corrosion inhibitor for C-steel in hydrochloric acid medium*, Journal of Materials and Environmental Science, 2012, **3**, 294.
106. Y. Tang, F. Zhang, S. Hu, Z. Cao, Z. Wu and W. Jing, *Novel benzimidazole derivatives as corrosion inhibitors of mild steel in the acidic media. Part I: Gravimetric, electrochemical, SEM and XPS studies*, Corrosion Science, 2013, **74**, 271-282.
107. J. Y. Chen, X. B. Chen, J. L. Li, B. Tang, N. Birbilis and X. G. Wang, *Electrosprayed PLGA smart containers for active anti-corrosion coating on magnesium alloy AMLite*, Journal of Materials Chemistry A, 2014, **2**, 5738-5743.
108. D. G. Shchukin and H. Mohwald, *Surface-engineered nanocontainers for entrapment of corrosion inhibitors*, Advanced Functional Materials, 2007, **17**, 1451-1458.
109. X. L. Guo, B. Hurley and R. G. Buchheit, *Encapsulation of NaVO₃ as Corrosion Inhibitor into Microparticles and its Active Corrosion Protection for AA2024 Based Upon Inhibitor Control Release*, Corrosion, 2015, **71**, 1411-1413.
110. E. Koh, S. Lee, J. Shin and Y. W. Kim, *Renewable Polyurethane Microcapsules with Isosorbide Derivatives for Self-Healing Anticorrosion Coatings*, Industrial & Engineering Chemistry Research, 2013, **52**, 15541-15548.
111. V. V. Gite, P. D. Tatiya, R. J. Marathe, P. P. Mahulikar and D. G. Hundiware, *Microencapsulation of quinoline as a corrosion inhibitor in polyurea microcapsules for application in anticorrosive PU coatings*, Progress in Organic Coatings, 2015, **83**, 11-18.
112. R. J. Marathe, A. B. Chaudhari, R. K. Hedao, D. Sohn, V. R. Chaudhari and V. V. Gite, *Urea formaldehyde (UF) microcapsules loaded with corrosion inhibitor for enhancing*

- the anti-corrosive properties of acrylic-based multifunctional PU coatings*, Rsc Advances, 2015, **5**, 15539-15546.
113. M. Zheludkevich, S. Poznyak, L. Rodrigues, D. Raps, T. Hack, L. Dick, T. Nunes and M. Ferreira, *Active protection coatings with layered double hydroxide nanocontainers of corrosion inhibitor*, Corrosion Science, 2010, **52**, 602-611.
 114. D. V. Andreeva, E. V. Skorb and D. G. Shchukin, *Layer-by-layer polyelectrolyte/inhibitor nanostructures for metal corrosion protection*, Acs Applied Materials & Interfaces, 2010, **2**, 1954-1962.
 115. D. Snihirova, S. Lamaka, M. Taryba, A. Salak, S. Kallip, M. Zheludkevich, M. Ferreira and M. Montemor, *Hydroxyapatite microparticles as feedback-active reservoirs of corrosion inhibitors*, Acs Applied Materials & Interfaces, 2010, **2**, 3011-3022.
 116. A. Jafari, S. Hosseini and E. Jamalizadeh, *Investigation of smart nanocapsules containing inhibitors for corrosion protection of copper*, Electrochimica Acta, 2010, **55**, 9004-9009.
 117. S. R. White, N. Sottos, P. Geubelle, J. Moore, M. R. Kessler, S. Sriram, E. Brown and S. Viswanathan, *Autonomic healing of polymer composites*, Nature, 2001, **409**, 794-797.
 118. X. Liu, J. Le and M. Kessler, *Microencapsulation of self-healing agents with melamine-urea-formaldehyde by the Shirasu porous glass (SPG) emulsification technique*, Macromolecular Research, 2011, **19**, 1056-1061.
 119. B. Blaiszik, N. Sottos and S. White, *Nanocapsules for self-healing materials*, Composites Science and Technology, 2008, **68**, 978-986.
 120. L. Yuan, A. J. Gu and G. Z. Liang, *Preparation and properties of poly(urea-formaldehyde) microcapsules filled with epoxy resins*, Materials Chemistry and Physics, 2008, **110**, 417-425.

121. B. J. Blaiszik, A. R. Jones, N. R. Sottos and S. R. White, *Microencapsulation of gallium-indium (Ga-In) liquid metal for self-healing applications*, Journal of Microencapsulation, 2014, **31**, 350-354.
122. C. J. Fan and X. D. Zhou, *Preparation and barrier properties of the microcapsules added nanoclays in the wall*, Polymers for Advanced Technologies, 2009, **20**, 934-939.
123. W. Wang, L. K. Xu, F. Liu, X. B. Li and L. K. Xing, *Synthesis of isocyanate microcapsules and micromechanical behavior improvement of microcapsule shells by oxygen plasma treated carbon nanotubes*, Journal of Materials Chemistry A, 2013, **1**, 776-782.
124. M. M. Caruso, B. J. Blaiszik, H. H. Jin, S. R. Schelkopf, D. S. Stradley, N. R. Sottos, S. R. White and J. S. Moore, *Robust, Double-Walled Microcapsules for Self-Healing Polymeric Materials*, Acs Applied Materials & Interfaces, 2010, **2**, 1195-1199.
125. L. M. Meng, Y. C. Yuan, M. Z. Rong and M. Q. Zhang, *A dual mechanism single-component self-healing strategy for polymers*, Journal of Materials Chemistry, 2010, **20**, 6030-6038.
126. H. Y. Li, R. G. Wang, H. L. Hu and W. B. Liu, *Surface modification of self-healing poly(urea-formaldehyde) microcapsules using silane-coupling agent*, Applied Surface Science, 2008, **255**, 1894-1900.
127. M. Jacquemond, N. Jeckelmann, L. Ouali and O. P. Haefliger, *Perfume - containing polyurea microcapsules with undetectable levels of free isocyanates*, Journal of Applied Polymer Science, 2009, **114**, 3074-3080.

128. X. X. Liu, H. R. Zhang, J. X. Wang, Z. Wang and S. C. Wang, *Preparation of epoxy microcapsule based self-healing coatings and their behavior*, Surface & Coatings Technology, 2012, **206**, 4976-4980.
129. R. K. Hedao, P. P. Mahulikar, A. B. Chaudhari, S. D. Rajput and V. V. Gite, *Fabrication of Core-Shell Novel Polyurea Microcapsules Using Isophorone Diisocyanate (IPDI) Trimer for Release System*, International Journal of Polymeric Materials and Polymeric Biomaterials, 2014, **63**, 352-360.
130. D. Raps, T. Hack, M. Kolb, M. L. Zheludkevich and O. Nuyken, *Development of corrosion protection coatings for aa2024-T3 using micro-encapsulated inhibitors*, 2010: American chemical society, Washington DC, US.
131. E. Koh, S. Y. Baek, N. K. Kim, S. Lee, J. Shin and Y. W. Kim, *Microencapsulation of the triazole derivative for self-healing anticorrosion coatings*, New Journal of Chemistry, 2014, **38**, 4409-4419.
132. T. Dispinar, C. A. L. Colard and F. E. Du Prez, *Polyurea microcapsules with a photocleavable shell: UV-triggered release*, Polymer Chemistry, 2013, **4**, 763-772.
133. B. McFarland and J. A. Pojman, *Effects of shell crosslinking on polyurea microcapsules containing a free-radical initiator*, Journal of Applied Polymer Science, 2015, **132**, 11.
134. P. D. Tatiya, R. K. Hedao, P. P. Mahulikar and V. V. Gite, *Novel polyurea microcapsules using dendritic functional monomer: synthesis, characterization, and its use in self-healing and anticorrosive polyurethane coatings*, Industrial & Engineering Chemistry Research, 2013, **52**, 1562-1570.

135. J. Hickey, N. A. D. Burke and H. D. H. Stover, *Layer-by-layer deposition of clay and a polycation to control diffusive release from polyurea microcapsules*, Journal of Membrane Science, 2011, **369**, 68-76.
136. G. Wu, J. L. An, D. W. Sun, X. Z. Tang, Y. Xiang and J. L. Yang, *Robust microcapsules with polyurea/silica hybrid shell for one-part self-healing anticorrosion coatings*, Journal of Materials Chemistry A, 2014, **2**, 11614-11620.
137. S. Kang, M. Baginska, S. R. White and N. R. Sottos, *Core-Shell Polymeric Microcapsules with Superior Thermal and Solvent Stability*, Acs Applied Materials & Interfaces, 2015, **7**, 10952-10956.
138. D. Borisova, H. Möhwald and D. G. Shchukin, *Influence of embedded nanocontainers on the efficiency of active anticorrosive coatings for aluminum alloys part II: influence of nanocontainer position*, Acs Applied Materials & Interfaces, 2012, **5**, 80-87.
139. T. Chen and J. Fu, *pH-responsive nanovalves based on hollow mesoporous silica spheres for controlled release of corrosion inhibitor*, Nanotechnology, 2012, **23**, 235605.
140. T. Chen and J. Fu, *An intelligent anticorrosion coating based on pH-responsive supramolecular nanocontainers*, Nanotechnology, 2012, **23**, 1-12.
141. G. Williams, H. McMurray and M. Loveridge, *Inhibition of corrosion-driven organic coating disbondment on galvanised steel by smart release group II and Zn (II)-exchanged bentonite pigments*, Electrochimica Acta, 2010, **55**, 1740-1748.
142. M. W. Patchan, B. W. Fuller, L. M. Baird, P. K. Gong, E. C. Walter, B. J. Vidmar, I. Kyei, Z. Y. Xia and J. J. Benkoski, *Robust Composite-Shell Microcapsules via Pickering Emulsification*, Acs Applied Materials & Interfaces, 2015, **7**, 7315-7323.

143. L.-T. T. Nguyen, X. K. D. Hillewaere, R. F. A. Teixeira, O. van den Berg and F. E. Du Prez, *Efficient microencapsulation of a liquid isocyanate with in situ shell functionalization*, Polymer Chemistry, 2015, **6**, 1159-1170.
144. M. W. Patchan, L. M. Baird, Y.-R. Rhim, E. D. LaBarre, A. J. Maisano, R. M. Deacon, Z. Xia and J. J. Benkoski, *Liquid-filled metal microcapsules*, Acs Applied Materials & Interfaces, 2012, **4**, 2406-2412.
145. M. Huang and J. Yang, *Salt spray and EIS studies on HDI microcapsule-based self-healing anticorrosive coatings*, Progress in Organic Coatings, 2014, **77**, 168-175.
146. S. S. Jada, *The structure of urea—formaldehyde resins*, Journal of applied polymer science, 1988, **35**, 1573-1592.
147. I. Updegraff, *In Encyclopedia of Polymer Science and Engineering*, 1985: Wiley-Interscience, New York, US.
148. F. MacRitchie, Mechanism of interfacial polymerization, Transactions of the Faraday Society, 1969, **65**, 2503-2507.
149. Y. M. Ma, L. Zhang and G. Y. Nie, *Study on Effects of the Nano Reinforcing Material on the Mechanical Properties of Self-healing Composites*, 2014: Trans Tech Publications Ltd, Stafa, Switzerland.
150. J. D. Rule, N. R. Sottos and S. R. White, *Effect of microcapsule size on the performance of self-healing polymers*, Polymer, 2007, **48**, 3520-3529.
151. M. Li, M. R. Chen and Z. S. Wu, *Enhancement in thermal property and mechanical property of phase change microcapsule with modified carbon nanotube*, Applied Energy, 2014, **127**, 166-171.

152. E. C. Suloff, *Sorption behavior of an aliphatic series of aldehydes in the presence of poly (ethylene terephthalate) blends containing aldehyde scavenging agents*, Virginia Polytechnic Institute and State University, phd thesis, 2002.
153. P. J. Flory and J. Rehner Jr, *Statistical mechanics of cross - linked polymer networks II. Swelling*, The Jourenel of Chemical Physics, 1943, **11**, 521-526.
154. T. Canal and N. A. Peppas, *Correlation between mesh size and equilibrium degree of swelling of polymeric networks*, Journal of Biomedical Materials Research Part A, 1989, **23**, 1183-1193.
155. A. Jonquière, D. Roizard and P. Lochon, *Use of empirical polarity parameters to describe polymer/liquid interactions: correlation of polymer swelling with solvent polarity in binary and ternary systems*, Journal of Applied Polymer Science, 1994, **54**, 1673-1684.
156. N. Schneider, J. Illinger and M. Cleaves, *Liquid sorption in a segmented polyurethane elastomer*, Polymer Engineering & Science, 1986, **26**, 1547-1551.
157. N. A. Peppas and S. R. Lustig, *The Role of Cross - links, Entanglements, and Relaxations of the Macromolecular Carrier in the Diffusional Release of Biologically Active Materials*, Annals of The New York Academy of Sciences, 1985, **446**, 26-40.
158. B. Yang, W. Huang, C. Li and L. Li, *Effects of moisture on the thermomechanical properties of a polyurethane shape memory polymer*, Polymer, 2006, **47**, 1348-1356.
159. D. Sun, H. Zhang, X.-Z. Tang and J. Yang, *Water resistant reactive microcapsules for self-healing coatings in harsh environments*, Polymer, 2016, **91**, 33-40.
160. H. Zhang, P. Wang and J. Yang, *Self-healing epoxy via epoxy–amine chemistry in dual hollow glass bubbles*, Composites Science and Technology, 2014, **94**, 23-29.

161. B. C. A and S. R. W, *Apparatus for coating particulate material by thermal evaporation*, 1958, US2846971A, US patent.
162. V. N. Talash, V. A. Lavrenko and O. A. Frenkel, *Preparation and properties of iron powder plated with nickel and cobalt*, Powder Metallurgy and Metal Ceramics, 2002, **41**, 342-346.
163. H. J. Zhang and Y. Liu, *Preparation and microwave properties of Ni hollow fiber by electroless plating-template method*, Journal of Alloys and Compounds, 2008, **458**, 588-594.
164. F. Svahn, Å. Kassman-Rudolphi and E. Wallen, *The influence of surface roughness on friction and wear of machine element coatings*, Wear, 2003, **254**, 1092-1098.
165. P. L. Menezes and S. V. Kailas, *Influence of surface texture and roughness parameters on friction and transfer layer formation during sliding of aluminium pin on steel plate*, Wear, 2009, **267**, 1534-1549.
166. J. Lancaster, presented in part at the Proceedings of the Institution of Mechanical Engineers, Gothenburg, Sweden, 5.28-5.29, 1969.

List of Publications

Book chapter

Nay Win Khun, He Zhang, **Dawei Sun** and Jinglei Yang, Multifunctional polymeric composites with wear-resistant, toughening, and self-healing features (Multifunctionality of Polymer Composites, Chapter 19, p, 588-615).

Publications

1. **Dawei Sun**, He Zhang, Xiuzhi Tang, Jinglei Yang, Synthesis of isocyanate filled microcapsules with excellent water resistance for self-healing anticorrosion coatings. **Polymer**. 2016, 91:p. 33-40.
2. **Dawei Sun**, Jinliang An, Gang Wu, Jinglei Yang, Double-layered reactive microcapsules with excellent thermal and non-polar solvent resistance for self-healing coatings. **Journal of Materials Chemistry A**, 2015. 3: p. 4435-4444.
3. Naywin Khun, He Zhang, **Dawei Sun**, Jinglei Yang, Tribological behaviors of binary and ternary epoxy composites functionalized with different microcapsules and reinforced by short carbon fibers. *Wear*, 2016, 350: p89-98.
4. Gang Wu, Jinliang An, **Dawei Sun**, Xiuzhi Tang, Yong Xiang and Jinglei Yang*, Robust microcapsules with polyurea/silica hybrid shell for one-part self-healing anticorrosion coatings. *Journal of Materials Chemistry A*, 2014. 2(30): p. 11614-11620.
5. Naywin Khun, **Dawei Sun**, Mingxing Huang, Jinglei Yang, Chee Yoon Yue, Wear resistant epoxy composites with diisocyanate-based self-healing functionality. *Wear*, 2014. 313(1): p. 19-28.

6. **Dawei Sun**, He Zhang, Xin Zhang, Jinglei Yang. Encapsulation of liquid agents within metal shell by chemical plating on liquid surface, (Manuscript finished).
7. **Dawei Sun**, Yongbing Chong, He Zhang, Ke Chen, Jinglei Yang. The preparation and characterization of double-resistant microcapsules showing outstanding self-healing and self-lubricating functions in epoxy coatings. (Manuscript finished)
8. **Dawei Sun**, Jinglei Yang. Encapsulation of liquid wax within metal shell through chemical plating technique. (Manuscript finished)
9. **Dawei Sun**, Jinglei Yang. The preparation of self-healing anticorrosion coating with super thin thickness. In preparation.
10. **Dawei Sun**, Jinglei Yang. Wear resistant epoxy composites with self-lubricating function by embedding encapsulated isocyanates within metal shell. In preparation.